Aalborg University

# Application of Reconstituted High-Density Lipoproteins for Cancer Immunotherapy

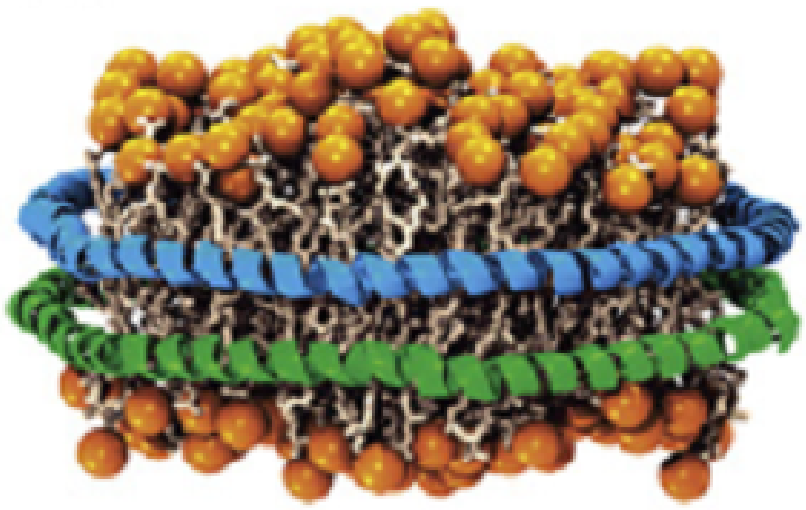

**Master's thesis**

Dennis Pedersbæk

10.08.2017

AALBORG UNIVERSITY
*Students' report*

**Department of**
**Physics and Nanotechnology**
Nanotechnology
Skjernvej 4A
9220 Aalborg Ø

**Title:** Application of Reconstituted High-Density Lipoproteins for Cancer Immunotherapy

**Semester Theme:** Master's Thesis

**Project period:** August 2016 - August 2017

**Name:** Dennis Pedersbæk

**Supervisors:**
Jens Bæk Simonsen
Evamaria Petersen
Thomas Lars Andresen

**Number of pages:** 65
**Appendix (A and B):** 5 pages
**Finished:** 10.08.2017

# Abstract

Drug delivery systems (DDSs) have shown great promise to improve the therapeutic effect of many conventional free drugs. Cancer treatment has been the focus of many DDSs, and as it has been recognised that the immune system has an important role in tumour development, DDSs have also been utilized for cancer immunotherapy to deliver immune modifiers to certain immune cells for stimulation of an immune response against the cancer cells.

The primary focus of this study is high density lipoprotein (HDL), since it has several properties which are advantageous for DDSs, including the small size of approximately 10 nm, the long circulation half-life and high tolerance in humans, as well as the fact that HDLs can be recognised by endogenous receptors. The HDLs can either be isolated from blood or reconstituted from apolipoproteins such as apolipoprotein A-I (apoA-I) and lipids. It is possible to design reconstituted HDL (rHDL) with various lipid compositions and incorporated drugs, thus making the rHDL applicable for various biomedical applications.

Discoidal rHDLs were in this project formulated with apoA-I (purified from human plasma) and with varying lipid composition. It was found that the rHDL could be designed to associate preferably with monocytes in whole human blood, which can be used for cancer immunotherapy by delivering adjuvants to activate the monocytes. It was also possible to obtain a preferred monocytes association when using rHDL with a neutral lipid composition, which is in marked contrast to liposomes, where potentially toxic cationic lipids are required to achieve a similar effect. A toll-like receptor 7 agonist was incorporated as the adjuvant in the rHDL, which resulted in secretion of cytokines effective for an anti-cancer immune response when incubated in whole human blood. It was also found that the rHDLs were capable of delivering antigen to isolated dendritic cells in a way that it could be presented to cytotoxic T-cells that can eliminate cancer cells.

The adjuvant and antigen delivery are important for effective cancer immunotherapy. Hence, although some of the experiments need to be confirmed explicitly by replication, the present study clearly indicates the great potential of using rHDLs in DDSs applicable for cancer immunotherapy.

AALBORG UNIVERSITY
*Students' report*

**Department of**
**Physics and Nanotechnology**
Nanotechnology
Skjernvej 4A
9220 Aalborg Ø

## Dansk resumé

Drug delivery systemer har vist stort potentiale til at forbedre den terapeutiske effekt af mange konventionelle frie drugs, især til at udvikle forbedrede kræftbehandlinger. Eftersom det er blevet anerkendt, at immunsystemet har stor betydning for udvikling af en kræfttumor, er drug delivery systemer også blevet brugt til cancer immunterapi, hvor der benyttes immunaktiverende drugs til at stimulere immunsystemet, så det kan genkende og eliminere kræftcellerne.

Dette projekt benytter high density lipoprotein (HDL) til at udvikle et drug delivery system, der kan bruges til cancer immunterapi. HDL har mange egenskaber, der er fordelagtige for drug delivery systemer, hvilket inkluderer den lille størrelse (∼10 nm), lange cirkulationstid og høje tolerance i mennesker, samt at HDL kan blive genkendt af endogene cellereceptorer. HDL kan enten blive isoleret fra blod eller rekonstitueret fra apolipoproteiner, f.eks. apolipoprotein A-I (apoA-I), og lipider. Det er muligt at formulere rekonstitueret HDL (rHDL) med mange forskellige lipid kompositioner og inkorporerede drugs, hvilket gør det muligt at designe rHDL til mange forskellige biomedicinske applikationer.

Diskformet rHDL blev i dette project formuleret med apoA-I (som var oprenset fra plasma) og med forskellig lipidkomposition. Det viste sig, at rHDL kunne blive designet til at associere fortrinsvis med monocytter i fuldblod. Dette kan udnyttes til cancer immunterapi, hvor man med immunaktiverende drugs kan aktivere monocytterne. HDL med neutral lipidkomposition associerede også monocytterne, hvilket er i stærk kontrast til liposomer, hvor potentielle toksiske kationske lipider er nødvendige for at få lignende effekt. En toll-like receptor 7 agonist (immunaktiverende drug) blev inkorporeret i rHDLen, hvilket resulterede i udskillelser af cytokiner, når de blev inkluderet i fuldblod, hvilket potentielt kunne assistere et anti-cancer immunrespons.

rHDL blev også brugt til at levere antigen til isolerede dendritske celler, og det var muligt for rHDL at levere antigenerne på en måde, så de kunne blive præsenteret til cytotoksiske T-celler, som kan eliminere kræftcellerne.

Både immunaktiverende drugs og antigener er vigtige for et effektiv anti-cancer immunrespons. Selvom det er nødvendigt at gentage flere af projektets eksperimenter for entydigt at bekræfte de observerede effekter, viser studiet dog tydeligt, at der er stort potentiale i at benytte rHDL til cancer immunterapeutiske drug delivery systemer.

# Preface

The Master's thesis is based on work conducted by Dennis Pedersbæk from August 2016 to August 2017, thus it is comprising 60 ECTS. The experiments of the project were conducted at DTU, Technical University of Denmark, at The Colloids & Biological Interface Group (DTU Nanotech), although Dennis Pedersbæk is affiliated with Aalborg University as a student. Evamaria Petersen has been the supervisor from AAU while Jens B. Simonsen and Thomas L. Andresen have been the supervisors from DTU.

The sources that are used in the report will have an assigned number, which will be presented in brackets similar to: [1] when referred to. The list of all sources is found in the bibliography. A reference presented after a full stop refers to the entire preceding section or until interrupted by a previous reference. A reference which only refers to a specific part of the text, will be presented before either the full stop or comma. References in a figure caption refers to the source of the figure. Figures without a reference in the caption are made by the author of the thesis himself. The front figure is from "Evaluation of Reconstituted High-Density Lipoprotein (rHDL) as a Drug Delivery Platform – a Detailed Survey of rHDL Particles ranging from Biophysical Properties to Clinical Implications" by Jens B. Simonsen[1].

Dennis Pedersbæk


## *Acknowledgements*

First of all, I would like to thank Thomas L. Andresen for giving me the opportunity to join the research group to do my Master's thesis, and Jens B. Simonsen for extraordinary daily supervision. Furthermore, a lot of people have assisted with the experiments of the project. Lotte Nielsen gave valuable support with the use of the HPLC system. Both Ditte Villum Madsen and Mie Hübbe conducted the flow cytometry measurements of the project. Martin Kisha Kræmer both synthesised the antigen SIINFEKL, and measured TMX-201 concentration of some samples. Casper Hempel took the TEM image, and Frederik Teudt assisted with the ELISA measurements. They all deserve thanks and acknowledgements for their effort.

# List of abbreviations

**APC**: Antigen Presenting Cell

**ApoA-I**: Apolipoprotein A-I

**BSA**: Bovine serum albumin

**CD**: Cluster of Differentiation

**cDC**: Conventional Dendritic Cell

**CETP**: Cholesteryl Ester Transfer Protein

**CHS**: Monocholesterylsuccinate

**CMC**: Critical Micelle Concentration

**CTLA-4**: T-Lymphocyte Associated Protein 4

**CVD**: Cardiovascular Disease

**DC**: Dendritic Cell

**DDS**: Drug Delivery System

**DMPC**: 1,2-dimyristoyl-*sn*-glycero-3-phosphocholine

**DOPE-PDP**: 1,2-dioleoyl-*sn*-glycero-3-phosphoethanolamine -N-[3-(2-pyridyldithio) propionate]

**DOPG**: 1,2-dioleoyl-*sn*-glycero-3-phospho-(1'-*rac*-glycerol).

**DOTAP**: 1,2-dioleoyl-3-trimethylammonium-propane

**ELISA**: Enzyme-Linked Immunosorbent Assay

**EPC**: 1,2-dioleoyl-*sn*-glycero-3-ethylphosphocholine

**EPR**: Enhanced Permeability and Retention

**FBS**: Fetal Bovine Serum

**FFA**: Free Fatty Acids

**FSC**: Forward Scatter

**HDL**: High-Density Lipoprotein

**HPLC**: High-Performance Liquid Chromatography

**HSA**: Human Serum Albumin

**IDL**: Intermediate-Density Lipoprotein

**IFN**: Interferon

**IL**: Interleukin

**LCAT**: Lecithin Cholesterol Acyltransferase

**LDL**: Low-Density Lipoprotein

**LPS**: Lipopolysaccharide

**mDC**: Monocyte-Derived Dendritic Cell

**MFI**: Mean Fluorescence Intensity

**MHC**: Major Histocompatibility Complex

**OD**: Optical Density

**PBS**: Phosphate-Buffered Saline

**PD-1**: Programmed Cell Death Protein 1

**pDC**: Plasmacytoid Dendritic Cell

**PEG**: Polyethylene Glycol

**PGA**: Poly(glycolide)

**PLA**: Poly(lactide)

**PLGA**: Poly(lactide-*co*-glycolide)

**POPC**: 1-palmitoyl-2-oleoyl-*sn*-glycero-3-phosphocholine

**PTA**: Phosphotungstic Acid

**rHDL**: Reconstituted High-Density Lipoprotein

**SDS**: Sodium Dodecyl Sulfate

**SEC**: Size-Exclusion Chromatography

**SSC**: Side Scatter

**SR-BI**: Scavenger Receptor Class B Type I

**TEM**: Transmission Electron Microscopy

**TLR**: Toll-Like Receptor

**VLDL**: Very Low-Density Lipoprotein

**WHB**: Whole Human Blood

# Contents

# 1. Introduction

Nanotechnology has during the last decades aspired a promising novel discipline in science which is derived from the classical scientific disciplines such as engineering, physics, chemistry, and biology [2]. In 1959 Richard Feymann imagined writing *Encyclopedia Britannica* on a head of a pin, thereby exploring the possibilities of nanotechnology, though the term "Nanotechnology"was not used until 1974 [2]. Since then, there has been an increased interest in nanotechnology, especially as a tool for optimization of electronic chips [2], however, other areas of science have also utilized the manipulation of materials at the nanoscale (arbitrarily defined 1-100 nm), and promising materials are developed in the area of biotechnology and medicine [2,3]. For example, biosensors, which are designed to detect biological analytes, can be develop with nanomaterials to increase their sensitivity as wells as lower their detection limits down to individual molecules [4].

The application of nanotechnology to medicine is termed nanomedicine, and encompasses both therapeutic and diagnostic applications [5,6]. For therapeutic purposes the use of nanoscaled drug delivery systems (DDSs) have aspired as a promising method for treatment of various diseases [5,6,7,8], since the DDSs have the potential to improve many of the pharmacological properties of the conventional drugs, e.g. drug solubility, rapid break-down of the drug *in vivo* and unspecific drug delivery [6,7]. DDSs can be designed to deliver drugs directly to target organs thereby minimizing side-effects associated with drug toxicity to healthy cells [7,9]. It is also possible to deliver two or more drugs with some DDSs, hence, visualisation of the drug delivery can be obtained by co-delivering imaging agents [10]. The DDSs can be designed to alter the pharmacokinetics and biodistribution of drugs as well as to function as a drug reservoir which can release the drug continuously, hence, it is possible to design DDSs for various applications [7].

A DDS can be designed with the purpose only to release drugs in a sustained manner thereby obtaining a prolonged therapeutic effect, e.g. such DDS can be designed using fibers [11], however, many DDSs are designed for intravenous administration, and nanoparticles are often used for these applications [7]. There are several types of nanoparticles which can be used for DDSs, and they can be modified in several ways [5]. The nanoparticles can either encapsulate or be conjugated to the drug, and they can be designed to deliver the drug to a specific target [5,12]. The nanoparticles can protect the drugs from unwanted interactions with the environment, increase the stability of the drugs and they have the possibility to increase the solubility of hydrophobic drugs [9,13].

One of the major focuses of DDSs has been cancer therapy, which has shown great potential [3,6,10], and have resulted in several clinically approved products [10,12]. The traditional cancer treatments such as surgery, radiation and chemotherapy are often associated with threatening side-effects due to toxicity to healthy cells [12]. Hence, much effort have been put into development of DDSs which can deliver chemotherapeutics directly to the tumour thereby avoiding these side-effects [3,5,6].

Alternatively, or complementary, to the traditional cancer treatments is cancer immunotherapy which has aspired as a promising approach for cancer treatment [14]. The tumour microenvironment often suppress an effective immune response against the cancer cells, and the principle of cancer immunotherapy is to stimulate the immune system to overcome this suppression and eliminate the cancer cells [15,16]. There are various methods which can be used for cancer immunotherapy, for example some of the pathways which suppress the immune response in the microenvironment can be blocked [14]. Another interesting approach for cancer immunotherapy is cancer vaccine where tumour antigens are delivered to certain immune cells which then can initiate an immune response against cancer cells [17]. Besides the delivering of antigen, the immune response also needs to be boosted which can be achieved by using adjuvants such as toll-like receptor (TLR) agonists which can trigger the activation of the immune response [17,18]. Nanoparticle based DDSs are promising candidates for both antigen and adjuvant delivering to immune cells [16,17].

The primary focus of this project is the use of reconstituted high-density lipoprotein (rHDL) as they have several advantages over other commonly used nanoparticles for DDSs[19]. The rHDL mimics the biological HDL, which is involved in the natural transport of cholesterol to the liver[1], hence, the potential utilization of the natural transport properties as well as the biocompatibility and biodegradability which should be ensured, illustrates the great potential of rHDLs for DDSs. The rHDL will in this project be utilized in a novel DDS for cancer immunotherapy.

## 1.1 Nanoparticles for drug delivery

In the following sections more insight will be given into some of the approaches used for drug delivery as well as examples of some nanoparticles commonly used for DDSs. Thus, this will give the basic for the subsequent discussion of the potential of using rHDL for DDSs.

### 1.1.1 Passive and active targeting

Nanoparticles can be designed to target the desired site either passively or actively. Passive targeting of tumours often utilize the enhanced permeability and retention (EPR) effect. This phenomenon encompasses two effects[13]:

- **The vascular permeability** of blood vessels around tumours due to a defective endothelium, which is permeable to both smaller and larger molecules, including the nanoparticles. This effect can result in an increased leakage of nanoparticles into the tumour tissue.[13]
- **The enhanced retention** of macromolecules due to poor lymphatic drainage from the tumour tissue. Hence, the nanoparticles will not be cleared from the tumour tissue, and consequently accumulate here.[13]

The principles of the EPR effect are illustrated in figure 1.1. The clinically approved products for cancer treatment are primarily based on this passive targeting though several examples of more complex nanoparticles that can target tumour actively are described in literature[10]. The active targeting involves ligands which can bind specifically to receptors on the cell surface[12]. The ligands can be antibodies, polysaccharides or peptides which, conjugated to the nanoparticles, can bind to certain receptors that are over-expressed on the target cells, e.g. cancer cells[13]. The active and passive targeting can also work in combination where the EPR effect is responsible for the accumulation of nanoparticles in the tumour tissue while the ligands on the nanoparticles are reasonable for the receptor mediated uptake into the cancer cells.

Although these targeting approaches are often considered with respect to a more effective chemotherapeutic cancer treatment, similar targeting principles apply for immunotherapy as well. For example the EPR effect can be utilized when nanoparticles with immune modifiers are to be delivered to the tumour tissue[16]. Immune cells can also be targeted passively by directing them to sites which are rich in specific types of immune cells, e.g. smaller nanoparticles (<100 nm) can more easily enter the lymphatic system and be directed to the

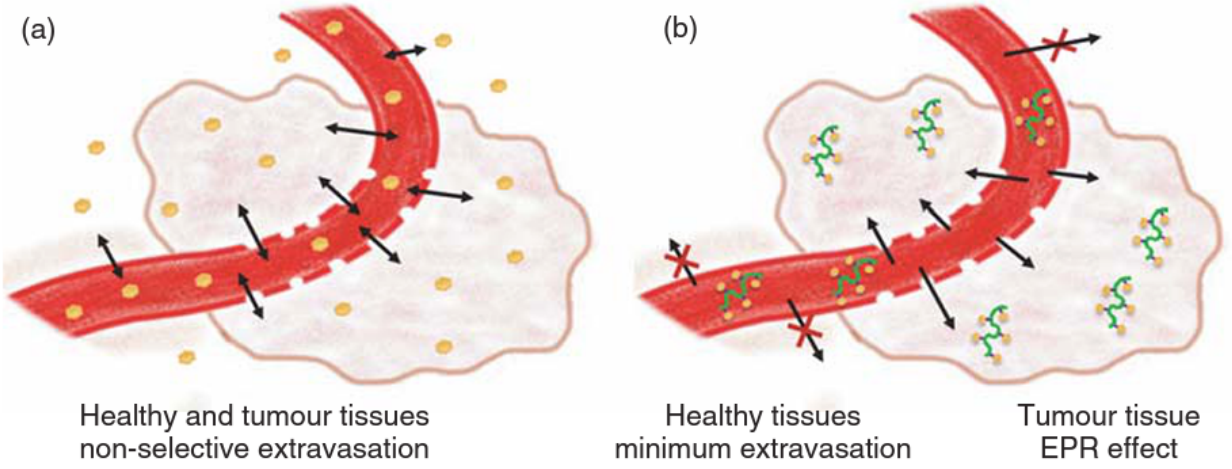


**Figure 1.1:** Illustration of the EPR effect. **(a):** Small molecules, e.g. free drugs, can diffuse freely into both healthy and tumour tissue **(b):** while larger molecules such as the nanoparticles only diffuse through the leaky blood vessels around the tumour tissue and accumulate due to poor lymphatic drainage.[13]

lymph nodes [23]. Furthermore, ligands can be used to actively target receptors that are specific for certain immune cells [16,23].

### 1.1.2 Examples of nanoparticles used for drug delivery

Several types of nanoparticles have shown great potential as carriers in DDSs. The drugs can be incorporated in the nanoparticles and thus improve the therapeutic effect of the drugs compared to conventional free drugs [7]. It is important to consider the biocompatibility and biodegradability when designing nanoparticles for biomedical applications. The biocompatibility ensures that the particles by themselves are nontoxic and do not evoke a immune response while the biodegradability ensure that the particles can be broken down in biological systems [13].

In figure 1.2 three types of nanoparticles are shown. These nanoparticles are commonly used in DDSs, and brief insight into each of them will be given in the following sections. However, it must be kept in mind that there are various other types of nanoparticles which can be used for DDSs, e.g. gold nanoparticles or carbonnanotubes [20]. The use of lipoproteins, and in particular rHDL, which are the primary focus of this project will be discussed in subsequent sections.

#### Polymeric nanoparticles

Figure 1.2 A show a polymeric nanoparticle. It is possible to design polymeric nanoparticles with various polymers, and both hydrophobic and hydrophilic drugs can be incorporated [24]. Synthetic polymers are commonly used as the polymeric material of the nanoparticles, however, natural polymers such as proteins or polysaccharides have also been considered as potential candidates [25]. The large variation in purity of natural polymers and the fact that they often require cross-linking which can denature the drugs have generally made synthetic polymers the preferred choice for drug delivery applications [25]. In order for the polymers to be applicable for biomedical applications, it is required that they are both biocompatible and biodegradable. There are several synthetic polymers which meet this requirement for example poly(glycolide) (PGA), poly(lactide-*co*-glycolide) (PLGA) and poly(lactide) (PLA) [13,24]. The size of the polymeric nanoparticles can be varied between 10 nm to 1000 nm, however, typically the size is approximately 100 nm [13]. The preparation of smaller polymeric nanoparticles are more difficult due to low stability during the polymerization process, which can result in aggregation to larger particles [26].

The polymeric nanoparticles protect the incorporated drugs from interactions with the environment thereby increasing their circulation half-life and making it possible to target the tumour passively by the EPR effect [24]. It is also possible to obtain active targeting by attaching ligands to the surface of the polymeric nanoparticles, though this surface modification would make the preparation more complex which can result in low reproducibility and batch-to-batch variations that consequently can make clinical transition more difficult [24]. The drugs can be released from the polymeric nano-

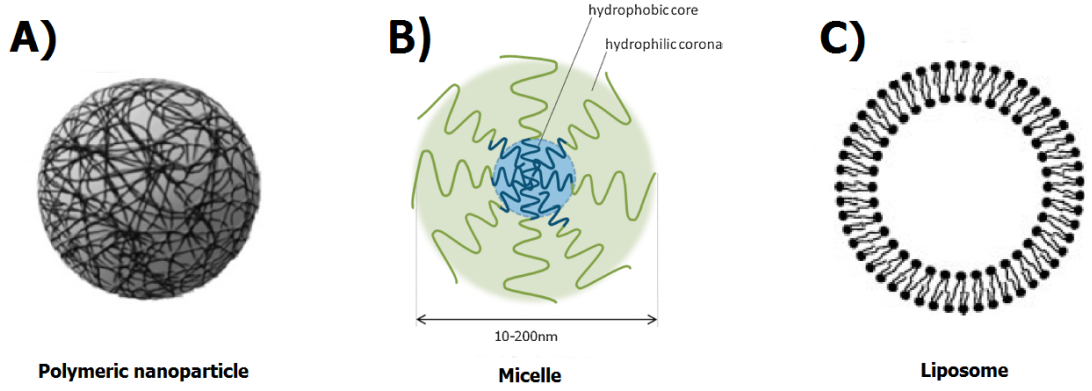


**Figure 1.2:** Illustration of three types of nanoparticles which can be used for DDSs. **(A):** Polymeric nanoparticle (image from [20]) **(B):** Micelle formed from a diblock copolymer (image from [21]) and **(C):** Liposome (Image from [22]).

particles in a sustained manner, and the release profile depends on the type of the used polymer [13]. The release of drug can either be caused by diffusion of the drug molecules through the polymeric matrix or the polymer itself can degrade either via surface or bulk erosion, leading to drug release [13,24]. The possible utilization of both targeting and a sustained release is one of the major advantages of using polymeric nanoparticles [25]. However, in order to prepare the polymeric nanoparticles often toxic solvents are required [25], which might lead to toxicity of the final product if the preparation is not handled carefully. Furthermore, though it is possible to incorporate hydrophilic drugs, there is a risk of a rapid drug leakage when incubating hydrophilic drug loaded nanoparticles with blood [25].

Although the polymeric nanoparticles have shown great potential as carrier in DDSs, there are several limitations which must be kept in mind, and other nanoparticles might be more suitable for some applications.

### Micelles

Micelles, as illustrated in figure 1.2 B, are small soluble particles which consist of amphiphilic molecules such as diblock copolymers or lipids. In aqueous solution the hydrophobic interaction will drive the self-assembly of the amphiphiles into micelles with the hydrophobic part forming the core and the hydrophilic part forming the shell around the core, when the concentration of amphiphilic molecules excess the critical micelle concentration (CMC) [9]. Hydrophobic drugs can be incorporated in the core which obviously improve the solubility issues of hydrophobic drugs [7]. The drug can either be physically entrapped in the core by hydrophobic interactions or chemically conjugated to the hydrophobic part of the polymer prior to assembly into micelles [27].

Typically, amphiphilic block copolymers are used for DDSs. They have a relatively low CMC (in the micromolar range) compared to classic micelles with surfactants or lipids and are able to form micelles smaller than 100 nm [9,27]. The micelles used for drug delivery are typically in the size range of 10-200 nm [28] and have relatively narrow size distribution [29]. The properties of the micelles can be tuned by varying the polymer type or length, e.g. the CMC can vary depending on the length of the polymer chain, and some amphiphilic polymers might not be able to form micelles [9]. The small size of micelles, and the fact that the size easily can be tuned by varying the length of the polymer chains are some of the advantages of using micelles for drug delivery [26]. DDSs using micelles often aim to target the tumour, and due to the small size and the hydrophilic shell, which is typically composed of polyethylene glycol (PEG), they are able to avoid detection by the immune system, thereby obtaining an increased circulation time, which can result in a more effective accumulation in the tumour due to the EPR effect [9,28,29]. The release of drug from the micelles can be tuned by varying the length and type of the hydrophobic part of the block copolymer [28].

The stability of the micelles is another important concern. The micelles will dissemble when below the CMC, which will result in instant drug release [26]. Though, it has been found that polymeric micelles can be relatively stable in serum (with a half-life of approximately 9 hours) [21], there are several parameters concerning the stability which need to be kept in mind when designing novel micelle based drug delivery systems, e.g. disassembly *in vivo* might not correlate with the CMC measured *in vitro*, since protein or cells in the blood might affect the stability of the micelles [21,26].

### Liposomes

A liposome is a spherical vesicle consisting of a phospholipid bilayer that constitutes the shell of the liposome which encapsulate the aqueous interior, as illustrated in figure 1.2 C. The liposome was the first nanoparticle to be researched as potentially nanocarrier for drugs delivery systems [10], and since then a great amount of research has been using liposomes in order to develop effective drug delivery systems, which have resulted in several clinically approved products [30,31]. The basis structure of the liposomes are obviously inspired by nature, since the lipid bilayer morphology mimics the cellular membranes [30]. Hence, the liposomes are generally considered to be safe due to the biocompatibility and biodegradability of the lipids [30].

It is possible both to deliver hydrophilic and hydrophobic drugs with the liposomes since hydrophilic drugs can be incorporated in the aqueous core while hydrophobic drugs can be incorporated in hydrophobic bilayer [13]. The encapsulated drugs are consequently protected from undesired interaction with healthy cells

which could otherwise lead to side-effects[30]. However, there have been some difficulties in retention of some drugs in serum, since serum proteins can affect the release of drugs[31]. This is particularly true for hydrophobic drugs since the permeability through the lipid bilayer is higher for these drugs than hydrophilic drugs[31]. This problem has been addressed by loading the drugs with a pH gradient, e.g. by using a slightly acidic pH in the interior of the liposomes, amines of the drugs can be loaded thus inducing a charge which limits the possibility for drug release through the lipid bilayer, however, the retention of some drugs are still problematic[31].

In order to achieve longer circulation time and minimize the uptake of the liposomes by the immune system, PEGylation, i.e. coating the surface of the liposomes with PEG, is a commonly used approach[24,31]. PEGylation of the liposomes increases their circulation half-time from minutes to hours[27]. These so-called stealth liposomes have especially proven to be useful for passive targeting of tumours by the EPR effect, which have resulted in the clinically approved product Doxil[31]. Active targeting can be achieved by incorporation of ligands to the lipid bilayer. However, the preparation of ligand-targeting liposomes are more difficult to control and can lead to poorly defined systems[31]. Furthermore, the incorporation of ligand can hinder the diffusion to the target tissue, can cause recognition and elimination by the immune system and the targeting ligand can be deactivated by non-specific binding of serum proteins, hence, the ligand-targeting liposomes have had limited clinical success[30].

The liposomes used for drug delivery systems are typically in the range of 50-450 nm[30] with approximately 100 nm sized liposomes commonly used[22]. The preparation of smaller liposomes becomes increasingly difficult, and it is very difficult, if not impossible, to obtain liposomes smaller than 50 nm, due to a required high degree of curvature of the lipid bilayer[26].

Clearly, there are various possibilities to modify and design the liposomes suitable for several applications by changing the lipid composition of the liposomes, PEGylation of the lipids or incorporation of ligands[30,31]. For example it is possible to choose lipids which induce a charge on the liposomes. The charge of the liposomes can affect the interaction with the cells. Furthermore, incorporation of cholesterol in the lipid bilayer will reduce the permeability of the bilayer thereby increasing both the retention of the encapsulated drugs and the stability of the liposomes.[30]

### 1.1.3 Lipoproteins for drug delivery

As the main focus of this project is HDL, a deeper insight into lipoproteins in general and their applications in DDSs will be given initially, followed by a more detailed description of HDL.

Although, it is possible to achieve biocompatibility and biodegradability with the nanoparticles presented in the previous sections, i.e. polymeric nanoparticles, micelles and liposomes, there has been concerns using synthetic nanoparticles due to potentially toxicities issues or immunogenicity[32,33]. Hence, this has inspired the use of biological particles for drug delivery, amongst which the lipoproteins have attached much focus due to their natural transport properties which potentially can be utilized for drug delivery[32]. These properties include accumulation at various important targets and a long circulation time relative to other nanoparticles[32].

Lipoproteins can be divided into four major classes: Chylomicron, very low-density lipoprotein (VLDL), low-density lipoprotein (LDL), and HDL, as illustrated in figure 1.3[32,34]. The size, density, function, lipid composition and the apolipoprotein composition differ between the lipoproteins[34]. The biological function of each lipoproteins is represented in figure 1.4 and discussed below.

Chylomicrons are the largest lipoproteins with sizes ranging from 75 to 1200 nm. Their main function is transfer of dietary fat, i.e. triglycerides, cholesterol and other lipids. The triglycerides are released from the chylomicrons through hydrolysis by lipoprotein lipases which result in free fatty acids (FFA). The lipoprotein lipases are located in muscle and other tissues which requires FFA. The chylomicrons remnants are hereafter taken up by the liver. The VLDL are 30-80 nm in diameter. They are involved in the transport of triglyceride and cholesterol from the liver to the blood, where the triglycerides are delivered as FFA to muscles and other tissues, as it was the case for chylomicrons. The remnants, which are rich in cholesteryl esters, are called intermediate-density lipoprotein (IDL) and are 15-35 nm in diameter. The IDL can either be taken up

by the liver or be converted into LDL by removal of more triacylglycerol. The main functions of the LDL is delivery of cholesterol to the peripheral tissue. Nascent HDL are formed in the peripheral tissue, and can pick up cholesterol, e.g. cholesterol released into the plasma from dying cells or excess cholesterol from the peripheral tissue, and mature into the spherical HDL. The HDL will eventually deliver the cholesterol to the liver. [32,35]

Lipoproteins are known to be important for cardiovascular disease (CVD). High levels of LDL are associated with risk of CVD due to possible formation of atherosclerotic plaques. Therefore, LDL is often referred to as bad cholesterol. On the other hand, HDL can remove cholesterol from the peripheral tissue, thus reducing risk of CVD, hence, it is known as the good cholesterol. Drugs used to treat risk of CVD generally aims to lower LDL levels. One could also imagine that increasing HDL level could be another approach, however, though much effort has been put into the development of such drugs, they have generally not shown therapeutic benefit. [32]

Most DDSs using lipoproteins are based on LDL or HDL, since their circulation time in blood is much longer than the circulation time of the other lipoproteins, e.g. the circulation half-life of chylomicrons is only a few minutes. Furthermore, the penetration into target sites is more efficient with the smaller lipoproteins. Hence, chylomicrons and VLDL are rarely used for DDSs, and will not be discussed further. LDL based drug delivery

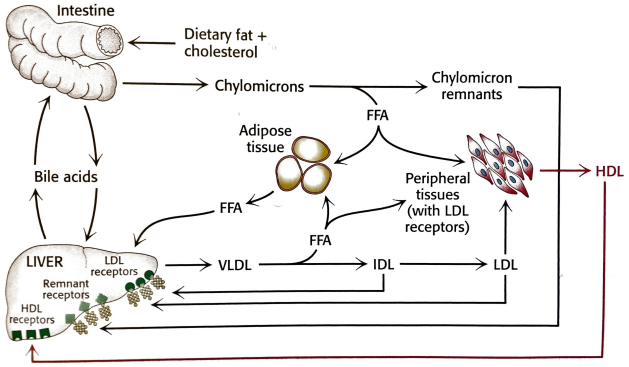


**Figure 1.4:** Simplified illustration of the biological fate of the lipoproteins. [35]

often utilize the fact that LDL can interact with the LDL receptor which are present both on cancer cells and macrophages. Hence, LDL can be used for chemotherapeutic drug delivery to cancer cells or to treat atherosclerosis by delivering drugs to the macrophages at atherosclerotic plaques. The drug can be encapsulated in the hydrophobic core of LDL. Furthermore, targeting ligands can also be conjugated to the LDL thus directing it to different targets which does not necessarily have the LDL receptor. However, the large apolipoprotein B-100 of LDL can irreversibly aggregate when isolated thus making it difficult to modify the LDL for drug delivery. HDL is, in contrast, compromised of smaller apolipoproteins, mainly the apolipoprotein A-I (apoA-I), which can be isolated without aggre-

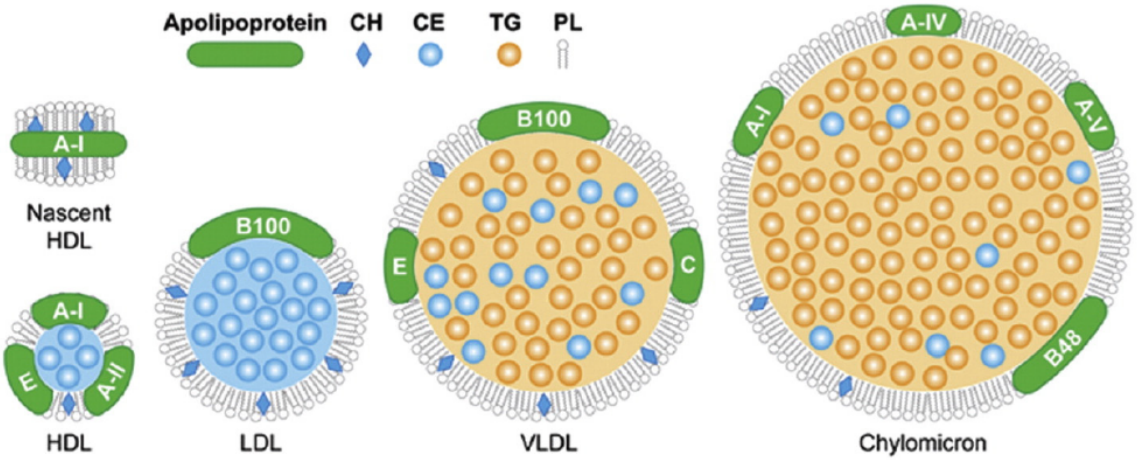


**Figure 1.3:** Illustration of the different types of lipoproteins. The following abbreviations are used: Cholesterol (CH), cholesteryl ester (CE), triglycerides (TG) and phospholipids (PL). The nascent HDL is the discoidal HDL which is the focus of this project. [32]

gation. Hence, HDL can be self-assembled from components making it possible to design and reconstitute it for the specific applications. This is one of the reasons that HDL has attracted most focus as a carrier for DDSs, and it is also the focus of this project. The following sections will consider HDL for drug delivery in more details. [32]

### 1.1.4 HDL particles

In figure 1.3 it was illustrated that there are two forms of HDL. The structure of the HDL differs since the nascent HDL is discoidal while the mature HDL is spherical. As previously discussed, the main function of the HDL particles is believed to be removal of excess cholesterol from the peripheral tissue [19,34]. The biological fate of endogenous HDL is illustrated in more detail in figure 1.5. The apoA-I is obtained from the liver or intestine, which after association with lipids forms the nascent discoidal HDL (referred to as pre-$\beta$HDL in the figure). The discoidal HDL can take up cholesterol which are converted into cholesteryl esters by the lecithin cholesterol acyltransferase (LCAT). The cholesteryl esters are highly hydrophobic and will consequently be internalized into the core of the HDL thereby forming spherical HDL. As more cholesteryl esters are internalized into the HDL, the spherical HDL will increase in size. The spherical HDL can also exchange cholesteryl esters for triglycerides from other lipoproteins through a process mediated by the cholesteryl ester transfer protein (CETP). The spherical HDL will eventually return to the liver where the cholesterol and triglycerides will be delivered through a process mediating by the scavenger receptor class B type I (SR-BI). Note that other lipoproteins such as LDL interact with the liver through the LDL receptor. [19]

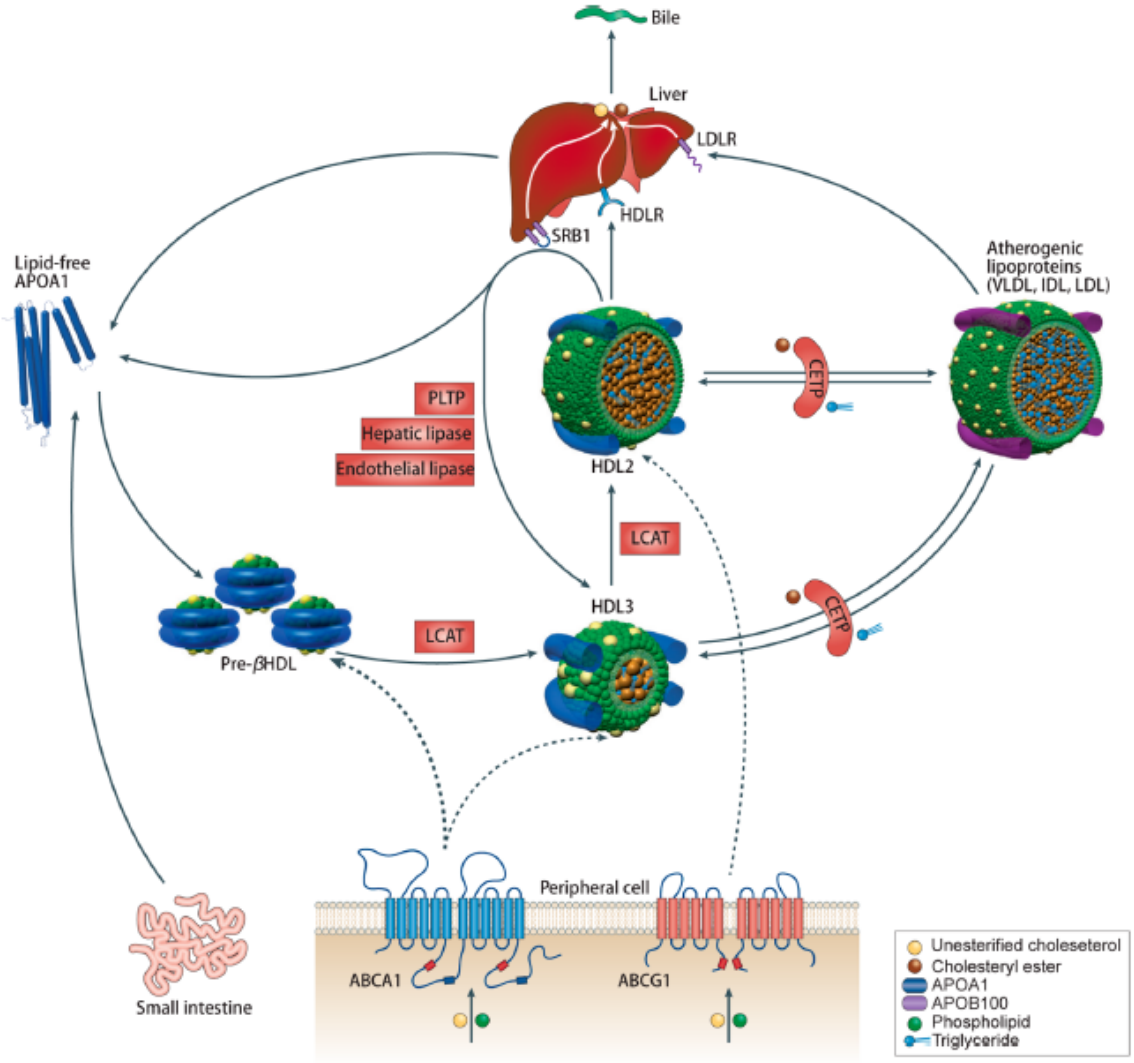


**Figure 1.5:** The biological fate of endogenous HDL. [19]

An illustration of the discoidal HDL, which is the focus of this project, is seen in figure 1.6. The biological discoidal HDL with a size of approximately 9.6 nm is comprised of two apoA-I proteins and a phospholipid bilayer[1]. Mimics of this 9.6 sized HDL is often used for drug delivery applications[1], however, it has been observed that discoidal rHDL with larger sizes can be obtained. These larger sized rHDLs also contained more apoA-I protein per particle, i.e. DMPC/cholesterol rHDLs with diameters of approximately 12, 20, 30 and 40 nm were found to contain 2, 4, 6 and 8 apoA-I proteins, respectively[37].

### 1.1.5 rHDL particles for drug delivery

HDL applicable for drug delivery can either be isolated from human plasma or reconstituted from apolipoproteins and lipids[19]. In order to reduce risk of infectious agents and to ensure reproducibility most research are primarily focussed on using rHDL[38]. rHDL can deliver both hydrophobic and hydrophilic drugs, since hydrophobic drugs can be internalized into the core of the rHDL while hydrophilic drugs can be adsorbed or conjugated to the hydrophilic surface of the rHDL[19]. rHDL particles have several advantages over other particles used for drug delivery systems, e.g. small size (7-12 nm), long circulating half-time (12-24 h) and relatively high tolerability in humans[19]. Furthermore, rHDLs can without surface modifications interact with certain cell receptors, e.g. SR-B1, thereby delivering their cargo specifically to certain targets[1,19]. The SR-B1 receptor is for example often over-expressed in cancer cell, thus allowing for selective delivery of anticancer drug to the cancer cells via this receptor[1,38]. Note that both discoidal and spherical HDL can be recognized by the SR-B1 receptor[32].

As an example of a rHDL based DDS, Ji Wang et al.[36] developed a discoidal rHDL which consisted of paclitaxel, soy phosphatidylcholine and monocholesterylsuccinate (CHS) as well as CHS-modified apoA-I (denoted cP-d-rHDL). They used CHS instead of cholesterol to prevent the transformation to spherical rHDL, since the transformation has been shown to result in drug leakage from the rHDL. As previously discussed, LCAT converts cholesterol into cholesteryl esters which can be internalized in the rHDL causing the formation of spherical rHDL. Hence, since LCAT cannot react with CHS, the transformation to spherical rHDL was diminished. They studied the effect of these cP-d-rHDL and compared them with commercial paclitaxel (Taxol) and CHS-modified paclitaxel-loaded liposomes (denoted cP-liposome). As seen from their result presented in figure 1.7, which shows the concentration of paclitaxel in the tumour, using cP-d-rHDL clearly enhanced the delivering of paclitaxel to the tumour compared to commercial paclitaxel, cP-liposome and the non-modified paclitaxel-loaded rHDL (P-d-rHDL).[36]

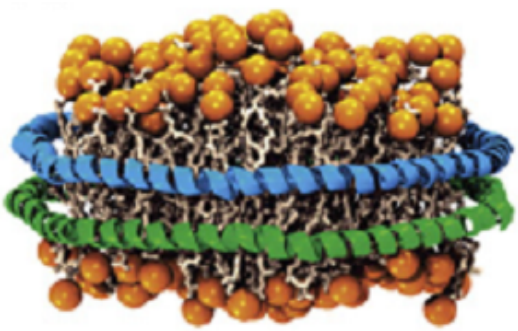

**Figure 1.6:** The discoidal HDL particles which consist of phospholipids and stabilizing apolipoprotein, e.g. apoA-I.[1]

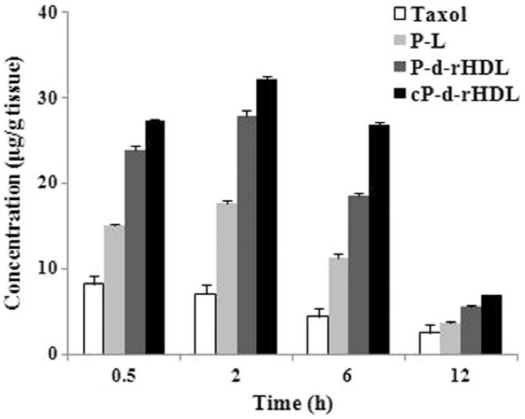


**Figure 1.7:** The results from the study of Ji Wang et al.[36] showing the concentration of paclitaxel in the tumour (human breast cancer cells, MCF-7) after intravenous administration of Taxol, cP-liposome (P-L), P-d-rHDL and cP-d-rHDL in mice models.[36]

## 1.2 Cancer immunotherapy

Some basis aspects of the immune system will initially be described before discussion of cancer immunotherapy. Finally, the use of rHDL for cancer immunotherapy will be addressed.

### 1.2.1 The immune system

The immune system is a complex system designed to protect the body from pathogen entry and destroy these pathogen if they enter the body. Hence, it needs to distinguish between the bodies own cells and foreign pathogenic agents which it needs to eliminate[39]. The immune system is complex and comprises a variety of cells and biological pathways[40]. The following section will only focus on certain types of leukocytes (white blood cells, i.e. immune cells), thus keeping the principles relatively simple, though the complexity of the immune system still have to be kept in mind.

The immune system can be divided into two major categories: the innate and adaptive immunity. The innate immune system provides the immediate defense against infectious agents with both physical (e.g. skin) and chemical barriers (e.g. low pH or digestive enzymes). If the infectious agents have overcome the physical and chemical barriers, the cells of the innate immune systems can respond with short notice. This include phagocytic cells such as monocytes, macrophages and dendritic cells (DCs) which can engulf foreign material. The innate immune system is a nonspecific system which does not provide any memory, i.e. there is not a more effective response during a secondary exposure. In contrast, the adaptive immune system provides a specific response and the response is more effective for secondary exposures. It responds to infectious agents which have entered the body, and it can take days to weeks before the effect of the response becomes apparent. Cells of the adaptive immune system include B-cells and T-cells, which are also called lymphocytes. Activation of a B-cell occurs when it encounters a specific antigen and results in secretion of antibodies. The activated B-cells which secrete antibodies are called plasma cells. The secreted antibodies can bind to the pathogen which eventually can cause elimination of the pathogen. Activation of T-cells requires aid by other so-called antigen presenting cells (APCs). The APCs can be macrophages and DCs which, after phagocytosis of the pathogen, can activate T-cells by presenting pathogen antigens to the T-cells. Hence, the APCs provides an important link between the innate and adaptive immune system.[39,40]

Lymphocytes represent 20-35% of the leukocytes in the blood, while an increased amount of these cells are located in the lymph nodes. It is primarily in the lymph nodes that the APCs present antigen to the T-cells. The APCs, such as macrophages and dendrictic cells, resides mainly in the tissue, but can after phagocytose of foreign material travel to the lymph nodes where they can present the antigen. After activation, the T-cells can leave the lymph nodes to seek for the pathogen expressing the specific antigen. Monocytes are another type of leukocytes. It is the largest of the leukocytes and represent 3-7% of the leukocytes in the blood. Monocytes originate from the bone marrow, and after they enter the bloodstream, they function as phagocytes for a few days. The monocytes can also leave the bloodstream and differentiate into either macrophages or DCs. The DCs derived from monocytes are called monocyte-derived DCs (mDCs), but there are also other types of DCs which include plasmacytoid DCs (pDCs), conventional DC1s (cDC1) and cDC2s. These different subsets of DCs can have different properties and biological functions. Another major class of leukocytes is the granulocytes which encompasses neutrophils, eosinophils and basophils which represent 55-90%, 1-3% and 0.5 % of leukocytes in blood, respectively. The main function of the neutrophils is phagocytosis while eosinophils and basophils are, among other things, involved in the destruction of large eukaryotic pathogens. Note that there are other types of leukocytes but it is beyond the scope of this project to describe all of them in detail.[40,41]

The presentation of antigen to T-cells occurs through the major histocompatibility complex (MHC). There are two classes of MHC proteins, the MHC class I (MHC-I) and MHC class II (MHC-II). The MHC-I are expressed on nearly all cells while the MHC-II are expressed only on APCs. In order for a peptide to be presented by the MHC-II, it requires endocytic uptake and degradation of the corresponding protein, hence, peptides from the cytosol cannot normally reach the MHC-II. On the other hand, peptides expressed on the MHC-I is normally obtained from the cytosol and not

the peptides in the endosomes.[35] However, DCs have the potential to circumvent this general rule, and present peptides from the endosomes to the MHC-I in a process known as cross-presentation[42]. Antigens presented by the MHC-I can signal for cell destruction, e.g. antigens are presented to cytotoxic T-cells through the MHC-I.[35]

An example of the cascade of reactions that happen, when an antigen activates a B-cell or a DC present an antigen to a T-cell, is seen in figure 1.8. As it is evident from the figure, there are several types of T-cells. The antigen can be presented to a T helper cell through the MHC-II. The activated T helper cell can aid the activation of other native T-cells, which can result in secretion of cytokines and differentiation of the native T cells into memory T-cell or effector cells such as cytotoxic T-cells. The activation of cytotoxic T-cells requires antigen presentation through the MHC-I, e.g. from DCs which can cross-present antigens as previously discussed. The activated cytotoxic T-cells can specifically

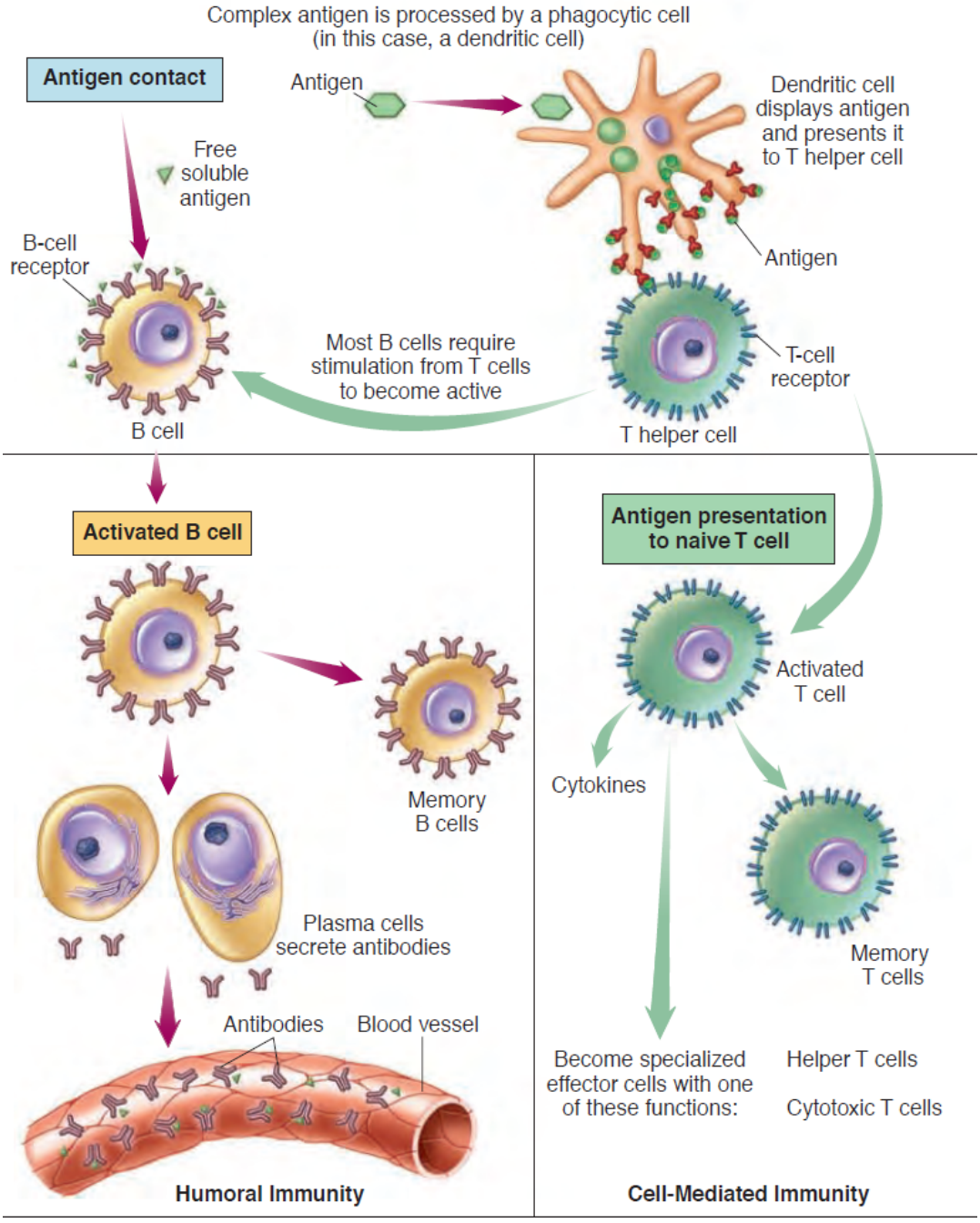


**Figure 1.8:** Illustration of the cascade of reactions and cells involved in initiation of a humoral or cell-mediated immune response.[40]

recognise and eliminate the pathogen. This immune response is called a cell mediated immune response. The T-cell types can be distinguish by certain surface proteins such as cluster of differentiation (CD) receptors, e.g. T helper cells express CD4 while cytotoxic T-cells express CD8. The activated T helper cell can also aid the activation of B-cells, which will result in plasma cells that secrete antibodies. This response is called a humoral immune response. [39,40]

In order to achieve an effective immune response, the secretion of cytokines from the leukocytes are also necessary. Cytokines are a group of molecules which simulate the immune response by binding to cell surface receptors on the leukocytes. They can for example regulate growth and activation of lymphocytes. There are several different cytokines with various functions, however, since the cytokines interleukin-6 (IL-6), IL-10, IL-12p70 and interferon-$\alpha$ (IFN-$\alpha$) are relevant for this project, they will be discussed briefly in the following. [39,40]

**IL-6** can be secreted from a variety of cells including endothelial cells, macrophages and T-cells. It is a pro-inflammatory cytokine which can stimulate the growth of B-cells. However, too much IL-6 is often associated with prolonged and uncontrolled inflammatory, which is one of the characteristics of cancers. Hence, IL-6 is mainly considered to have negative effects in regards to cancer treatment, since it is related to tumour growth and metastasis. [43]

**IL-10** is expressed from many types of leukocytes which include lymphocytes, monocytes and DCs. It is an anti-inflammatory cytokine which consequently is involved in feedback regulation of an immune response. Since it can inhibit the cell-mediated immune response, it can limit the effect of the immune response against cancer cells. [44]

**IL-12p70** is comprised of the subunits IL-12p40 and IL-12p35. It is mainly secreted from monocytes, macrophages and DCs. It has an important role in the development of a cell-mediated immune response, e.g. it is important for the induction of IFN-$\gamma$, another cytokine which is of major importance for the cell mediated immune response, since it improves the antigen presentation to T-cells. Furthermore, IL-12p70 also enhances the activation of cytotoxic T-cells. [44]

**IFN-$\alpha$** can be secreted from several different types of cells including pDCs, monocytes, macrophages and lymphocytes. pDCs are considered to be the primary source of IFN-$\alpha$ since they can secrete large amounts when activated. The secretion of IFN-$\alpha$ from monocytes is for example much less than from pDCs. IFN-$\alpha$ aid the activation of cytotoxic T-cells, and enhance the expression of MHC-I on tumour cells, and are consequently considered to be advantageous for an anticancer immune response. [44,45]

### 1.2.2 Principles of cancer immunotherapy

The primary aim of cancer immunotherapy is to stimulate the immune system to eliminate the cancer cells. A more effective treatment than the conventional cancer treatments such as chemotherapy or radiation, can be obtained by utilizing the specificity of the immune system. Combination of immunotherapy with conventional cancer treatments have also shown great promise for an improved therapeutic efficacy. [46]

There are several approaches which can be used for cancer immunotherapy, and for a better understanding of these, it is relevant to consider how the immune system responds to cancer cells. An overview of possible interactions between the immune system and the cancer cells is seen in figure 1.9. Certain danger signals and tumour antigens can appear after development of cancer cells. Both the innate and adaptive immune systems can respond to these signals, since they can be reconsigned as foreign. For example can tumour antigen be taken up by APCs such as DCs, which can can lead to activation of cytotoxic T-cell that can eliminate the cancer cells. In this case, the tumour is in the elimination phase. As previously discussed, cytokines are important for an effective immune response, and some of the important cytokines for an anti-cancer effect are indicated in figure 1.9, and include IFN-$\gamma$, IL-12 and IFN-$\alpha$. However, the cancer cells can transform to cancer cells which are not recognised by the immune system. The tumour will then enter the equilibrium phase, where the tumour neither grow due to immunological elimination of some cancer cells nor diminishes due to some cancer cells which are not recognised by the immune system. It is only considered to be the adaptive immune system which function in the equilibrium phase. Eventually, more cancer cells can transform, e.g. by loss of the

tumour antigen, and the tumour can enter the escape phase. It is in this phase that the tumour becomes clinically apparent. The tumours microenvironment will now suppress the anti-cancer functions of the immune system. For example by secretion of anti-inflammatory cytokines such as IL-10. Cancer immunotherapy aims to affect this progress and shift to tumour to the elimination phase by initiating a cell mediated immune response. [15]

Some of the used approaches for cancer immunotherapy are as follows:

**Checkpoint blockade**

As evident from figure 1.9, tumour growth is promoted by the expression of certain molecules such as the T-lymphocyte associated protein 4 (CTLA-4) and the programmed cell death protein 1 (PD-1), which inhibits the function of cytotoxic T-cells. The principle of checkpoint blockade is to use antibodies to block these molecules, thus maintaining T-cell function which eventually can cause tumour elimination. This concept has resulted in clinically approved products which are saving lives of many cancer patients. [14]

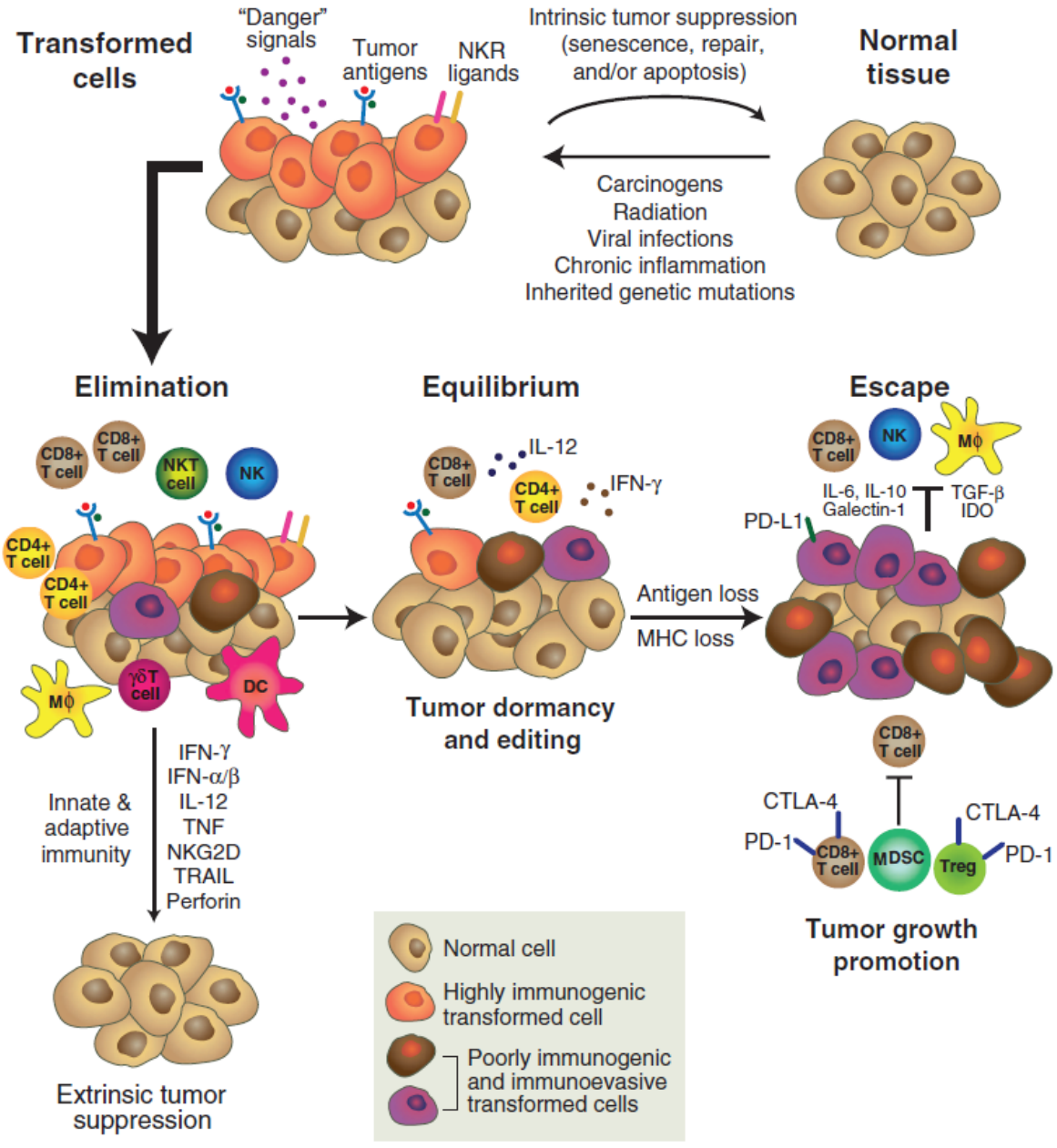


**Figure 1.9:** Illustration of how the immune system can respond to tumour development. [15]

### Cytokine therapy

The importance of cytokines for effective elimination of the tumour is also illustrated in figure 1.9. This has lead to cancer immunotherapy where cytokines are used to boost the immune system. This could be the cytokines IL-2 and IFN-$\alpha$ which are important for the activation of cytotoxic T-cells. Both these cytokines have been FDA approved for cancer treatment. Another approach for cytokine-based therapy could be the neutralisation of anti-inflammatory cytokines such as IL-10.[44]

### Adoptive cell transfer

The principle of this therapy is to remove T-cells capable of fighting the cancer from the patients, grow them *ex vivo* and transfer them back into the patient. The cytokine IL-2 is often injected along with the T-cells, since IL-2 can promote the growth of T-cells. The tissue around the tumour often contain T-cells with anticancer activity, hence, such a tissue sample is taken from the patient and the appropriate T-cells are selected and grown. However, for many types of cancer it is difficult to collect tumour specific T-cells. In order to make the therapy application for more cancer types, some efforts have gone into modifying removed T-cells, which do not have anti-cancer activity, with receptors that do recognise tumour antigen.[14]

### Cancer vaccine

In contrast to other conventional used vaccines, cancer vaccination is therapeutic rather than prophylactic, hence, it would be administered to the patients after the detection of cancer. The therapy has demonstrated potential to completely eliminate solid tumours, thus showing great promise as an effective cancer treatment. The aim of cancer vaccine is to induce tumour specific cytotoxic T-cells. This can be achieved by delivering antigens to DCs which in turn can present the antigens to the T-cells. Note that cross-penetration is required for antigen presentation to cytotoxic $CD8^+$ T-cells if the antigens are taken up by endocytosis. The delivery of antigen to DCs can be achieved either by removing DCs from the patient and culturing them *ex vivo* with tumour specific antigen before injecting them back into the patient, or DCs can be targeted *in vivo* for antigen delivery. The DC targeting *in vivo* often uses nanoparticle based DDSs, and are consequently of most relevance for this project.[14,17]

Besides delivering antigen it is also important to boost the DC activation for an effective cancer vaccination. This can be achieved by using adjuvants such as the TLR agonists[17]. The TLRs can detect pathogenic motifs, and, when activated, they can initiate a proinflammatory response[39]. Administration of free TLR agonists have limitations such as poor cellular uptake, unfavourable biodistribution and can result in secretion of too many cytokines, i.e. cytokine storm, which can cause severe side-effects[19]. Some of these limitation could be avoided by delivering the TLR agnoist with a nanoparticle based DDS[19]. The nanoparticles also have the potential to co-deliver antigen and adjuvant, and since both antigen and adjuvant are required for an effective activation of an anti-cancer immune response, the nanoparticle based DDSs have shown great potential for cancer vaccines[17]. The adjuvant can also be delivered without tumour antigen in order to boost the immune system, which can cause secretion of cytokines important for an anti-cancer immune response, while the antigens can be taken up from dead cancer cells, e.g. cancer cells killed by chemotherapeutic agents[18].

### Examples of nanoparticle based drug delivery systems for cancer immunotherapy

Several types of nanoparticles have been used for cancer vaccine immunotherapy. A few examples will be given below.

Samar Hamdy et al.[47] designed PLGA nanoparticles with encapsulated antigen to actively target the mannose receptor which are present on DCs. When the antigen was delivered to the DCs, they observed antigen specific T-cell activation. The PLGA nanoparticles also have the potential to co-deliver TLR agonists, thereby enhancing the immune response.[47] Similar PLGA nanoparticles have also been used to target other receptors on DCs, e.g. the CD40, for delivery of antigen and TLR agonist[48]. Instead of using polymeric nanoparticles, Thomas C.B. Klauber et al.[49] used liposomes for targeting the dendritic cell immunoreceptor, which are present on DCs and monocytes, to deliver a TLR7 agonist. An effective targeting and resulting cytokine secretion were observed, and they suggest that the liposomes could be co-formulated with antigen or used in combination with other cancer treatments such as chemotherapy or radiotherapy for a more effective treatment.[49]

Pia T. Johansen et al.[50] also used liposomes as carriers in a DDS for cancer immunotherapy. However, they aimed to targeted monocytes and used a TLR7 agonist to stimulate the immune response. The monocyte activation by the TLR7 agonist can cause cytokine secretion, and induce the monocytes to differentiate into DCs which in turn can migrate to lymph nodes and activate T-cell. The TLR7 is located in the endosomes of the monocytes, hence, a endocytic uptake of the liposomes is required. Interestingly, they found that by using a slightly cationic lipid composition in the liposomes, they could target monocytes specifically over lymphocytes and granulocytes. They used POPC as the neutral lipid and DOTAP as the cationic lipid and found that when using 7-10% of DOTAP in the liposomes, 75-95% of the monocytes were associated with the liposomes after one hour of incubation. Although cationic lipids can be toxic, they observed no cytotoxicity when using only low amounts of cationic lipids in the liposomes. They also confirmed that the TLR7 agonist loaded liposomes could initiate an immune response by measuring the cytokines IL-6 and IL-12p40, see figure 1.10, and they proved that the monocytes differentiated into DCs when treated with the TLR7 agonist.[50]

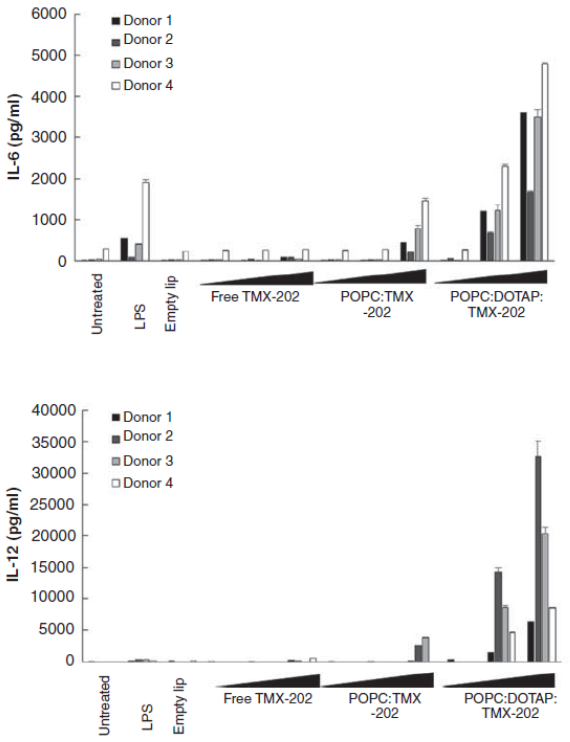


**Figure 1.10:** The results from Pia T Johansen et al.[50] showing that their slightly cationic liposomes could cause an immune response and secretion of IL-6 and IL-12p40 in whole human blood. The lipid composition of the liposomes were POPC:DOTAP:TMX 81:14:5. The used TMX-202 concentrations were of 0.1, 1.0 and 10.0 $\mu$M.[50]

### 1.2.3 rHDL for immunotherapy

The endogenous HDL is generally considered to be anti-inflammatory. This is, among other things, because HDL can bind and neutralize lipopolysaccharide (LPS), which is a potent TLR4 agonist from gram-negative bacteria, thereby minimizing the immune response. HDL can also interact with the TLR4, which recognises LPS, and impair its functions. Furthermore, HDL can remove cholesterol from the cell membranes of macrophages, DCs and lymphocytes which can down-regulate their normal proinflammatory properties, e.g. it can cause a decrease in the expression of the MHC-II in macrophages and DCs which in turn can decrease T-cell activation. The free apoA-I can also induce secretion of IL-10 which can limit the differentiation of monocytes into DCs.[51,52] In contrast to these anti-inflammatory properties of HDL, it has also been found that HDLs can exert an overall proinflammatory from macrophages by causing an increased secretion of cytokines such as IL-12, and reduction in the amount of secreted IL-10. However, this proinflammatory effect seems to be specific for macrophages, and it is recognised by the same study identifying this proinflammatory effect that HDLs do exert anti-inflammatory effects on other leukocytes.[53]

Although, HDLs can exert anti-inflammatory they have various properties which are of major advantage for cancer immunotherapy. This include the fact that they are highly biocompatible and biodegradable with a resulting high tolerance and long circulation time in humans. Furthermore, the size of the rHDL is optimal for delivery to the lymph nodes, and it is possible to deliver multiple drugs, e.g. both adjuvant and antigen.[19]

rHDLs have been used for several types of cancer immunotherapies. For example Maria C. Ochoa et al.[54] used rHDL to optimize cytokine therapy with the IL-15 cytokine. IL-15 aid the activation of cytotoxic T-cells, however, free IL-15 has a short circulation half-life. Hence, in order to increase the circulation half-life, and thereby the therapeutic efficiency of IL-15 treatment, Maria C. Ochoa et al.[54] incorporated IL-15 in

rHDL which resulted in an increased amount of activated cytotoxic T-cells with anti-tumour activity.[54]

Another interesting study by Rui Kuai et al.[55] used rHDL to co-deliver antigen and a TLR9 agonist to the DCs. They formulated discoidal rHDL using apoA-I mimicking peptides instead of the full length apoA-I, and with a lipid composition of DMPC and 4 mol% dioleoyl-sn-glycero-3-phosphoethanolamine-N-[3-(2-pyridyldithio) propionate] (DOPE-PDP). The DOPE-PDP was used to conjugate the antigen to the rHDL, and since the conjugation is reduction sensitive, it facilitates the intracellular release of the antigen in the DCs. They observed effective delivering to the DCs and were able to treat certain types of cancer in mice models. Furthermore, they showed that the treatment could be improved by applying the rHDL in combination with checkpoint blockade treatment, i.e. they used anti-PD-1 and anti-CTLA-4, and they were able to completely eliminate tumours in >85% of the treated mice. Furthermore, they observed an effective rejection of the cancer cells when re-challenging the surviving mice with the same type of cancer 70 days later, illustrating the effective memory of the adaptive immune system, which is evoked during cancer vaccination.[55]

## 1.3 The aim of this project

The project aims to investigate several aspects concerning discoidal rHDL (rHDL will in the following refer to the discoidal rHDL if not stated otherwise). This include the formulation and characterization of rHDL as well as its potential as carrier in a DDS for cancer immunotherapy. Supply of apoA-I is obviously required for the formulation of rHDL, and since the amount of apoA-I in human blood is relatively high, i.e. the concentration of apoA-I in plasma is 1.0-1.5 mg/mL[56], it should be feasible to purify relatively high amounts of apoA-I from human blood. Following the guidelines for purification of apoA-I described elsewhere[57], the purification process will be set up and optimized with the available laboratory equipment, thereby ensuring continuously supply of apoA-I. After the supply of apoA-I is ensured, studies concerning formulation of rHDL will also be conducted.

The main aim of the project is to design rHDL applicable for cancer immunotherapy. Inspired by the results of Pia T. Johansen et al.[50], rHDL with similar lipid composition will be formulated in order to investigate,

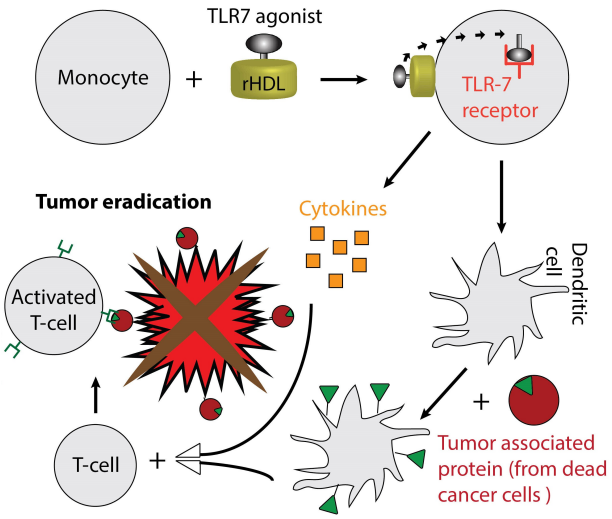


**Figure 1.11:** Illustration of the concept of the project. The rHDL loaded with TLR7 agonist, designed to associate with monocytes, can cause activation of the monocytes which can result in cytokine secretion and differentiation of the monocytes into mDCs. The mDCs can present antigens (obtained from tumour associated proteins) to the cytotoxic T-cells that can eliminate the cancer cells.

if the rHDL can have similar monocyte targeting properties, and, if such properties are found, it might also be possible to deliver the TLR7 agonist to the monocytes. The rHDL might yield an even better delivery due to its smaller size and recognition by endogenous cellular receptors. The concept of the approach is illustrated in figure 1.11. When only TLR7 agonist is used in the rHDL, the possible cancer treatment relies on DCs to take up tumour associated proteins, and present the resulting antigens to the T-cells.

Obviously, rHDLs differ from liposomes and it might not be straightforward to incorporate a positively charged lipid into the particles, since it might interfere with the apoA-I protein, thus hindering the self-assembly of the rHDLs, e.g. it has been found in literature that incorporation of the cationic DMTAP in DMPC rHDL impaired the formation of monodispersed 9.6 nm sized rHDL particles[58]. Hence, it will be investigated if DOTAP can be incorporated in a POPC based rHDL. Note that the overall net charge of the rHDL might not be positive even when DOTAP is incorporated since the apoA-I has a net negative charge around pH 7.4[59]. However, the net charge must be more positive for a rHDL containing DOTAP than a rHDL which only contain neutral POPC.

Other lipids will also incorporate into the POPC based rHDL, namely the anionic DOPG and the cationic EPC. The EPC mimics the POPC better than DOTAP, as it is seen from the chemical structure presented in figure 1.12, hence, it is interesting to study the effect of using EPC as the cationic lipid instead of DOTAP. Furthermore, DMPC rHDL will also be formulated. DMPC differs from POPC by the fact that it is saturated while POPC is unsaturated. This might affect the packing into the rHDL and consequently affect its properties. The structure of the lipids used in the project are illustrated in figure 1.12.

The association of the rHDLs with leukocytes will be studied, and the effect by changing the lipid composition with the aforementioned lipids will be evaluated. Furthermore, it will be assessed if the rHDL with TMX-201, a potent TLR7 agonist, can induce secretion of cytokines effective for an anti-cancer immune response. Experiments will also be conducted to evaluated if rHDL are capable of delivering antigen to DCs such that the DCs can present the antigen by the MHC-I to cytotoxic T-cells.

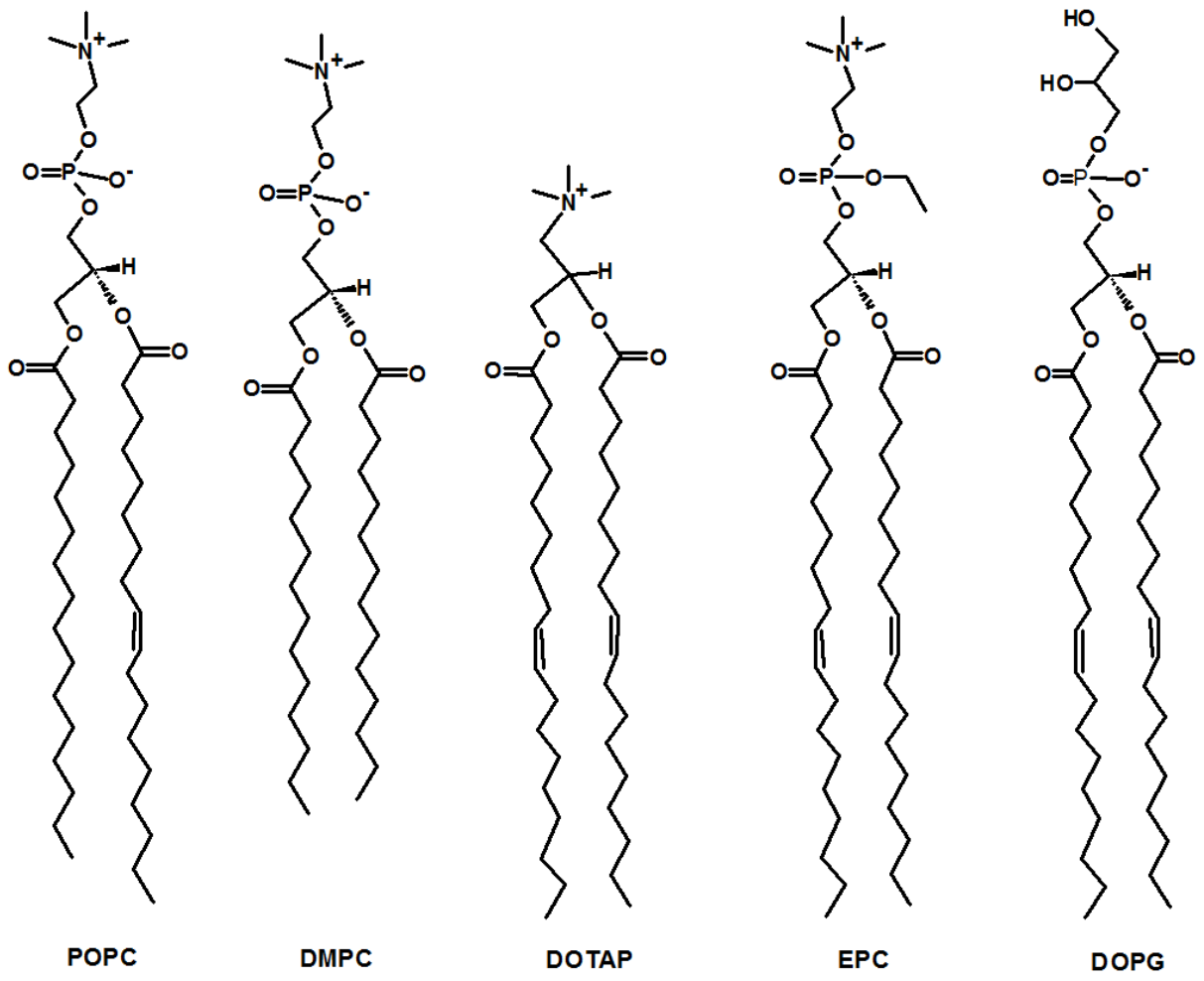


**Figure 1.12:** Structure of the lipids used in the project. POPC and DMPC have no net charge, while DOTAP and EPC are positively charged and DOPG is negatively charged. The full name of the lipids are as follows: **POPC**: 1-palmitoyl-2-oleoyl-*sn*-glycero-3-phosphocholine, **DMPC**: 1,2-dimyristoyl-*sn*-glycero-3-phosphocholine, **DOTAP**: 1,2-dioleoyl-3-trimethylammonium-propane, **EPC**: 1,2-dioleoyl-*sn*-glycero-3-ethylphosphocholine **DOPG**: 1,2-dioleoyl-*sn*-glycero-3-phospho-(1'-*rac*-glycerol).

# 2. Theoretical background of the used methods

Several experiments were conducted during the project, and various methods were used. The basic principles of the methods will be discussed in the following chapter while the subsequent chapter will describe materials and experimental procedures related to each experiment.

## 2.1 High-Performance Liquid Chromatography

High-Performance Liquid Chromatography (HPLC) can be used for the separation of substances in a sample, e.g. it can be used for the purification of proteins as well as analysis of the components in a sample. The sample is applied to the top of a column which consists of beads that can interact with the substances of the sample, thus causing them to be separated and eluted at different times. The separation can depend on properties of the substances such as size and charge. A solvent, i.e. the mobile phase, continuously flow through the column. Note that HPLC is enhanced version of standard chromatography where finer column material is used which allows for more interaction sites and resulting higher resolution, however, it also requires an applied pressure which is why the term high-pressure liquid chromatography is sometimes used for HPLC as well. The eluted substances from the sample can for example be detected by measuring absorbance. The detector is typically located immediately after the column. The elution of proteins can be followed by measuring the absorbance at 220 nm or 280 nm, since the absorbance at 220 nm can be related to the peptide bonds while the absorbance at 280 nm can be attributed to amino acids with aromatic rings, i.e. tryptophan, tyrosine and phenylalanine. Obviously, the signal at 220 nm would often be higher than at 280 nm, but in some cases, the signal at 280 nm can be preferred since the high signal at 220 nm might lower the resolution. The separation methods used by the HPLC in this project will be discussed in the following. [35,60]

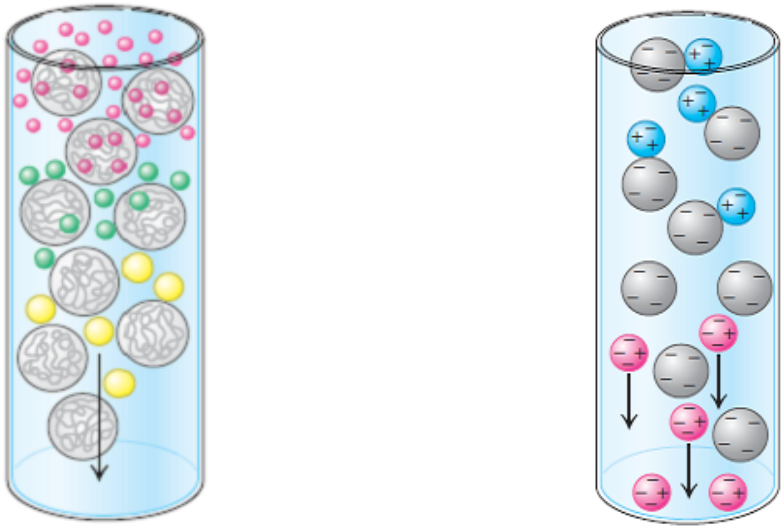

**(A)** **(B)**

**Figure 2.1:** The principles of the columns used on the HPLC system. **(A):** The column for SEC. The larger molecules cannot enter the beads and are therefore eluted sooner than the smaller molecules. **(B):** The column used for cation exchange chromatography. The positive charged molecules bind to the column while the negative charged molecules are eluted. Salt in the mobile phase buffer can be used to elute the bound molecules. Anion exchange chromatography uses similar principles, however, the beads are positively charged, and binds negatively charged molecules. [35]

**Size-exclusion chromatography**

Size-exclusion chromatography (SEC) can be used to separate the substances in a sample according to size. The column consists of porous beads made of insoluble but hydrated polymer. Smaller molecules can enter the beads while larger molecules cannot, thus more volume is accessible to the smaller molecules than for the larger molecules. This results in larger molecules being eluted from the column sooner than smaller molecules. Intermediate sized molecules can occasionally enter the beads and will consequently be eluted at an intermediate position. The principle of the column is illustrated in figure 2.1 A.[35,60]

In this project SEC was used both for the purification of apoA-I and for analysis of the formulated rHDL.

**Ion-exchange chromatography**

Ion-exchange chromatography can separate molecules according to their charge. Positively charged molecules can for example bind to a column consisting of anionic charged beads, while the non-bound negatively charged molecules will be eluted. The bound molecules can be released from the beads by increasing the salt (e.g. NaCl) concentration in the elution buffer. The positively charged ions from the salt (e.g. $Na^+$) will compete with the protein for binding to the column, and since the salt ions have a high density of charge, it will cause the elution of the bound molecules. This process is known as cation exchange chromatography, and is illustrated in figure 2.1 B. Contrarily, anion exchange chromatography columns bind molecules of negative charge using positive charged beads. Note that the pH of the buffers used as mobile phase is important, as it can affect the charge of proteins.[35]

In this project, both cation and anion chromatography were used for the purification of apoA-I.

## 2.2 Electrophoresis

Electrophoresis describes the phenomenon that a molecule with a net charge will move when subjected to an electric field. The method can be used for the analysis of purity in a protein sample, since it can separate proteins according to their size.A polyacrylamide gel is often used as supporting media during electrophoresis due to the fact that it is chemically inert. A voltage is applied over the gel, typically with the anode at the bottom of the gel. The proteins will move in the gel with a velocity that are proportional to the charge, as indicated by the following equation which describes the velocity ($v$) of a molecule with a certain charge ($z$) in an electric field ($E$). $f$ is the frictional coefficient:

$$v = \frac{E \cdot z}{f}$$

The frictional coefficient depends both on the shape and mass of the molecules as well as the viscosity of the gel. The method is known as native page when conducting it under non-denaturing conditions, and it is evident from the above equation that both the size and charge can affect the separation of proteins on a native page.[35]

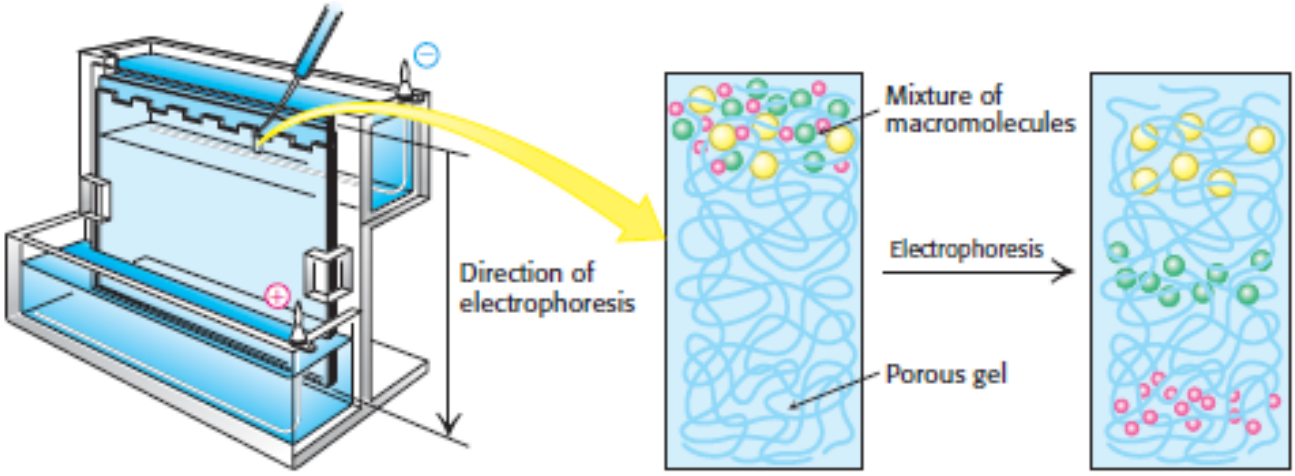


**Figure 2.2:** Illustration of the SDS-page method. The protein samples are pretreated with SDS, loaded to a polyacrylamide gel and a voltage is applied over the gel. The resulting electric field over the gel causes the molecules in the gel to move against the anode. The SDS induces a large negative charge on the proteins making the resulting charge independent of the original charge of the native proteins. Under these conditions, the smaller molecules migrate with a higher velocity than the larger molecules, hence, the proteins can be separated by mass.[35]

In order to separate the protein merely by mass, one can use SDS-polyacrylamide gel electrophoresis (referred to as SDS-page). For this methods, the protein samples are first denatured by sodium dodecyl sulfate (SDS) which is an anionic detergent that disrupt almost all noncolavent interactions. A reducing agent can also be added in order to reduce disulfide bonds. Approximately one SDS anion for every two amino acids residues binds to the denatured protein. This means a large negative charge will be added to the protein by the binding of SDS, and since this charge is usually much greater than the charge of the native protein, the charge of the complex is essentially determined by the amount of bound SDS which in turn is proportional to the mass of the protein. Obviously, the charge will then be higher for the larger proteins, however, larger protein will also have a higher frictional coefficient. The increase in frictional coefficient will decrease the velocity more than the additional charge will increase it, hence smaller proteins will migrate with higher velocity through the gel than larger proteins, thus resulting in separation by mass as illustrated in figure 2.2. [35]

The proteins can be visualized as bands in the gel after the separation by staining them with for example coomassie blue. Staining with coomassie blue allows for the detection down to 0.1 $\mu$g protein [35]

SDS-page was used in the project for the analysis of fractions collected during the purification of apoA-I. Also, it was used to assess the purity and yield after each purification step. Native page was used for the analysis of rHDLs with different lipid composition.

## 2.3 Transmission Electron Microscopy

Transmission Electron Microscopy (TEM) can be used to image a sample. It uses an electron beam which can be absorbed or scattered in all directions when it hits the sample. TEM detects the electrons transmitted through the sample, and a contrast will appear because of the difference in electron density between the substances in the sample and the surrounding media. The short wavelength of electrons makes it possible to visualise nanosized structures. [62]

In order to achieve better contrast, it is possible to stain the samples. There are two possibilities for staining the samples, either using a stain that bind to the specimens in the samples or a stain that provides contrast around the specimens, referred to as positive and negative staining, respectively. Heavy metal salts can be used for the stains, since they scatter electrons more strongly than lighter atoms in for example proteins or lipids, thereby providing improved contrast. [63]

For this project TEM was used to characterize the size of the rHDL, and negative staining was used to improve the contrast.

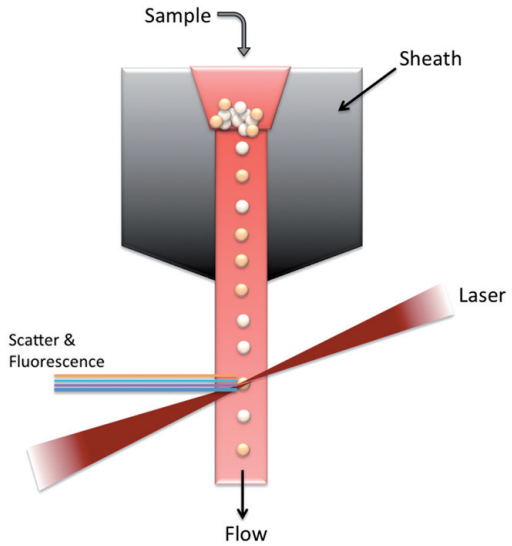


**Figure 2.3:** Illustration of the flow cytometry principles. Single cells pass through the laser beam while the scattered light and the fluorescence are measured. [61]

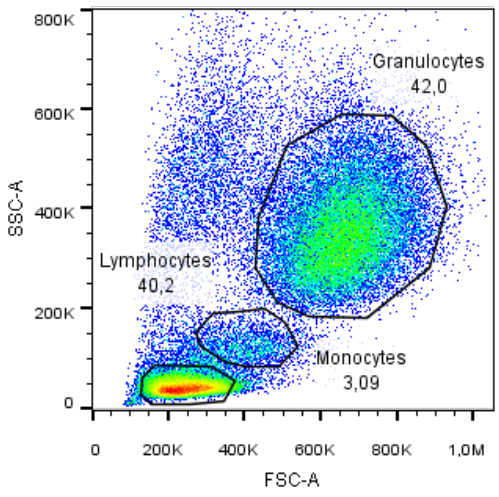


**Figure 2.4:** Illustration of a dual-parameter histogram with FSC and SSC from a flow cytometric analysis of a human blood sample. It can be used to distinguish between granulocytes, lymphocytes and monocytes. (Data from experiments of the project)

## 2.4 Flow Cytometry

Flow cytometry can be used to measure optical and fluorescence properties of single cells or particles. The set-up is illustrated in figure 2.3. A flow cytometer is designed in such a way that cells pass through a laser beam one by one. The light from the laser beam is scattered by the cells, and since the scattering depend on the structural and morphological properties of the cell, it is possible to obtain valuable information by measuring the light scattering. The light scatter can be divided into forward scatter (FSC) and side scatter (SSC). FSC is proportional to the size of the cell while the SSC is related to the internal complexity of the cell, hence, the scattered light can be used to identify different cell types. This effect is illustrated in figure 2.4, which in a dual-parameter histogram shows how granulocytes, lymphocytes and monocytes can be distinguish using only FSC and SSC. Fluorescence can also be detected, and by using a fluorescence marker for a specific cell type, e.g. by conjugation of the fluorescence marker to an antibody specific for the cell type, it is possible to obtain an even better identification of the cells. Furthermore, fluorescence from particles associated with the cell can also be detected. [61]

A variety of information can be obtained during the flow cytometry analysis since several fluorescence markers can be used. In order to analyse the data, it is necessary to set gates based on some characteristics of the analysed cells, thus resisting the further analysis to cells displaying these characteristics. A fluorescent marker can for example be used to assess if the cells are alive or dead, and the gate can be set such that the following analyses are resisted to cells which are alive. [61]

In this project flow cytometry was used to determine the association of different formulation of rHDLs with granulocytes, lymphocytes and monocytes. Furthermore, it was used to assess the antigen presentation by DCs when delivering antigens to isolated DCs with the rHDLs. The association of rHDLs in each cell type were studied by measuring the fluorescence signal from the incorporated fluorophore atto488.

## 2.5 ELISA

Enzyme-linked immunosorbent assay (ELISA) can be used to quality the amount of proteins/peptides, i.e. antigen, in a sample by using antibodies which specifically recognise the antigen. There are several types of ELISAs, and one of these is the sandwich ELISA, as illustrated in figure 2.5. For this method monoclonal antibodies specific for the antigen are adsorbed to the bottom of a well. The antigens will bind to the antibodies when they are added to the well, while the rest of the substances in the sample can be washed out. Enzyme linked antibodies which can bind to the antigens are then added. Unbound antibodies are hereafter removed by washing the well. The enzyme can catalyse a colorless substrate into a colored product, hence, when the colorless substrate is added a color can appear due to the enzyme catalysed reaction. The rate of color formation is proportional to the amount of enzyme linked antibody present which obviously will be proportional to the amount of antigens, thus allowing for quantitative estimation of the antigen by measuring absorption of the well. [35]

In this project, sandwich ELISA was used to assess the cytokine secretion in whole human blood (WHB) after treatment with rHDLs loaded with a TLR7 agonist.

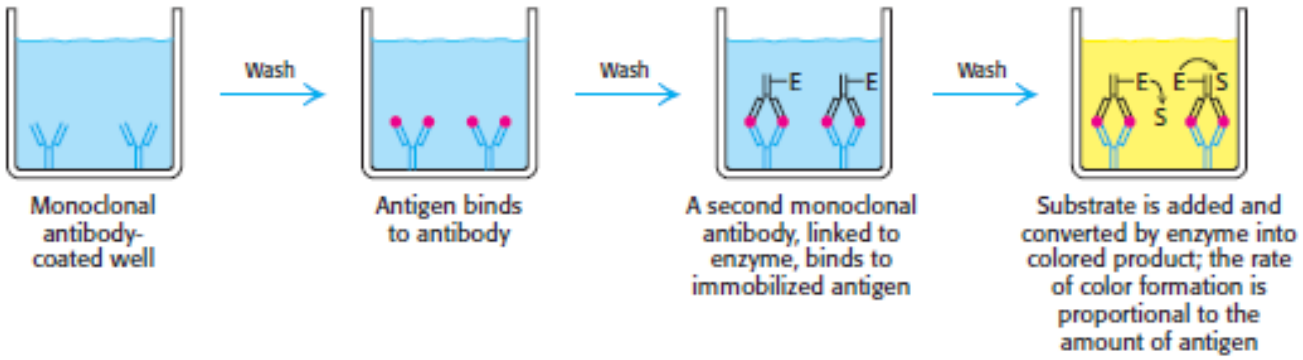


**Figure 2.5:** Illustration of the sandwich ELISA method. [35]

# 3. Materials and Methods

## 3.1 Purification of apoA-I

The purification of apoA-I was conducted in order to ensure supply of apoA-I for formulation of rHDL. The used purification process was similar to procedures described elsewhere[64], though it was optimized over several runs of the experiments. The description of the purification process in the following section is based on the optimized process.

### Materials

Human plasma was supplied from RegionH Blodbank, Hvidovre Hospital (Denmark). Affi-Gel® Blue Media supplied from Bio-Rad (USA). Phosphate-buffered saline (PBS) tablets and sodium cholate were supplied from Sigma Aldrich (Denmark). Several buffer solutions were used for the purification and these are presented in table 3.1. Reference to the used buffers will be made based on the notation in the table. Every components used for the buffers were supplied from Sigma Aldrich. All buffers were filtrated through a 0.45 $\mu$m Cellulose Nitrate Membrane filter from Whatman (Germany).

### Experimental Procedure

An overview over the purification steps are seen in figure 3.1. A HPLC system from Shimadzu was used throughout the purification process, and the volume shift of the fraction collector on the HPLC system was determined experimentally before using it for the purification, see appendix A. The purification steps will be described in more details below.

- The human plasma was thawed and 1 M $CaCl_2$ was added to the plasma so that it yielded a final concentration of 10 mM $CaCl_2$. The solution

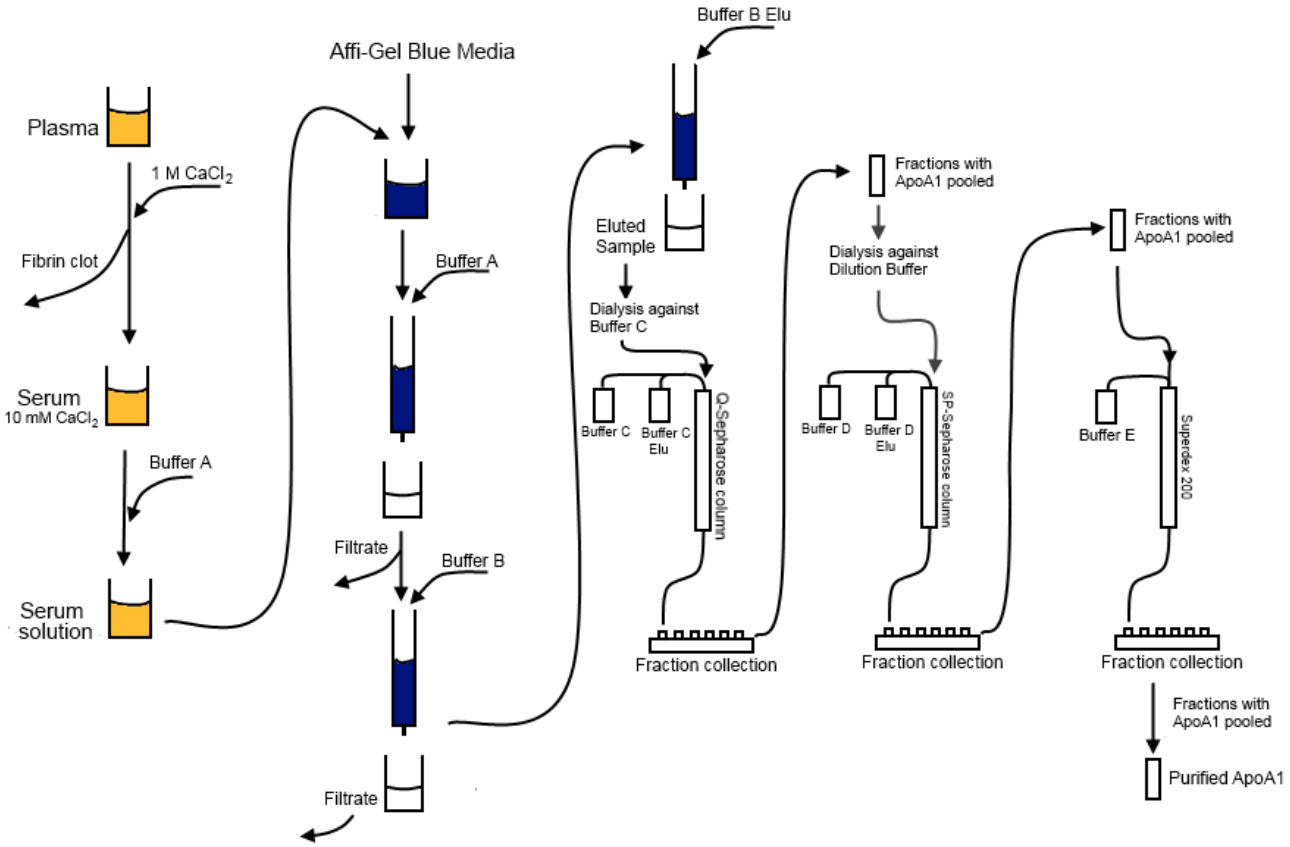


**Figure 3.1:** Overview over purification steps used to purify apoA-I.

was left for 2 hours with occasional stirring. This caused the fibrin clot to aggregate, allowing for easy removal hereof. In order to ensure that all the fibrin clot was removed, the samples was centrifuged (4500g for 20 minutes at 4 °C), and the supernatant was collected. By removing the fibrin clot, serum was obtained.

- The serum was diluted, 1 part to 3 parts of buffer A. The obtained solution was added to approximately 100 mL of Affi-Gel® Blue Media which contains beads that can bind the hydrophobic moieties of apoA-I. Albumin is also known to bind to the beads, however, the high NaCl concentration of buffer A should release the albumin. The solution was left overnight at 4 °C with gentle stirring. The next day, the solution was poured into a column, as seen in figure 3.2, and the beads were washed herein with buffer A until the absorbance of the filtrate at 280 nm was less than 0.025. The beads were then washed with buffer B (200 -300 mL) in order to remove the high salt concentration. The beads were removed from the column and stored in buffer B elu overnight at 4 °C with gently stirring. Since buffer B elu contains the detergent cholate, it should release apoA-I from the beads. After being stored at room temperature for 2-3 hours the following day, the solution was once again added to the column, and the filtrate was collected until the absorbance hereof at 280 nm again was so low that the majority of apoA-I presumably had been released and collected. The collected batches which had significant absorbance at 280 nm were pooled, and further concentrated by spinning through a centrifugal filter unit with a molecular weight cut-off of 10,000 Da. The volume of the concentrated sample was approximately 50 mL.

- The solution was dialysed against buffer C in order to exchange triton X-100 and cholate. The obtained solution was loaded to a HiPrep Q FF 16/10 column from GE Healthcare (will be referred to as Q-Sepharose column in the following) using the HPLC system. The Q-Sepharose column is an anionic column and should thus bind the anionic moieties of apoA-I, which are present at pH 8. The column was prewash with Buffer C. After loading the column and washing with two

**Figure 3.2:** The column used for the purification steps using Affi-Gel® Blue Media.

| Buffer | Composition | pH |
|---|---|---|
| Buffer A | 50 mM Tris<br>1 mM $CaCl_2$<br>3 M NaCl<br>5 mM EDTA | 8.0 |
| Buffer B | 50 mM Tris<br>1 mM $CaCl_2$<br>5 mM EDTA | 8.0 |
| Buffer B Elu | 50 mM Tris<br>1 mM $CaCl_2$<br>5 mM EDTA<br>5 mM Sodium Cholate | 8.0 |
| Buffer C | 20 mM Tris<br>1 mM $CaCl_2$<br>5 mM EDTA<br>0.1% Triton X-100 | 8.0 |
| Buffer C Elu | 20 mM Tris<br>1 mM $CaCl_2$<br>5 mM EDTA<br>0.1% Triton X-100<br>1 M NaCl | 8.0 |
| Buffer D | 25 mM Potassium Acetate<br>1mM EDTA<br>0.1% Triton X-100 | 5.0 |
| Buffer D Elu | 25 mM Potassium Acetate<br>1mM EDTA<br>0.1% Triton X-100<br>1 M NaCl | 5.0 |
| Buffer E | 20 mM HEPES<br>100 mM NaCl<br>1 mM EDTA<br>20mM Cholate | 8.0 |
| Dilution buffer | 100 mM Potassium Acetate<br>1 mM EDTA<br>0.1% Triton X-100 | 5.0 |

**Table 3.1:** Overview over the used buffers. Note that the percentage of Triton X-100 is given with respect to volume.

column volumes of buffer C, apoA-I was eluted using a linear gradient with Buffer C elu (over five column volumes). Fractions of 2 mL were collected during the applied gradient. Based on the chromatogram obtained during the elution, fractions of interest were chosen and analysed further by SDS-page. The fractions which contained apoA-I were pooled and diluted in dilution buffer in order to obtain a volume suitable for dialysis. The sample was hereafter dialysed against the dilution buffer.

- The sample was then loaded onto a HiPrep SP HP 16/10 column from GE Healthcare (will be referred to as SP-Sepharose column in the following), which is a cationic column and should thus bind the cationic moieties of apoA-I which are present at pH 5. The column was prewashed with buffer D before the sample was loaded. After the sample was loaded, it was washed with two column volumes of buffer D, and the bound apoA-I was eluted with a linear gradient of buffer D Elu (over five column volumes). Fractions of 2 mL were collected. Fractions of interest were analysed by SDS-page and the fractions which contained apoA-I were pooled and concentrated.
- The sample was then applied to the Superdex 200 Increase 10/300 GL from GE Healthcare (will be referred to as Superdex-200 column in the following), which is a SEC column that separates the proteins by size. Fractions of 1 mL were collected. Fractions of interest were analysed by SDS-page, and the fractions which contained apoA-I were pooled. This yielded the final purified apoA-I.

## 3.2 Electrophoresis

Electrophoresis was conducted both under denaturing conditions (SDS-page) and non-denaturing conditions (native page). The same set-up was used for the experiments (XCell SureLock™ Mini-Cell Electrophoresis System), but the experimental approach and used materials differed, hence, the methods will be described separately in the following.

### 3.2.1 SDS-page

SDS-page was used continuously throughout the purification of apoA-I, both to estimate if the fractions collected from the HPLC system contained apoA-I, and to evaluate the purification process.

**Materials**

The used gels were NuPage® Novex® 4-12% Bis-Tris Gel, the running buffer was NuPAGE® MOPS SDS Running Buffer and the ladder was PageRuler™ Prestained Protein Ladder, all supplied by Thermo Fisher Scientific (Denmark). The SDS sample buffer was supplied from Sigma Aldrich. The used coomassie stain was primarily SimplyBlue™ SafeStain from Thermo Fisher Scientific, however, for some of the experiments a coomassie blue stain solution was prepared using 0.1% Brillant Blue G (w/v), 25% methanol (v/v), 5% acetic acid (v/v) and 70% milli-Q water (v/v), and a destain solution prepared using 25% methanol (v/v), 5% acetic acid (v/v) and 70% milli-Q water (v/v). All components for this coomassie blue stain and destain solution were supplied from Sigma Aldrich.

**Experimental Procedure**

The SDS-page experiments were conducted as follows:

- The sample and sample buffer were mixed (4:1) in an eppendorf tube
- The solutions were heated to 90 °C for 10 minutes
- The running gel buffer was poured over the set-up and the solutions were added to the wells.
- Electrophoresis was run at 150 V for approximately 75 minutes
- The gel was removed from the set-up and stained in the stain solution for 1 hour.
- The stain solution was removed. When using SimplyBlue™ SafeStain, the gel was washed with deionized water and left to destain in water overnight. When using the prepared coomassie blue stain solution, the gel was left in the prepared destain solution overnight.
- The destain solution was removed and pictures of the gel were taken. For some of the gels a Li-Cor Odyssey FC was used to image the gel.

The software imageJ was used to plot the intensity of the different lanes. Since a linear correlation between the integral measured over the peaks and the different concentration of apoA-I was found (see appendix A), minimum two samples of apoA-I with known concentrations were used in each experiment to estimate the amount of apoA-I, though it might be a very accurate estimate.

### 3.2.2 Native page

The native page is run under non-denaturing condition, hence, it should be possible to investigate assembled rHDL. This was used to assess if the charged lipids were incorporated in the rHDL.

#### Materials

The used gels were NuPage® Novex® 4-12% Bis-Tris Gel from Thermo Fisher Scientific. The running buffer contained 25 mM Tris base and 192 mM glycine. The sample buffer contained 310 mM Tris-HCl, 0.05% bromophenol blue and 50% glycerol. All components for the running buffer and sample buffer were supplied from Sigma Aldrich. SimplyBlue$^{TM}$ SafeStain from Thermo Fisher Scientific was used for staining.

#### Experimental Procedure

The native page protocol was as follows:

- The sample and sample buffer were mixed (4:1) in an eppendorf tube
- The running gel buffer was poured over the set-up and the solutions were added to the wells.
- The gel was run at 150 V until the front was at the bottom of the gel (approximately 6 hours)
- The gel was removed from the set-up and stained for 1 hour in the stain solution.
- The stain solution was removed and left to destain in deionized water overnight.
- The next day, the gel was removed from the water, and imaged using the Li-Cor Odyssey FC.

## 3.3 Formulation of rHDL

The rHDLs were formulated with both purified and supplied apoA-I. The lipid composition was varied by variation of the lipid type and lipid/protein ratio.

#### Materials

The supplied apoA-I was obtained by recombination methods and supplied by another research group, while the purified apoA-I was obtained as described in section 3.1. The used lipids (POPC, DMPC, DOTAP, EPC and DOPG) were all supplied from Avanti Lipids Polar (USA). Bio-Beads were obtained from Bio-Rad Laboratories (Dominican Republic). Sodium cholate hydrate was supplied from Sigma Aldrich. DOPE-atto488 and TMX-201 were supplied from ATTO-TEC (Germany) and PRC Ticinum Lab (Italy), respectively.

#### Experimental Procedure

It is possible to formulate rHDL by several methods. In this project, the detergent depletion method was used. The method was performed as follows:

- Lipid stock solutions of 25 mM were obtained by dissolving the lipids in PBS buffer containing 50 mM sodium cholate. DOPE-atto488 and TMX-201 were similarly dissolved in cholate.
- The lipids were mixed with the apoA-I solution such that the final lipid concentration was 2.5 mM as standard, however, in some of the experiments the final lipid concentration was higher.
- The Bio-Beads were added to the samples. The used mass (in mg) of Bio-Beads was approximately 60% of the volume of the sample (in $\mu$L).
- The samples were stored overnight at 4 °C with gentle shaking of the eppendorf tubes. For some of the experiments, the samples were stored at room temperature.
- The Bio-Beads were removed from the sample by attaching the eppendorf tube that contained the sample to the top of a falcon tube with a hole cut in the lid, see figure 3.3. By centrifugation (2500 rpm for 3-5 minutes) the liquid was spun into the falcon tube while the beads remained in the eppendorf tube.

SEC with the Superdex-200 column was used to characterize the obtained rHDL. The volume of the column was 24 mL, the used flow was 0.5 mL/min and each run was set to 50 min. The mobile phase was PBS buffer, and UV response at 280 nm was detected.

**Figure 3.3:** The set-up used to remove the Bio-Beads from the sample by centrifugation.

## 3.4 Transmission Electron Microscopy

The sample was added onto the grid (∼3 $\mu$L) and was left for 1 minute before excess solution was removed with filter paper. A 1% phosphotungstic acid (PTA) used for negative staining was hereafter added onto the grid (∼3 $\mu$L) and left there for approximately 3 minutes before removing excess stain solution with filter paper. The grid was now ready to be loaded into the TEM apparatus and imaged. The TEM images were taken by Casper Hempel, postdoc in the research group, and are printed with his permission.

## 3.5 rHDL association with leukocytes

The main aim of these experiments were to design rHDL for targeting of monocytes in whole human blood (WHB). The measurements were based on flow cytometry to detect the leukocytes and the associated rHDL. Granulocytes and lymphocytes were detected based on their morphology using FSC and SSC, while CD14 staining was used for the detection of monocytes. The fluorescence from atto488 incorporated in the rHDL was used to detect the rHDL.

### Materials

WHB from donors were tapped in Hiruidin tubes. PBS, PBS/FBS mixture (PBS + 1% Fetal Bovine Serum) and the human IgG used for blocking were supplied from Sigma Aldrich. CD14 antibody (CD14-APC Mouse $IgG_{2a,\kappa}$) and lysis buffer were supplied from BD Bioscience (USA).

### Experimental Procedure

The formulated rHDLs were mixed with RMPI media to yield a concentration of 2.5 mM lipids. The solution with rHDL and RMPI media was then mixed with 200 $\mu$L blood and incubated for 1 hour. Hereafter, the samples were centrifuged (200 g for 5 minutes) and the supernatant was removed. The samples were incubated with lysis buffer (diluted 10 fold prior the addition to the samples) for 15 minutes in order to lyse the red blood cells, before being washed twice with PBS/FBS mixture. This process using lysis buffer was repeated, however, the samples were only incubated for 5 minutes with the lysis buffer the second time. The IgG solution (diluted 25 fold from the stock) was added to the samples for blocking in order to avoid unspecific binding. The samples were transferred to a 96-well plate and the CD14 antibody (10 $\mu$L) was added to each sample. After being stored for 30 minutes on ice, the plate was spun (400 g for 8 minutes) and supernatant was removed. Two washing steps using PBS/FBS mixture for the first wash and PBS for the second wash were conducted. Finally, 100 $\mu$L PBS was added, and the flow cytometry analysis was run (using Gallios$^{TM}$ Flow Cytometer). The measurements were in practice conducted by Ditte Villum Madsen, PhD student in the research group, and the gating strategy was also set by her. All figures from the experiments are printed with her permission.

## 3.6 Antigen delivery to dendritic cells

The model antigen SIINFEKL is used for these experiments since the expression of this antigen on the MHC-I can be detected using a specific antibody. The cholesterol-anchored SIINFKEL has to be processed by the DCs in order for the MHC-I:SIINFEKL complex to be recognised by the antibody. The measurements were based on flow cytometry which could be used to detect this antibody as well as distinguish between different types of DCs using other antibodies. The amount of rHDL associating with the cells were assessed by detection of fluorescence from atto488 which was incorporated in the rHDL.

### Materials

The cholesterol-anchored SIINFEKL was synthesized by Martin Kisha Kræmer, PhD student in the research group. The live/dead marker (eBioscience$^{TM}$ Fixable Viability Dye eFluor$^{TM}$ 780) was supplied from Thermo Fisher Scientific, the antibody specific for MHC-I:SIINFEKL (APC anti-mouse H-$2K^b$ bound to SIINFEKL) was supplied from BioLegend (USA), and the FC block solution was supplied from BD Bioscience.

### Experimental Procedure

One million purified DCs from a splenocyte suspension were seeded in 1 mL medium for each sample to be tested. The medium with cells was distributed in a 24-well plate, the rHDL samples were added and the samples incubated overnight. The next day, the cells were stained with a live/dead marker (diluted 1000 fold from stock), before adding the FC block solution, which were used to block unspecific binding. Finally, the antibo-

dy specific for the MHC-I:SIINFEKL as well as other antibodies used to recognise the different types of DCs were added to the samples, and the analysis by flow cytometry was conducted. These measurements were conducted by Mie Linder Hübbe, PhD student in the research group, and the gating strategy was also set by her. All figures from the experiments are printed with her permission.

## 3.7 Study of cytokine secretion

ELISA was used to study the cytokine secretion in WHB caused by delivering a TLR7 agonist with rHDLs.

### Materials

WHB was tapped in Hirudin tubes from donors. RMPI and PBS were supplied from Sigma Aldrich. A washing buffer (0.05% Tween20 (v/v) in PBS) and reagent dilution (1% BSA (w/v) in PBS) were prepared for the ELISA measurements. A reagent dilution solution containing 0.5% (w/v) BSA and 0.05% (v/v) Tween20 in PBS was used for analysis of the cytokine IFN-$\alpha$. The required capture antibody, detection antibody and standards were all supplied in the ELISA kits from R&D Systems (Denmark) and diluted in the appropriate concentrations as given by the protocol from the specific ELISA kit. Capture antibody was diluted in PBS while detection antibody and standard were diluted in Reagent Diluent. The substrate was 1-Step$^{TM}$ Ultra TMB-ELISA from Thermo Fisher Scientific. The stop solution was a 1 M $H_2SO_4$ solution. Resiquimod (R848) was supplied from InvivoGen (France), and TMX-201 was supplied from PRC Ticinum Lab.

### Experimental Procedure

RMPI media was added to the WHB in 1:7 ratio. The samples were also diluted in RMPI media such that when mixing 50 $\mu$L sample with 350 $\mu$L WHB/RMPI solution, the final concentration of TMX-201 was 10 $\mu$M in the samples containing TMX-201. DMSO, free TMX-201 dissolved in DMSO and R848 were used as controls. The samples, mixed with the WHB/RMPI solution, were incubated at 37 °C for 1 hour before washing the cells twice with RMPI. The samples were centrifuged (400 g for 2 minutes) between each wash such that supernatant without cells could be removed. Hereafter, the samples with cells were distributed in a 96-well plate and incubated overnight. The next day the samples were transferred to eppendorf tubes and centrifuged (5000 g for 5 minutes), and the supernatant was transferred to another 96-well plate. The supernatant was analysed by ELISA using the following procedure. Note the exact procedure and concentrations depend on the used ELISA kit.

- The ELISA plate wells were coated with capture antibody and incubated overnight at 4 °C.
- The wells were washed by removing all the previous solution and adding 100 $\mu$L wash buffer to each well. The washing procedure was repeated three times.
- 100 $\mu$L reagent diluent was added to the wells in order to block unspecific binding. The wells were incubated with the reagent diluent for one hour at room temperature.
- After washing three times, 50 $\mu$L of sample, diluted in appropriate concentration with reagent dilution, was added to the wells. The standards were also added to the wells with a twofold dilution series and a well left blank. The plates were hereafter stored overnight at 4 °C.
- After washing three times, 50 $\mu$L detection antibody solution was added to the wells, and incubated for 2 hours at room temperature. For the IFN-$\alpha$ the substrate could be added directly hereafter because the enzyme was already conjugated to the detection antibody, however, for the other cytokines an additional step was required.
- The plates were washed three times and 50 $\mu$L enzyme (Streptavidin-HRP) solution was added to each well and incubated for 20 minutes at room temperature protected from light by aluminium foil (apply for analysis of IL-6, IL-10, IL-12p70).
- After washing the plates three times, 50 $\mu$L of substrate was added to the wells. When an appropriate color change was observed, 50 $\mu$L stop solution was added to each well (apply for analysis of all the cytokines).
- A Victor$^3$ multilabel counter from PerkinElmer (Denmark) was used to detect the absorbance of each well at 450 nm and 570 nm. The measurement at 570 nm was used to assess the background, and was subtracted from the measurement at 450 nm.

# 4. Results and Discussion

Several experiments have been conducted during the project, and the results will be presented and discussed in the following chapter. In order to obtain a better overview of the experimental results, the results from the purification of apoA-I, the formulation of the rHDL, the study of the association of rHDL with leukocytes and delivery of antigen by rHDL to DCs will be presented separately.

## 4.1 Purification of apoA-I from human plasma

The method used for the purification of apoA-I was optimized over several purification runs in order to obtain a sufficient yield and purity of apoA-I. The optimized protocol is described in section 3.1. In the following sections the results from the purification steps will be presented and discussed. Description of how the steps were optimized will be included as well. Refer figure 3.1 for overview of the purification process.

### 4.1.1 Evaluation of the purification step using Affi-Gel® Blue Media

The first purification step utilizes Affi-Gel® Blue Media, which consists of beads that can bind the hydrophobic moieties of apoA-I. This step was optimized in several ways. First of all, a suitable set-up was required for washing the beads and elution of apoA-I from the beads. The optimized set-up is seen in figure 3.2. Other set-ups were used, e.g. a 100 mL syringe with a Whatman No. 1 filter, however several practical difficulties, such as soaking the Affi-Gel® Blue Media sufficiently, made these set-ups unfavourable. The optimized set-up could hold a large volume and could be opened and closed which allowed for a quick removal of the liquid while open, and the beads to be soaked for a while when closed. Furthermore, it was found that the Affi-Gel® Blue Media had to be regenerated in a 2 M guanidine hydrochloride solution after each purification. This was found, since the second time the Affi-Gel® Blue Media was used for a purification experiment, significant lower amount of proteins was released from the beads than during the first purification experiment (measured by absorbance at 280 nm). Also, much apoA-I was found in the filtrates collected when washing the beads with buffer A (estimated by SDS-page), indicating that apoA-I did not bind sufficiently to the beads. The regeneration of the beads seemed to work effectively, and similar problems were avoided in later purification experiments.

For one of the successful purification experiments, fractions of the filtrates obtained from washing the beads were collected and analysed by SDS-page. The result can be seen in figure 4.1 where pure apoA-I and BSA (Bovine serum albumin) are used as references. It is evident that there are some apoA-I in the filtrates but

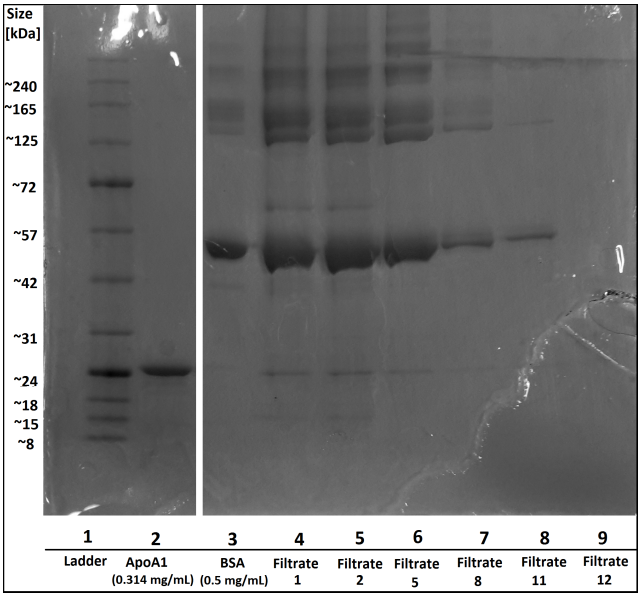


**Figure 4.1:** SDS-page analysis of the filtrate from washing the beads. Filtrate 1 was collected before washing, hence, it is from the solution containing Affi-Gel® Blue Media and serum. Filtrate 2 and later filtrates were collected from the washing of the beads with buffer A. The filtrate 11 had a OD of less than 0.025, hence, this was the last washing with buffer A. Filtrate 12 is the last filtrate collected from washing with buffer B.

it is clearly minimal. It seems reasonable to consider BSA as a reference for HSA (Human serum albumin), thus showing that much HSA is washed out in this washing process. It is interesting that filtrate 12 does not seem to contain any HSA. Filtrate 12 is collected after the washing with buffer without NaCl. As previously discussed, the beads can bind albumin effectively, but the high NaCl concentration of buffer A causes it to be released. Hence, either the remaining HSA binds to the beads when washing with buffer B, or there is simply not sufficient HSA left to yield a band. The importance of the washing process is clearly indicated by figure 4.1 since much of the unwanted proteins are removed.

### Elution of apoA-I

The elution of apoA-I from the Affi-Gel® Blue Media was conducted with a buffer containing cholate (buffer B Elu). Some studies were made concerning the release of the apoA-I from the beads which will be described in the following.

**Cholate or Triton X-100 as elution agent:** Triton X-100 has to be used as a detergent in later purification steps, which consequently require cholate and triton X-100 to be exchanged, e.g. by dialysis. If triton X-100 could be used as the elution agent, it should remove the need for the following dialysis, thus optimizing the purification process. The effectiveness of cholate and triton X-100 as elution agents were investigated by submerging 3 mL beads from after the washing step in both a cholate solution and a triton X-100 solution, and comparing the amount of released apoA-I, which was measured by SDS-page. The result can be seen in figure 4.2. It is clearly evident that triton X-100 does not seem to be an effective elution agent, thus cholate has to be used.

**The effect of temperature on the elution:** The temperature might also affect the elution of apoA-I, hence, in order to investigate the potential effect, the Affi-Gel® Blue Media solution obtained after the washing steps was stored with cholate at 4 °C overnight followed by 4 hours at room temperature the next day. Stirring was used both at 4 °C and room temperature. Samples were taken from the elution buffer after each storage period. The samples were analysed by SDS-page, and the results can be seen in figure 4.3. Using imageJ, the intensity was plotted, and the measured integral under the peaks were 10,604 and 12,410 for the sample after 4 °C and room temperature, respectively.

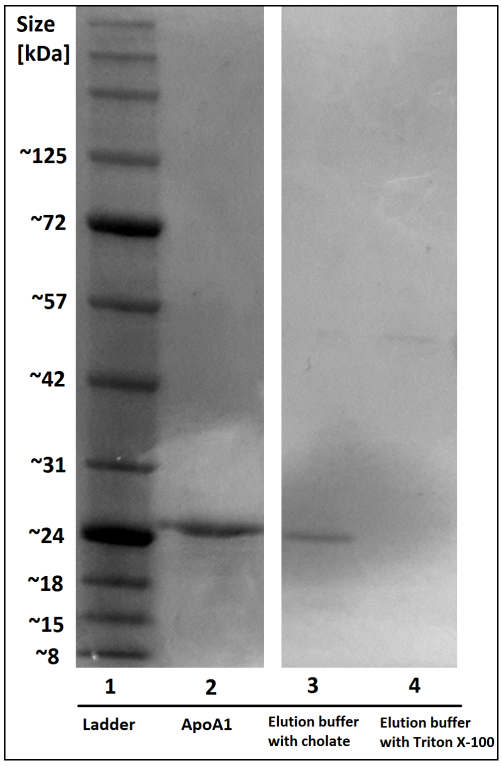


**Figure 4.2:** SDS-page used to investigate the potential of using either cholate or triton X-100 as elution agent in the buffer used for elution of apoA-I from Affi-Gel® Blue Media.

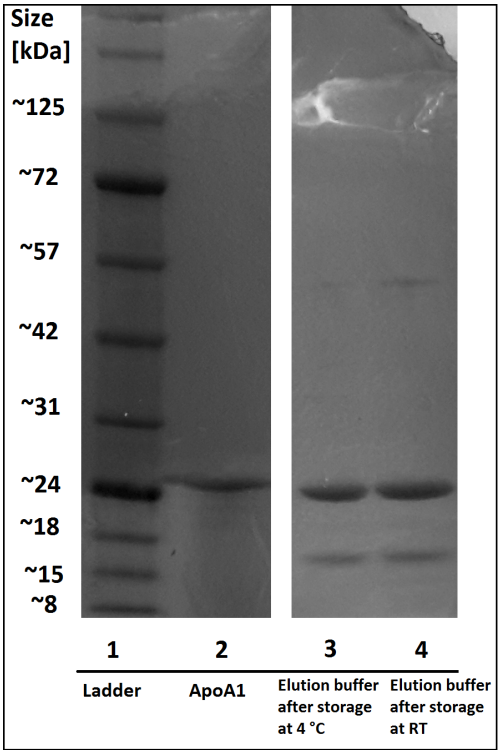


**Figure 4.3:** SDS-page used to investigate the effect of temperature on elution of apoA-I from Affi-Gel® Blue Media.

The low temperature does not seem to limit the elution of apoA-I, however, the storage at room temperature did seem to increase the amount of eluted apoA-I further. Hence, in further studies the solution is stored at room temperature for 2-3 hours after the incubation at 4 °C overnight. Note that the higher temperature can be unfavourable for the proteins, which is why the sample is not incubated at room temperature for more than 4 hours.

### 4.1.2 Evaluation of the purification step using Q-Sepharose column

The Q-Sepharose column is an anionic affinity column, thus it is supposed to bind the anionic moieties of apoA-I., which are present at pH 8. In the first purification run the solution obtained from the elution of apoA-I from the Affi-Gel® Blue Media was not concentrated nor dialysed. Equal volumes of the obtained

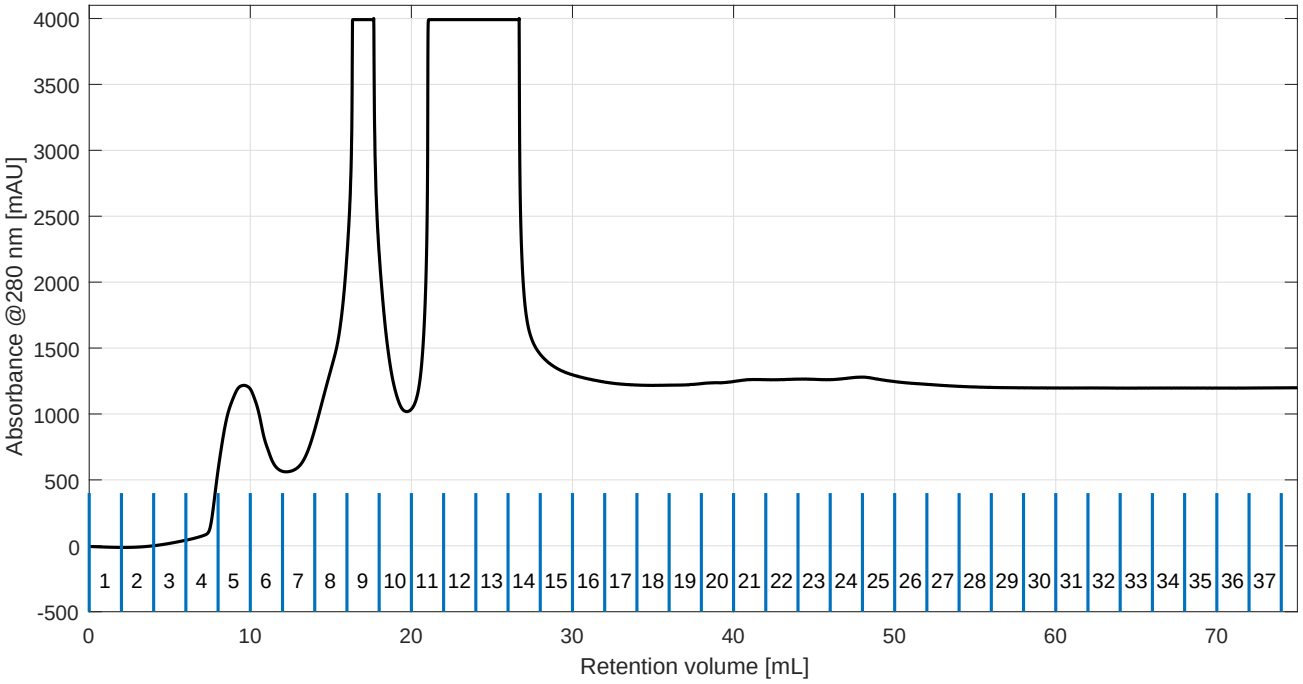


**Figure 4.4:** The chromatogram obtained from the elution on the Q-Sepharose column. The chromatogram is only shown after applying the gradient, however, it was prewashed with two column volumes of buffer C before the gradient was applied.

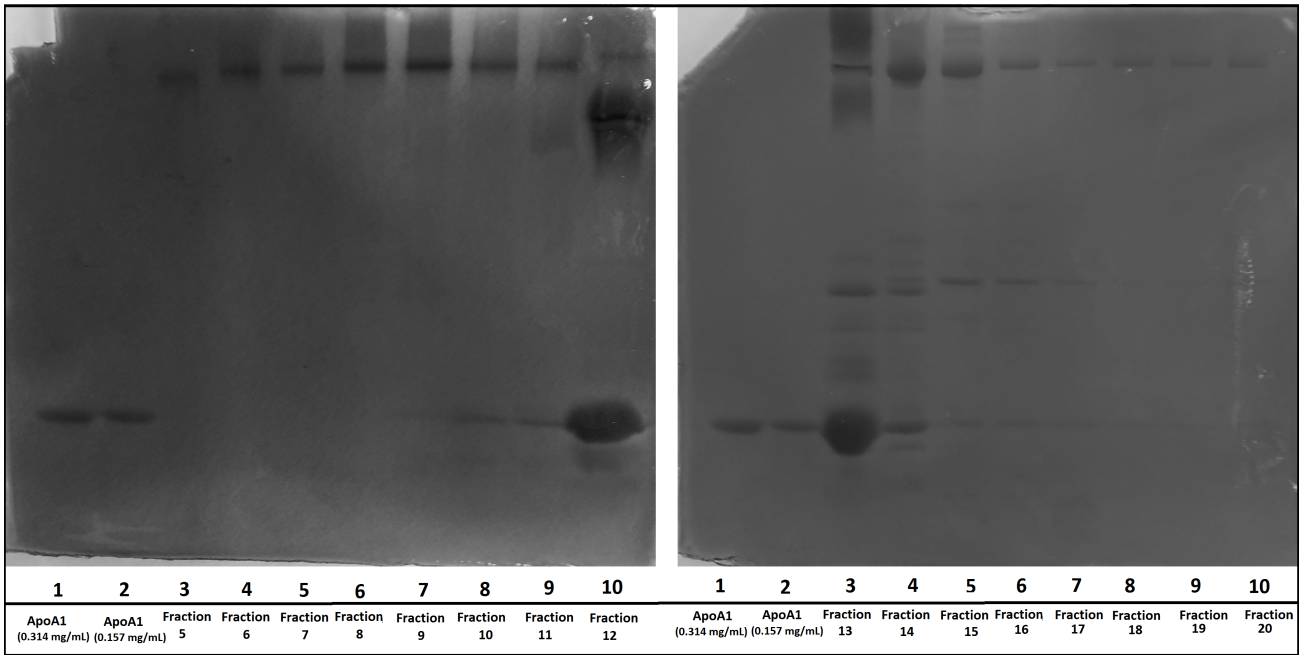


**Figure 4.5:** SDS-page on the collected fractions of interest. Fraction 12, 13 and 14 were pooled and used in the further purification processes.

solution and a buffer containing 25 mM Tris, 1 mM $CaCl_2$, 5 mM EDTA and 0.2 % Triton X-100 (pH 8) were mixed, yielding a total of approximately 200 mL. This volume was loaded to the Q-Sepharose column. The column was washed with two column volumes of buffer C in order to remove unbound substances, before a linear gradient of buffer C elu was applied. The resulting chromatogram had a peak briefly after the gradient was applied. However, the peak value was approximately 360 mAU, which was significantly lower than

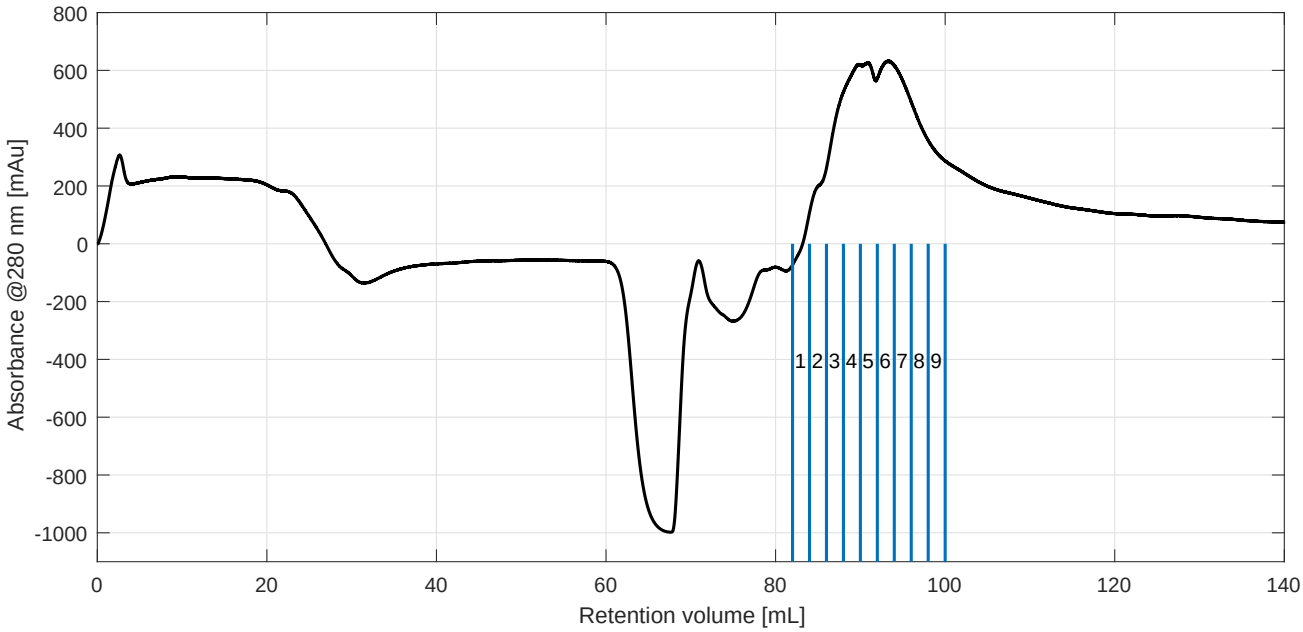


**Figure 4.6:** The chromatogram during the purification step using the SP-Sepharose column. The gradient with buffer D elu was applied after 40 mL. The fractions which were analysed further by SDS-page are shown and numbered.

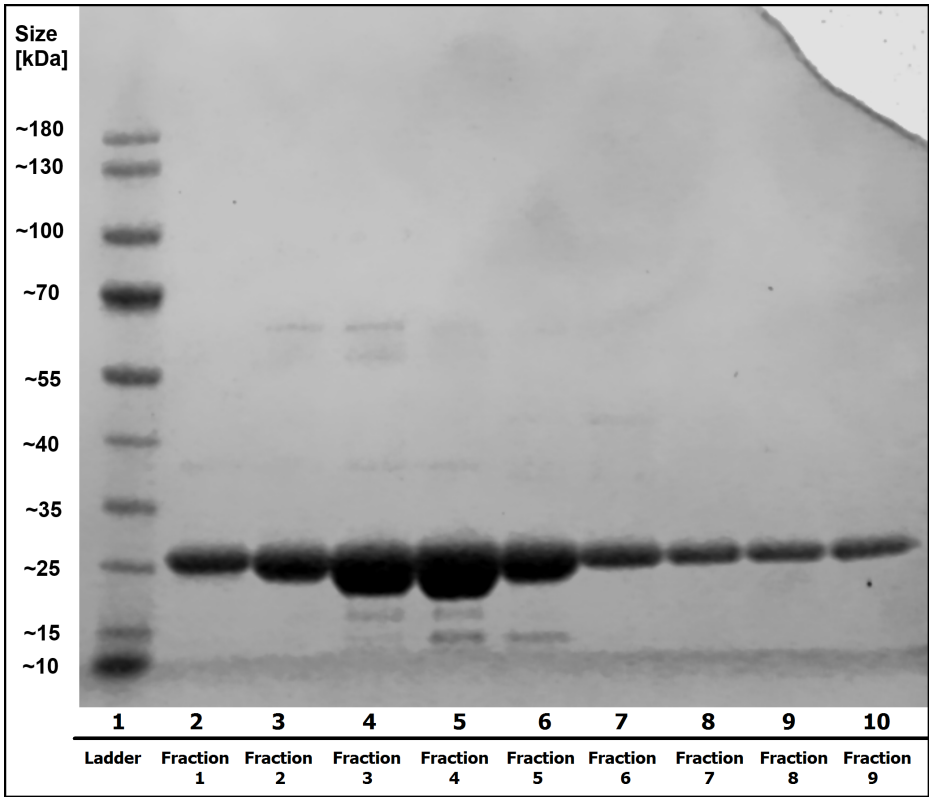


**Figure 4.7:** SDS-page analysing the collected fractions of interest obtained from the SP-Sepharose column. All the fractions were pooled and used in the further purification process.

expected. Fractions were collected during the elution, and the fractions correlated to the observed peak were analysed by SDS-page. It was found that some apoA-I indeed was eluted at this volume, but quantification of the amount of apoA-I, as described in appendix A, indicated that much less apoA-I was collected than loaded to the column. The waste collected when loading the sample was also analysed by SDS-page, and apoA-I was found in the waste in rather large quantities. Hence, it seems that apoA-I did not bind sufficiently to the column. This might be explained by the fact that too large volume was used. Cholate is present in buffer B elu, and it will consequently be present in the sample that is loaded to the column. Cholate is negatively charged[65], thus it can potentially bind to the column. When the relatively large volume is loaded to the column, it will clearly result in a relatively large amount of cholate being loaded as well. This might saturate the column, making it difficult for apoA-I to bind, thereby resulting in apoA-I in the waste as observed. This might be circumvented by concentrating the sample obtained after treatment with Affi-Gel® Blue Media, and using dialysis to exchange cholate with triton X-100. Obviously, there will still be some cholate present but since the amount is reduced, the column might not be saturated making it possible for apoA-I to bind more effectively. Note that triton X-100 is used to ensure that the proteins do not aggregate.

In later experiments, the sample obtained after treatment with Affi-Gel® Blue Media was concentrated and dialysed before being loaded to the column. In one of these runs approximately 40 mL concentrated sample (OD 1.16 at 280 nm) was loaded to the column and eluted with a linear gradient, which yielded the chromatogram seen in figure 4.4, where the collected fractions are indicated. The fractions of interest from this run were analysed by SDS-page, as seen in figure 4.5. Fraction 12 and 13 contain much apoA-I while fraction 14 also seem to contain some, thus, these fractions were pooled and used in the later purification steps.

### 4.1.3 Evaluation of the purification step using SP-Sepharose column

The pooled sample obtained after the Q-Sepharose column was dialysed against the Dilution Buffer in order to remove the NaCl and lower the pH, and subsequently loaded onto the SP-Sepharose column. After loading

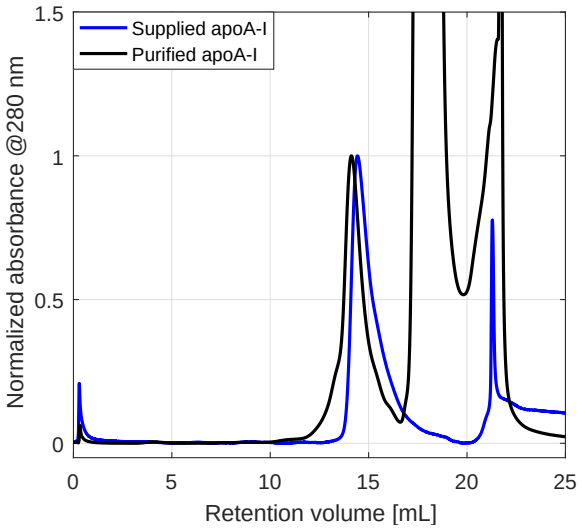


**Figure 4.8:** The chromatogram obtained when applying one of the concentrated fractions obtained after the SP-Sepharose to the Superdex-200 column. The measured absorbance is normalized with respect to the peak around 14 mL and compared with a chromatogram obtained from applying the supplied apoA-I to the column.

the sample, it was washed with buffer D before the gradient was applied. The obtained chromatogram is seen in figure 4.6. It is evident that a broad peak is observed during the washing which must be attributed to the proteins or other substances that do not bind to the cationic column. Obviously, this illustrates the importances of this column since a lot of unwanted proteins are removed. The negative peak in the chromatogram might be due to lack of triton X-100 at this eluted volume, since there is triton X-100 in the buffer which works as the reference, and triton X-100 absorb at 280 nm. Fractions collected during this negative peak was analysed by SDS-page, and did not seem to contain any detectable proteins. Fractions between retention volumes of 82 and 100 mL (shown and numbered in figure 4.6) were analysed by SDS-page, and the result is presented in figure 4.7. Most apoA-I seem to be in fraction 3 and 4, and there are minor impurities in some of the fractions, however, since all fractions seemed to contain apoA-I, they were pooled and used for the further purification process.

### 4.1.4 Evaluation of the purification step using Superdex-200 column

The fractions collected after the SP-Sepharose column were concentrated and applied to the Superdex-200 column, which can separate the proteins by size. The

chromatogram obtained from one of the purification runs are seen in figure 4.8, where the absorbance is normalized with respect to the peak around 14 mL, and compared to a chromatogram obtained by using some of the supplied apoA-I. Note that the peak observed around 17-19 mL most likely can be attributed to elution of triton X-100. The peak seen around retention volume of 13-16 mL can presumably be attributed to apoA-I, hence, fractions collected during this peak was pooled after confirming preference of apoA-I in each fraction by SDS-page. Absorbance at 280 nm of the pooled sample was measured by a Thermo Scientific$^{TM}$ NanoDrop$^{TM}$ Spectrophotometer, and by using the known extension coefficient and molecular weight of apoA-I, the concentration could be estimated.

### 4.1.5 Evaluation of the purification process

The discussion in the previous sections have focussed on each purification step, however, it seems relevant to consider the purification process as a whole and compare the purity and yield gained in each step. This was done for the second successful purification run which yielded approximately 12 mg apoA-I. This yield was estimated by the absorption at 280 nm, however, the yield can also be estimated by using SDS-page quantitatively, refer appendix A. The purity of apoA-I was also estimated by the SDS-page for each purification step. The purity consider in this case the amount of apoA-I relative to other proteins which are detectable by the SDS-page. The SDS-page of the samples taken after each purification step are seen in figure 4.9 A, while the estimated yield and purity are presented in figure 4.9 B. Note that it is difficult to define the band that is associated with apoA-I for serum, hence, the estimate of the amount of apoA-I in serum is associated with great uncertainty. It is, however, noted that the yield of approximately 74 mg from 50 mL plasma correspond well with the fact that human plasma contain 1-1.5 mg/mL apoA-I [56]. The band associated with apoA-I is more obvious for the other samples. Further-

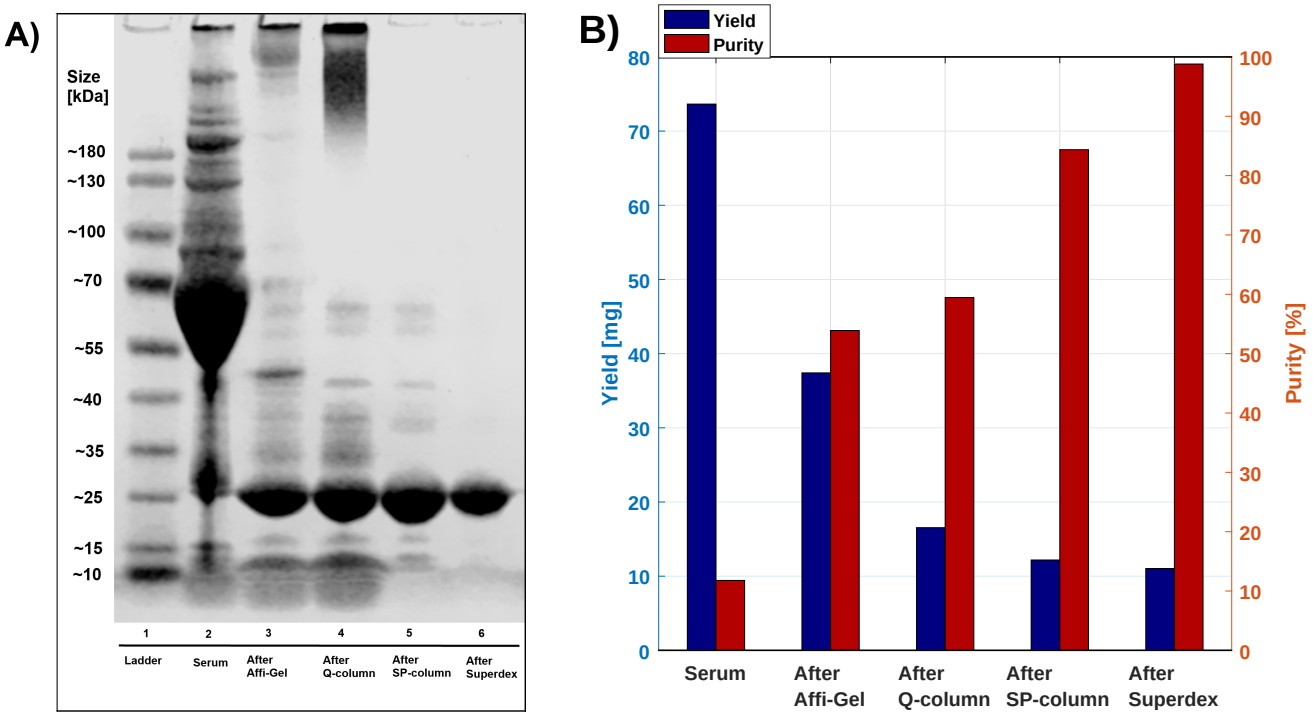


**Figure 4.9:** Overview over the effect of each purification step used in the purification of apoA-I. The following notations are used in the figures: Affi-Gel refers to Affi-Gel® Blue Media, Q-column refers to the Q-Sepharose column, SP column refers to the SP-Sepharose column and Superdex refers to the Superdex-200 column. **(A):** SDS-page samples taken after each step. In order to obtain bands of similar intensity, the samples were diluted differently. **(B):** Yield and purity after each purification step estimated by the SDS-page. Since SDS-page does not provide very accurate quantification, the yield should be considered with some uncertainty. The purity is in the case the amount of apoA-I relative to other proteins detectable by the SDS-page.

more, the dark areas in the top of some of the wells (especially well 3 and 4) are not included in the calculation as it is believed to be an artifact, since including them in the calculations yielded unreliable results.

It is evident that the yield decreases for each purification step while the purity increase till approximately 99% for the final sample. The serum obviously contains a lot of proteins, however, after the Affi-Gel® Blue Media a lot of these proteins are removed, e.g. the albumin which is believed to be associated with the large band between 55 and 70 kDa. The yield also decreases a lot during this step, probably since some apoA-I are also released during the washing of the Affi-Gel® Blue Media with buffer A, and because some apoA-I might not be released from the beads of the Affi-Gel® Blue Media by the elution buffer (buffer B elu). Apparently, the yield also decreases significantly when using the Q-Sepharose column, however, only a minor increase in purity is obtained. However, the purification step might still be important, since it potentially removes other substances than proteins, which are not detectable by the SDS-page. It is noted that the dark area in the top of the well 4 is removed after the SP-Sepharose column. One explanation for this band could be that it was related to debris from dead cells which, since cell membranes are generally negatively charged, are removed during the SP-Sepharose column which only bind cationic substances. The Superdex-200 column separates the proteins by size, and it is evident that proteins which are both smaller and larger than apoA-I are removed during this step. A high purity of approximately 99% is obtained after purification. The final yield of apoA-I is estimated by the SDS-page to be approximately 11 mg. This is fairly close to the yield estimate by the absorption though, it has to be kept in mind that quantification by SDS-page cannot be considered very accurate, and should primarily be used relatively to other samples in the same gel.

During the project two successful purification runs were conducted which yielded approximately 6 mg and 12 mg purified apoA-I, respectively. Hence, the second purification run yielded twice as much purified apoA-I as the first purification run, illustrating the importance of optimisation and experience with the method. The purified apoA-I was used for several experiments concerning the formulation of rHDL.

## 4.2 Formulation of reconstituted high-density lipoproteins

The formulation of rHDL can be affected by changing both the lipid composition and varying the lipid/protein ratio. Several studies were conducted in order to determine the effect of changing these parameters. The rHDLs were primarily characterized by SEC.

### 4.2.1 Formulation of rHDL with purified apoA-I

In order to assess if the purified apoA-I could be used to formulate rHDL, both the supplied and the purified apoA-I were used to formulate rHDL, and the obtained SEC chromatograms were compared. The rHDLs were formulated with DMPC and a lipid/protein ratio of 100. The result can be seen in figure 4.10. It is evident that both chromatograms have a peak around 11.5 mL. It was found that free apoA-I is eluted around 14-15 mL by running a pure apoA-I sample through the column, thus the particles seem to be larger, corresponding well

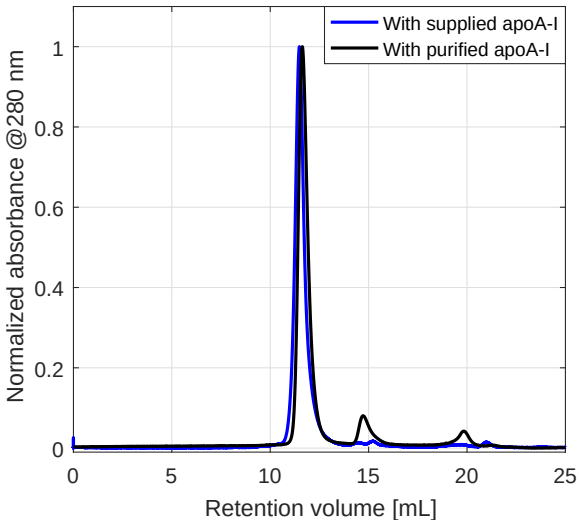


**Figure 4.10:** The chromatograms obtained from the rHDL formulated with DMPC and either the supplied or purified apoA-I. The chromatograms are normalized. Clearly, the chromatograms are similar indicating that rHDL was successfully formulated with the purified apoA-I.

with the assembly of rHDL. Furthermore, the two chromatograms clearly seem equivalent, thus indicating that rHDLs are successfully formulated with both supplied and purified apoA-I. It is further indicated that the approximated concentration of the purified apoA-I seems reasonable, since assuming a significant incorrect concentration would have shifted the lipid/protein ratio which would have resulted in an effect observable by the chromatogram (refer section 4.2.2). A minor peak is seen around 14-15 mL when using the purified apoA-I which could be free apoA-I, however, it could also be other proteins which are not discarded during the purification process.

### 4.2.2 The effect of the lipid/protein ratio

The lipid/protein ratio is an important parameter when formulating rHDL. In order to obtain rHDLs with a monodispersed distribution a certain optimal ratio is required. This optimal ratio can differ depending on the particular lipid composition used in the rHDL, since the surface area of the lipids might differ.[66] Hence, the effect of changing the lipid/protein ratio of rHDLs with either DMPC or POPC was investigated.

#### Optimal lipid/protein ratio for DMPC rHDL

The obtained chromatograms from SEC analysis of the rHDLs consisting of DMPC with varying lipid/protein ratio can be seen in figure 4.11. Note that these rHDLs particles were formulated with the supplied apoA-I. A major peak appears for all of the sample at the retention volume of approximately 11.5 mL. It is believed that this peak is associated with the rHDL of approximately 10 nm. The lipid/protein ratio of 50 results in a shoulder to the right of the major peak. It seems logically that the low ratio would result in some free apoA-I since there might be lack of lipids to form additional rHDLs with the free apoA-I, hence, the signal between 13-15 mL might be attributed to free apoA-I or apoA-I with only few associated lipids that therefore do not assemble into rHDL. In contrast, the lipid/protein ratio of 160 results in a shoulder to the left of the major peak, which might be attributed to larger rHDL particles. The 9.6 nm sized endogenous HDL consist of two apoA-I proteins, however, it is also possible to obtain rHDLs with more protein per particle[1]. The signal at 9-10 mL might correspond to these larger rHDL particles which consist of more than two apoA-I proteins. It might also be caused by aggregated rHDL particles, however, since there is no signal at the void (approximately 7-8 mL), it would only be smaller aggregated structures, hence, it does not seem to be an uncontrollable aggregation, and therefore the signal is believed to be associated with rHDLs. It is also notable that the major peak for the sample with the ratio of 160 seems

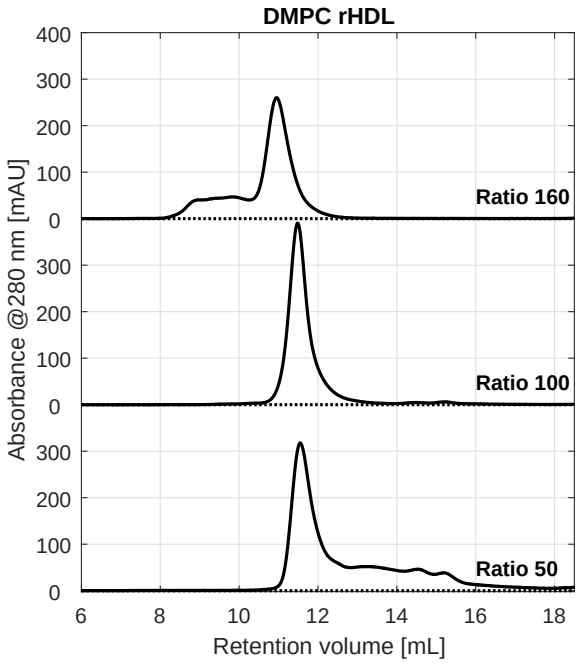


**Figure 4.11:** The SEC chromatograms obtained from the analysis of rHDLs formulated with DMPC and varying lipid/protein ratio.

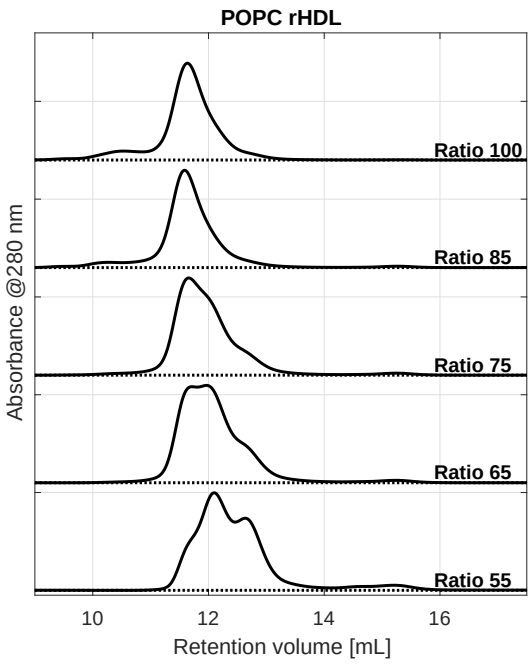


**Figure 4.12:** The SEC chromatogram obtained the analysis of rHDL formulated with POPC and varying lipid/protein ratios. Each chromatogram is normalized.

to differ slightly from the major peaks from the two other samples. This might be explained by the fact that more lipids are squeezed into the rHDL when higher ratios are used, which might result in larger particles. The extra lipids might also induce some structural changes in the rHDL, thus forming even larger rHDLs which still have only two apoA-I proteins but are eluted between 9-10 mL.

The ratio of 100 seems most optimal if a monodispersed distribution of the DMPC rHDLs is desired. A relatively sharp peak is obtained when using this ratio with minimal signal around 14-15 mL, thus indicating that nearly all of the apoA-I are associated in the rHDLs.

### Optimal lipid/protein ratio for POPC rHDL

The lipid/protein ratio was also varied for the rHDLs consisting of POPC. The chromatograms obtained by characterisation using SEC are seen in figure 4.12. As it was the case for the rHDLs consisting of DMPC, peaks are seen around 11.5 mL for all chromatogram which most likely are correlated to approximately 10 nm sized rHDL. It is evident that the ratio of 100 results in a minor shoulder to the left of the peak, indicating that lower ratios are desired if a monodispersed distribution of rHDLs are to be obtained. Hence, these results indicate that there is a difference in the optimal ratio depending on the lipid used in the rHDL. As previously discussed this difference can be attributed to the difference in surface area of the lipids, since the effective area of DMPC is ∼50 Å$^2$ while the effective area of POPC is ∼68 Å$^2$ [66]. From figure 4.12, it is seen that ratios lower than 75 result in a shoulder to the right of the peak which eventually results in a distant peak around 12.7 mL when ratio is lowered to 55. Furthermore, there seems to be an increase in the minor peak around 15 mL, which could correspond to free apoA-I. Thus, it is indicated that the most optimal ratio in order to obtain a monodispersed distribution of the POPC rHDLs is between 75 and 85, hence, a ratio of 80 was used for further studies when monodispersed POPC based rHDLs were desired. A full chromatogram obtained from investigation of POPC rHDL particles with a ratio of 80 is presented in figure 4.13. Although, the ratio is optimized, there still seem to be a minor shoulder to left of the major peak, and the distribution is wider than for DMPC rHDL. This illustrates that it is difficult to obtain a fully monodispersed distribution of POPC rHDLs which could be due to the fact that

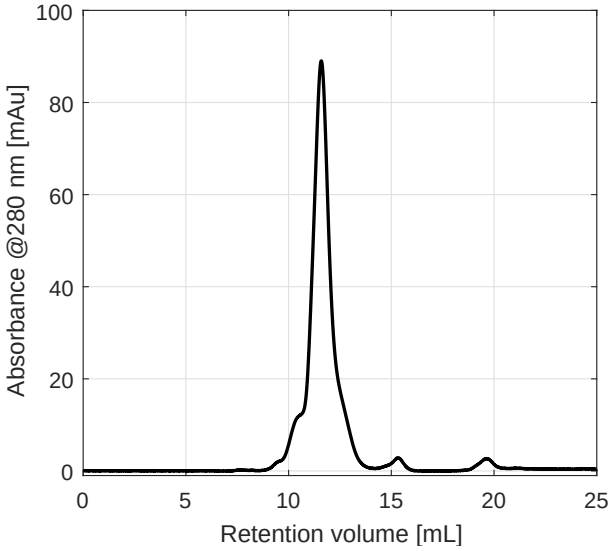


**Figure 4.13:** Chromatogram from SEC analysis of POPC rHDL formulated with a lipid/protein ratio of 80.

POPC is unsaturated, thus being more difficult to pack tightly in the rHDLs. However, POPC based rHDLs were still used for the experiments of this project. This is due to the fact that POPC rHDL mimics the endogenous HDL better than the DMPC rHDL, since nature mostly used unsaturated lipids [67], hence, POPC rHDL might be better suited for biomedical applications, and it is probably therefore POPC based rHDLs often are used for clinical trials [1].

### Increasing the lipid/protein ratio

As previously discussed, higher lipid/protein ratios than the optimal ratio seem to cause a shoulder to the left of the major peak which might be attributed to larger rHDL particles which consist of more than two apoA-I proteins. It could be interesting to increase the ratio further in order to assess if a monodispersed distribution of larger rHDL particles could be obtained. This was done for POPC rHDLs as well as for POPC:DOTAP 90:10 rHDLs. The incorporation of cationic DOTAP seems to cause a shift in the size distribution slightly to the left, which will be discussed in more detail in section 4.2.3. However, it could indeed be interesting to study the effect of increasing the ratio for these rHDLs as well, since DOTAP might prefer larger sized rHDLs, thus a monodispersed distribution of larger rHDL particles might be easier obtained for the POPC:DOTAP rHDL than for the POPC rHDL.

The results of these experiments are seen in figure 4.14. Note that the chromatograms are normalized, hence,

their total integral cannot in this case be considered as a relative indication of the amount of apoA-I. It is evident that as the lipid/protein ratio is increased for both POPC and POPC:DOTAP rHDLs, distant peaks appear at lower retention volumes. For the POPC rHDL using a ratio of 150, four peaks appear. The first peak around 7.7 might be caused by liposomes, since it appears around the void of the Superdex-200 column. Liposomes will yield a signal at the measured 280 nm due to light scatter, and they can indeed be formulated by the same approach used to formulate rHDL if conducted without apoA-I. This was done for the liposomes which were used to measure the void of the column, refer appendix A. Hence, the additional lipids which are available, when using higher ratios than the optimal ratio, might self-assemble into liposomes. The three peaks following the peak at the void could possibly be larger sized rHDL particles which consist of different amount of apoA-I. It is evident that distant peaks still appear when increasing the ratio from 150, though the two peaks immediately after the peak at the void seem to be smeared together and minor peaks/shoulders also appear.

In contrast to the effects observed for POPC rHDLs, the POPC:DOTAP rHDLs do not yield any peak at the void, thus these samples do seemingly not contain many liposomes. It is indeed interesting that though DOTAP shift the distribution slightly to the left when using ratios of 75 and 100, it apparently hinder the formation of liposomes when increasing the ratio further, which might be because DOTAP prefers the incorporation into larger rHDL particles instead of liposomes. Hence, it seems possible to obtain a higher yield of larger rHDL particles when using POPC:DOTAP than when solely using POPC in the rHDL. The three peaks which are observed when using a ratio of 150 remains distinguishable when increasing the ratio further. Although, the peaks at lower retention volume increase, and the peak at higher retention volumes decreases when the ratio is increased, there seem to be a limit to how much the distribution can be shifted as the effect is less pronounced when increasing the ratio above 200. Hence, though the amount of presumably larger rHDL particles increase, it seems that the self-assembly of smaller rHDLs of approximately 10 nm cannot be avoided. It does consequently not seem possible to obtain a monodispersed distribution of larger sized rHDL particles with neither the POPC rHDLs nor the POPC:DOTAP 90:10 rHDLs. Note that the presumably larger rHDL particles might be isolated by collecting fractions during SEC analysis.

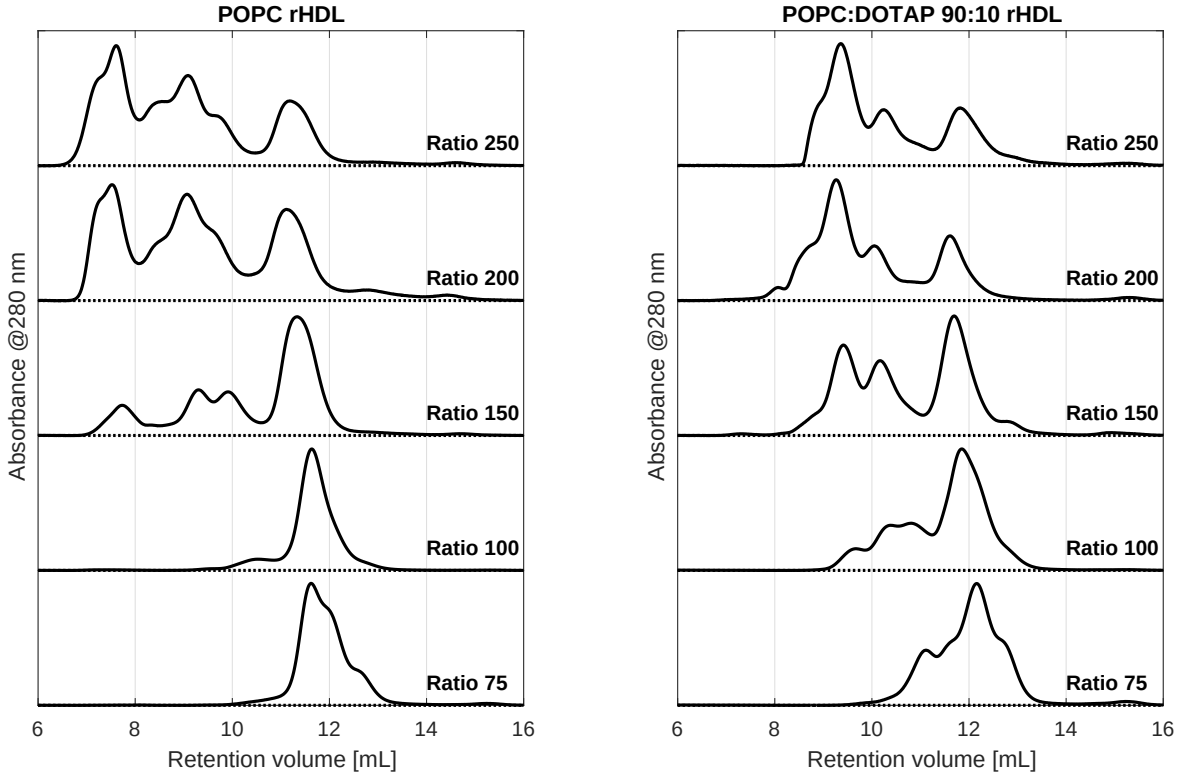


**Figure 4.14:** Investigation of the effect of varying the lipid/protein ratio of the POPC and POPC:DOTAP 90:10 rHDL. The SEC chromatograms are normalized and only the retention volumes of interest are shown.

This would allow for further analysis of the rHDL particles, and it could be interesting to determine if the larger rHDL particles actually did contain more than two apoA-I proteins per rHDL or if the additional lipids simply caused a structural change in the rHDLs such that larger sized rHDL particles were formed with only two apoA-I proteins per particle. Obviously, the isolated larger rHDL particles might not be stable, and the stability of each fraction needed to be studied as well. These studies were not conducted in this project, and the focus was mainly the rHDLs of approximately 10 nm, since these could be formulated with a somewhat monodispersed distribution.

### 4.2.3 Effect of a cationic lipid composition

In order to use similar lipid composition in the rHDL as Pia T. Johansen et al.[50] used for liposomes and thereby potentially obtaining specificity towards monocytes, incorporation of cationic lipids in the rHDL was required. POPC based rHDLs were formulated with various amount of the cationic lipids DOTAP and EPC in order to evaluate the effect of incorporating cationic lipids in the rHDL. The lipid/protein ratio was kept at 80. The result can be seen in figure 4.15. A minor shoulder to the left of the major peak appears when using both 5% and 10% of the cationic lipids in the rHDL. The shoulder observed when using 5% EPC seem arbitrarily large and is considered to be an artefact from either the preparation or the characterization, especially since the shoulder observed when using 10% EPC is less obvious. Although the shoulders which appear when using 5% and 10% cationic lipids seem slightly more pronounced than the shoulder which appears for the pure POPC rHDL, it is difficult to assess if the observed shoulders are caused by the incorporation of cationic lipids since a shoulder also appears for the POPC rHDL. A more obvious shift in the distribution is seen when incorporating 25% cationic lipids. A difference between POPC:DOTAP and POPC:EPC rHDL is also seen when using 25% of the cationic lipid. The distribution is shifted to the left for both samples, however, the POPC:EPC rHDL still seem to have a major peak

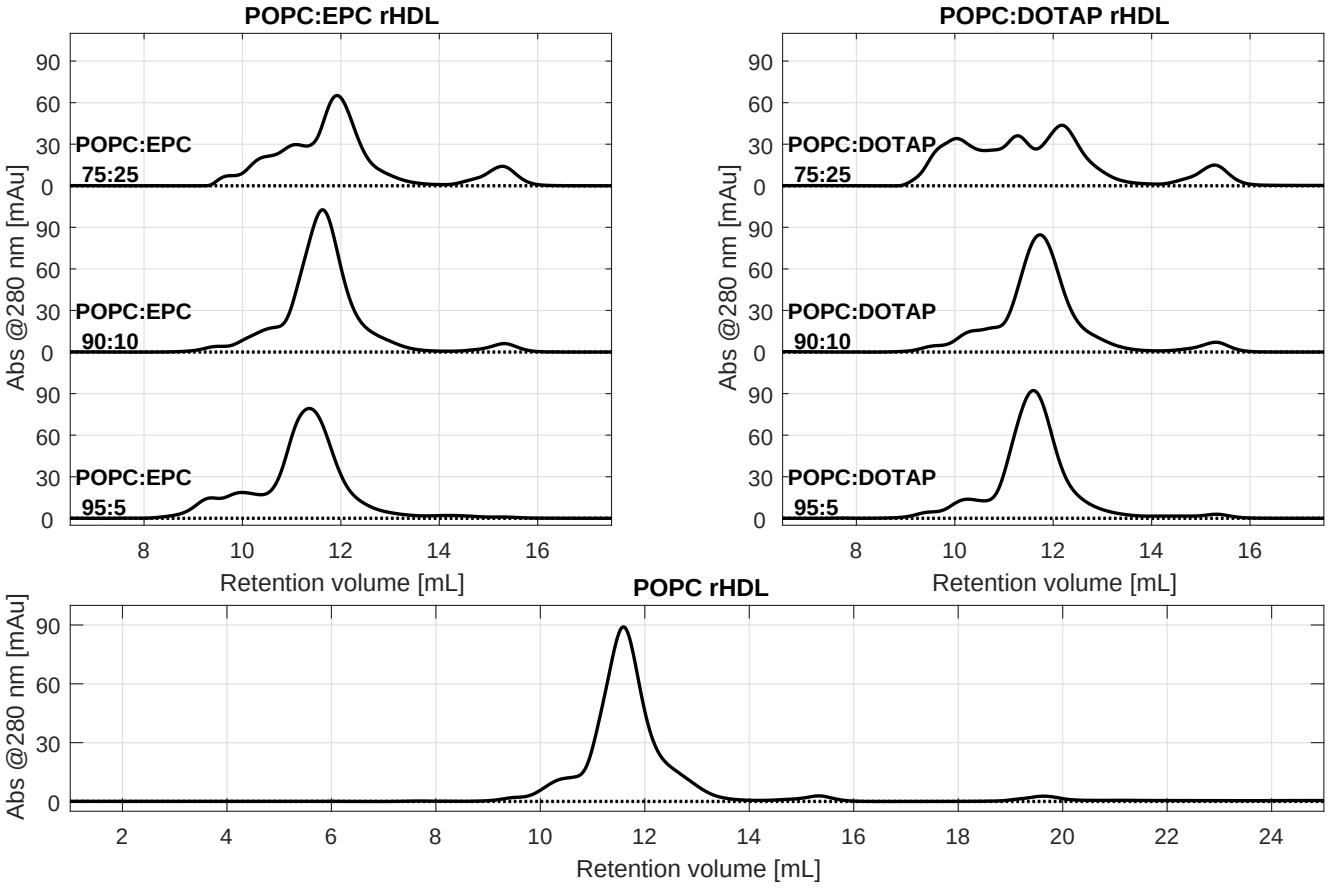


**Figure 4.15:** Chromatograms obtained from SEC analysis of rHDLs with various amount of DOTAP and EPC incorporated. The full chromatogram is shown for the POPC rHDL while only the retention volumes of interest are shown for the other samples, however, no peaks were observed at other retention volumes than shown.

at approximately the same position as POPC rHDL, whereas the POPC:DOTAP rHDL has three peaks of almost similar intensity. As seen from the structure of DOTAP and EPC, refer figure 1.12, EPC mimics POPC better than DOTAP, thus this might explain that it is more effectively incorporated. There might be some repulsion between the cationic part of the apoA-I and the cationic lipids, which could explain the observed shift in the chromatograms, since high amounts of EPC and DOTAP might be preferably incorporated in larger sized rHDL particles.

The incorporation of DOTAP was also conducted using POPC based rHDLs formulated with a lipid/protein ratio of 100, and similar effects were observed, however, with a more pronounced shift of the size distribution to the left when using 10% DOTAP. The results from these experiments are presented in figure 4.19 that also considers the stability of the rHDLs, which will be discussed later.

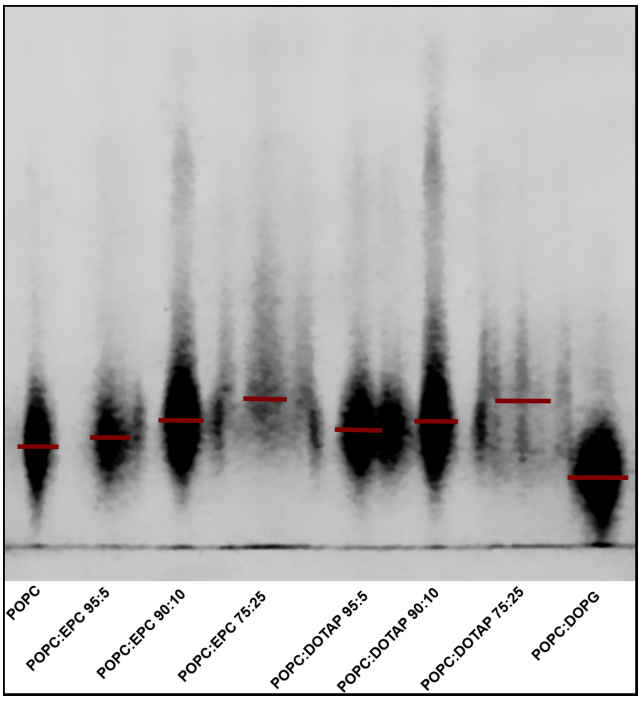


**Figure 4.16:** Native page analysis of fractions collected between retention volumes 11.5 - 12 mL during SEC analysis. Hence, they should have similar size and the movement should mainly depend on the charge of the rHDL.

### Incorporation of charged lipids

Native page was used to assess if the charged lipids were successfully incorporated into the rHDLs, thus resulting in rHDLs with varying charge. The native page does not denature the protein during electrophoresis, hence, it should be possible to analyse the assembled rHDL. The velocity of the rHDL during electrophoresis will then depend on the size and charge. It is evident from figure 4.15 that the addition of cationic lipids affect the size distribution of the rHDLs. Hence, in order to eliminate the effect of size during electrophoresis, fractions eluted from the SEC column between the same retention volumes were collected and analysed by native page. Although there might be a size distribution in the collected fractions, the size should be approximately equal across each fraction, hence, the movement during electrophoresis should mainly depend on charge. Fractions between retention volumes of 11.5 and 12 mL were collected. As seen from figure 4.15, this fraction encompasses the majority of the main peak for most of the formulations, however, some fractions will contain lower concentration of rHDL due to shift in the size distribution. The result for the analysis of the fractions using native page is seen in figure 4.16. rHDLs with POPC:DOPG 90:10 were also analysed. The middle of the bands are indicated by the red line since the bands are relatively wide, however, some of them also have a tail upwards in the gel which are neglected when setting the red line. The samples containing rHDL of POPC:EPC 75:25 and POPC:DOTAP 75:25 do not yield a well-defined band, possibly due to a too low concentration of rHDLs. This makes the red line mark rather arbitrary, though it set as an estimate of the middle of the band.

It is evident from the results of the native page that all the formulations migrate towards the anode which indicates that they all have an overall anionic charge though they are formulated with a cationic lipid composition. If the overall charge was cationic, they should most likely be detectable in the bottom of the well, but this was not found to be the case (note that the bottom of the well is not shown in the figure). Even the formulation with 25% cationic lipids did not seem to accumulate in the bottom of the well, however, it might not have been detectable due to the low concentration or more cationic lipids might have been incorporated in the larger sized rHDL particles which were not investigated. Although the bands are not separated much, it does seem that the rHDLs become slightly more cationic when using 5% and 10% cationic lipids (both EPC and DOTAP). rHDLs formulated with 10% cationic lipids yield a tail upwards in the gel, which might be

attributed to the positive charge since varying amount of incorporated cationic lipid might cause different migration velocities. The rHDL with a negatively charged lipid composition, i.e. POPC:DOPG 90:10 rHDL, seems to have migrated further down in the gel as expected if it was more negatively charged than the other formulations.

Considering the observed effects from the native page, it is evident that the charged lipids do seem to be incorporated in the rHDLs. However, the amount of charged lipids in the rHDL cannot be quantified using the native page. This could be an interesting parameter to study, especially since the charged lipids affect the size distribution of the rHDLs, i.e. it could be interesting to study if for example cationic lipids are preferably accumulated in larger sized rHDL particles. This quantitative evaluation might be achieved by analysing fractions eluted from the SEC column using mass spectroscopy, however, such studies were not conducted in this project.

### 4.2.4 Incorporation of drug and fluorophore

It is obviously important that the drug and fluorophore are effectively incorporated in the rHDL. The fluorop-

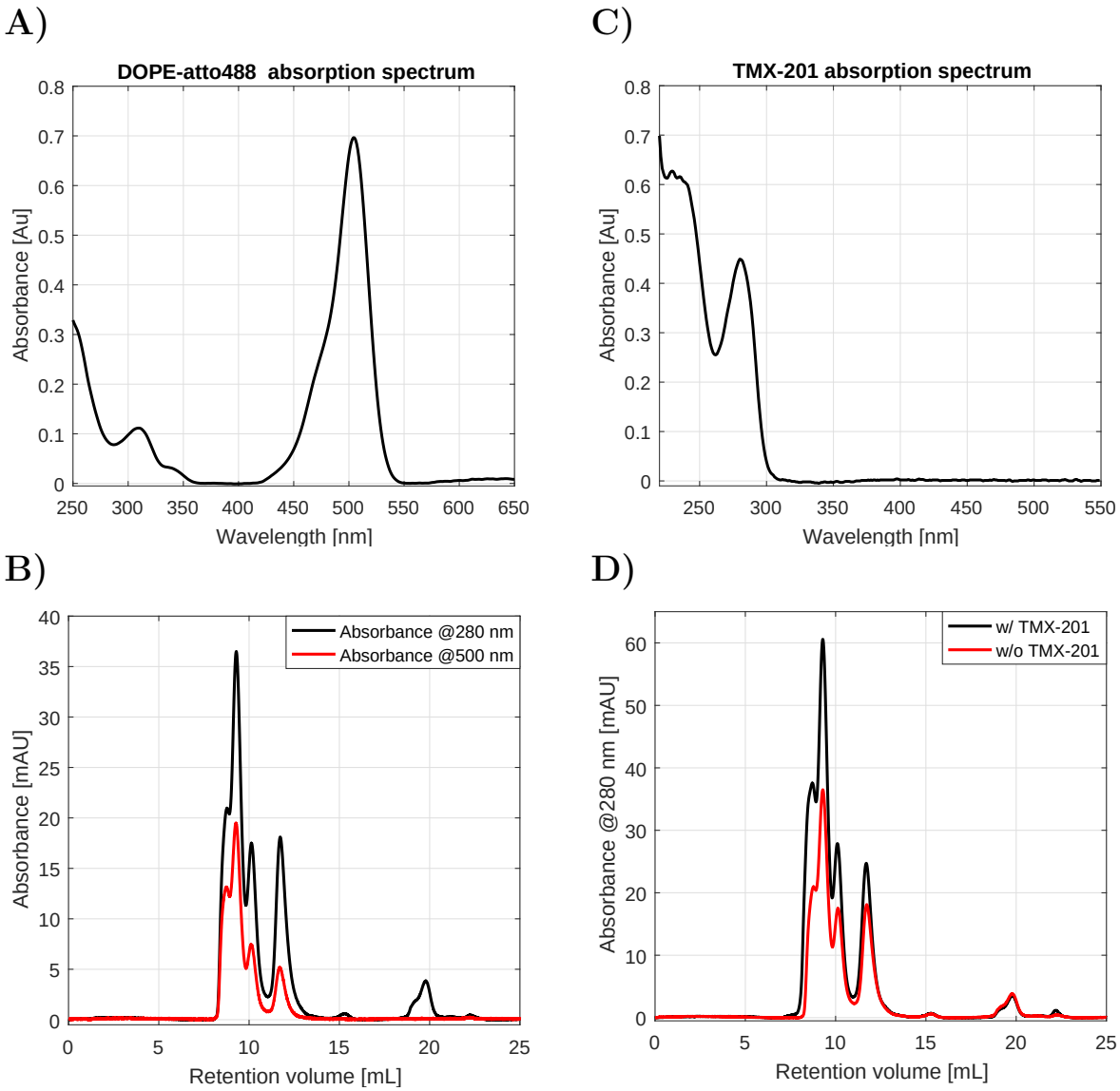


**Figure 4.17:** Investigating the incorporation of DOPE-atto488 and TMX-201 in the rHDL. **(A):** The absorption spectrum of DOPE-atto488. **(B):** SEC analysis of rHDL formulated with POPC:DOTAP:DOPE-atto488 89.9:10:0.1 and a lipid protein ratio of 200. The chromatograms obtained when measuring the absorbance at 280 nm and 500 nm peak at similar retention volumes indicating that DOPE-atto488 is effectively incorporated in the rHDL. **(C):** The absorption spectrum of TMX-201. **(D):** SEC analysis of POPC:DOTAP:TMX 85:10:5 rHDL and POPC:DOTAP 90:10 rHDL with a lipid/protein ratio of 200. The fact that the measured intensity is higher over the peaks for POPC:DOTAP:TMX 85:10:5 rHDL, indicates that TMX-201 is effectively incorporated in the rHDLs.

hore (atto488) was used to detect the rHDL during flow cytometry analysis, while TMX-201 was used to initiate an immune response by activation of TLR7.

The absorption of the DOPE-atto488 in solution was measured, as seen in figure 4.17 A. It has an absorption peak at approximately 500 nm. Hence, following the absorption at 280 nm and 500 nm during SEC analysis, it could be assessed if DOPE-atto488 and apoA-I were eluted at the same retention volume which would indicate an effective incorporation of DOPE-atto488 in the rHDL. Note that rHDL without DOPE-atto488 did not have a significant absorption at 500 nm. The result can be seen in figure 4.17 B where the 0.1 mol% DOPE-atto488 was incorporated in POPC:DOTAP 90:10 rHDL with lipid/protein ratio of 200. Clearly, the DOPE-atto488 seems to be well distributed over the entire size distribution of rHDLs.

When formulating rHDL with TMX-201, the TMX-201 first had to be dissolved in the cholate solution, which was achieved with some difficulties using heating and sonication. The expected concentration of dissolved TMX-201 was confirmed by Martin Kisha Kræmer by reverse phase HPLC. Considering the absorption spectrum of TMX-201, see figure 4.17 C, it is evident that it has a peak around 280 nm. This could potentially be detectable by SEC analysis as well, i.e. a higher signal would appear for the rHDL with TMX-201 relative to the rHDLs without TMX-201, if TMX-201 was incorporated effectively. This was indeed found to be the case, see figure 4.17 D, and since the measured intensities seem higher over all the observed peaks, it is indicated that TMX-201 is well distributed over the entire size distribution of rHDLs. POPC:DOTAP:TMX 85:10:5 rHDLs with lipid/protein ratio of 200 were used.

Cholesterol-SIINFEKL was also incorporated in the rHDL, however, it did not have an absorption characteristic that could be used to assess the incorporation by SEC. Hence, other methods have to be used to evaluate the incorporation into the rHDL, e.g. by analysing the collected fractions from SEC by mass spectroscopy.

### 4.2.5 Estimation of the rHDL size

It has previously been stated that it is believed that rHDL of ∼10 nm is eluted during SEC analysis at retention volume of approximately 11.5 mL. However, a more direct estimate of rHDL size is desirable, as it would also be a confirmation of the successful formation of rHDL. Note that the size of the formulated rHDL might differ from the endogenous 9.6 nm sized HDL.

Two approaches were used to characterize the size of the rHDL. First of all, the size was estimated by SEC after calibration of the Superdex-200 column with proteins of known size. The used proteins were eluted as seen in figure 4.18 A (the proteins were obtained from a standard Gel Filtration Calibration Kit HMW from GE Healthcare). Using the peak position of each protein, the following correlation between the mass of the protein ($M_w$) and retention volume ($V_R$) could be obtained:

$$\log_{10}(M_w) = -0.21 \cdot V_R + 7.8$$
$$\Updownarrow$$
$$M_w = 10^{(-0.21 \cdot V_R + 7.8)}$$

Rather than the protein mass, it is actually the hydrodynamic radius of the proteins that is related to the retention volume[68]. It is stated in literature[68] that the correlation between protein mass (in Dalton) and hydrodynamic radius (in nm) can be estimated as $R = 0.081 \cdot M^{1/3}$, if the proteins are assumed spherical. Using this, and the previous obtained expression for $M_w$, the correlation between the retention volume and the hydrodynamic radius ($R_H$) can be estimated as follows:

$$R_H = 0.081 \cdot \left(10^{-0.21 \cdot (V_R) + 7.8}\right)^{1/3}$$
$$\Updownarrow$$
$$V_R = \frac{7.8 - \log_{10}\left(\left(\frac{R_H}{0.081}\right)^3\right)}{0.21}$$

where the units of $R_H$ and $V_R$ is nm and mL, respectively. The invesitgated rHDLs are presumably discoidal, hence, the hydrodynamic radius might not be identical to the radius of the disc[69]. It is stated in literature[69] that the correlation between the hydrodynamic radius and the radius of a disk is:

$$R_H = \frac{3R_D}{2}\left([1+\alpha^2]^{1/2} + \frac{1}{\alpha}\ln(\alpha + [1+\alpha^2]^{1/2}) - \alpha\right)^{-1}$$

where $R_D$ is the radius of the disc and $\alpha = \frac{L}{2 \cdot R_D}$. The thickness of the disk is $L$, and since it for the rHDL is considered as the thickness of the lipid bilayer, it is set to be 4 nm. Using this expression as $R_H$ in the previous expression for $V_R$, a dependence between $R_D$ and $V_R$ can be obtained numerically. The result for the diameter of the disc is seen in figure 4.18 B, which indicates that the rHDLs eluted at retention volumes of 11.5 to

12 mL seemingly have sizes between 10.3 to 11.4 nm. This is reasonable though slightly higher than the expected 9.6 nm. There might be some approximations in the used expressions which caused this difference. Furthermore, since the lipid composition of the rHDL differs from the endogenous rHDL, the diameter might not be exactly the same, even though the apoA-I proteins constitute the boundaries of the rHDL.

Although the calibration of the Superdex-200 column gives better insight into the size of the rHDL, it is still a relatively indirect measurement. Hence, in order to make a more direct estimation of the size, TEM analysis was conducted. It would give a more accurate insight into the rHDL structure by imaging them in aqueous condition. This can be achieved by using cryo-TEM, howe-

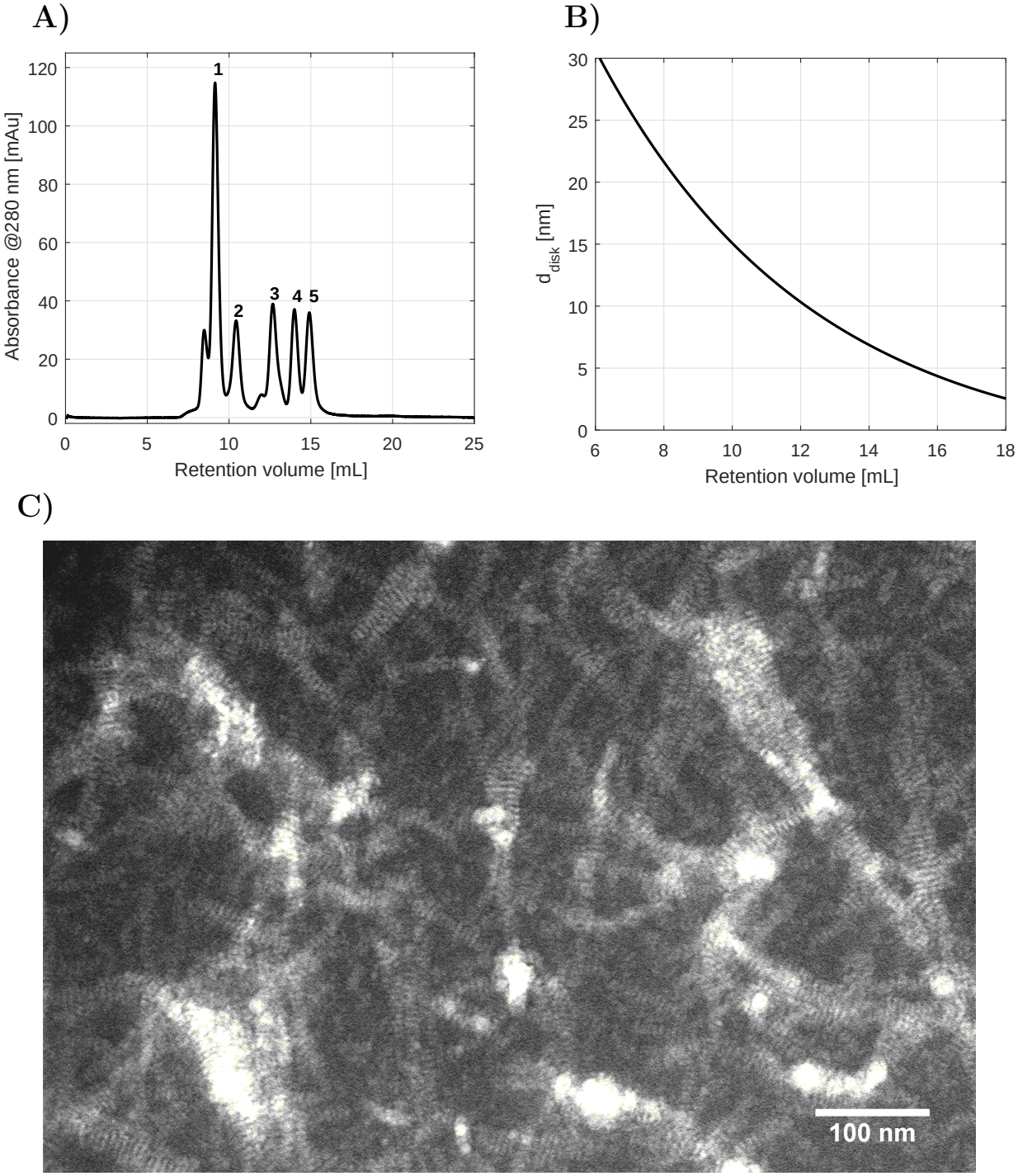


**Figure 4.18: (A):** Calbriation of the Superdex-200 column using proteins with different mass. The following proteins were used: 1) Thyroglobulin (669 kDa), 2) Ferritin (440 kDa), 3) Aldolase (158 kDa), 4) Conalbumin (75 kDa), 5) Ovalbumin (44 kDa). The corresponding peak is numbered in the figure. **(B):** The estimated correlation between the retention volume and the diameter of the discoidal rHDL particles. **(C):** TEM analysis using PTA as negative stain.

ver, though cryo-TEM measurements of some samples were conducted, it was not possible to observe the rHDLs clearly enough to make quantitative measurements due to too low contrast (data are consequently not shown). Hence, TEM analysis using negative stain was conducted instead. When using the negative stain PTA, rouleau structure appeared as expected, see figure 4.18 C. It has also been observed in other studies that PTA causes the formation of rouleau structure due to electrostatic interactions between the negative charge on PTA and positive charge on the head group of the phospholipids[63]. An average diameter of 11.75 ± 1.85 nm was measured from the rHDL rouleau structures. Again, this is slightly higher than the expected 9.6 nm, but fairly close to the estimate obtained from calibration of the Superdex-200 column. However, the boundaries of the rHDL rouleau structures in figure 4.18 C are not well-defined, hence, a great uncertainty is associated with the estimated size. More well-defined rHDL rouleau structures might appear if the concentration of rHDL in the investigated sample was lowered, since it might make it easier to obtain an image with better resolution, thereby obtaining a more accurate estimate of the rHDL size.

Although the size estimate from the TEM analysis is associated with great uncertainty, it is, however, a clear indication that rHDLs were successfully formulated and can be related to the peak seen around 11.5 - 12 mL during SEC analysis. Even though the size of the rHDL was estimated slightly higher than expected, the fact that the rHDLs behave as expected when using PTA and form rouleau structures further emphasizes the successful formation of rHDL. Another study, which also used apoA-I purified from human plasma, estimated the size of their rHDL with two apoA-I proteins to be ∼12 nm[37], illustrating that the size estimate might in fact be accurate, and that there are some flexibility in size even when restricted by two apoA-I proteins per rHDL. However, more studies are needed to confirm the exact size of the formulated rHDL.

### 4.2.6 Stability of the rHDL

The stability of the rHDL was evaluated by SEC, since changes in the size distribution, e.g. by aggregation or dissociation, would be detectable by SEC. The stability was investigated both when storing the samples at 4 °C for one week, and when storing the sample at 37 °C for 8 hours, since the temperature might have a significant effect on the stability.

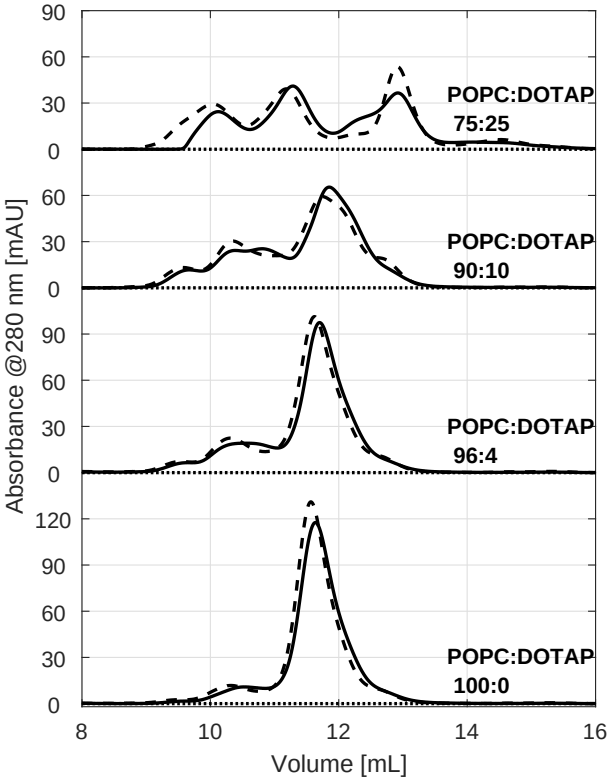


**Figure 4.19:** Investigation of the stability of the rHDLs at 4 °C using SEC. The rHDLs contained different mixtures of POPC and DOTAP, and were formulated with a lipid/protein ratio of 100. The solid lines represent the analysis taken immediately after preparation while the dashed line represent the analysis taken one week later. The same volume was loaded onto the Superdex-200 column for each sample.

The results from storing the samples at 4 °C are seen in figure 4.19. rHDL with POPC:DOTAP in varying ratios were used. The lipid/protein ratio was 100 for all the samples. The solid and dashed line represent the chromatograms immediately after preparation and one week later, respectively. It is evident that the chromatograms are similar indicating that the rHDLs are stable over one week at 4 °C. Furthermore, the peaks actually seem to be more distant after storage at 4 °C, which could be an indication of relaxation of unstable conformation into more stable rHDL conformation.

The results from storing the samples at 37 °C for 8 hours are seen in figure 4.20. It is evident that the storage at 37 °C clearly seem to affect several of the rHDL formulations by shifting the size distribution to larger

sizes, possibly due to aggregation. However, the effect seems to be minimal for the POPC rHDL while the DMPC and the POPC:DOPG 90:10 rHDLs seem to be stable over the 8 hours. The better packing of the saturated DMPC might explain the stability of DMPC rHDL while electrostatic interaction between the negative DOPG and apoA-I might explain the stability of the POPC:DOPG 90:10 rHDL. The instability at 37 °C of the rHDLs containing cationic lipids seems to be more pronounced as more cationic lipids are incorporated, and there does not seem to be a significant difference in the stability when comparing the rHDLs with either EPC or DOTAP incorporated. It is also noted that the amount of free apoA-I (attributed to peak around 14-15 mL) increase as the other peaks shift to lower retention volumes. It might be that the higher temperatures induces transformation to larger sized rHDL particles which might have more apoA-I proteins per particle. However, this transformation might also result in leakage of incorporated contents of the rHDL, e.g. drugs or fluorophore, thus obviously being unfavourable. During the experiments of this project where the rHDLs were incubated with blood at 37 °C, the incubation time was one hour, and though it is likely that the effect is less pronounced after only one hour, no stability measurements were taken to investigate this, thus, it might be that the observed instability already appear after one hour. Hence, the possible transformation to large sized rHDL particles have to be kept in mind when conducting experiments where the rHDL are incubated at 37 °C.

### 4.2.7 The possibilities of rHDL formulation

It is evident from the above discussion that rHDLs were successfully formulated with several lipid compositions. The DMPC rHDL yielded a clear monodisperse distribution when using the optimal lipid/protein ratio, while the POPC rHDL yielded a somewhat wider distribution with a minor shoulder to the left of the major peak. As previously discussed, this difference might be attributed to the fact that the saturated DMPC potentially packs better in the bilayer of the rHDL than the unsaturated POPC. It is also evident from figure 4.20,

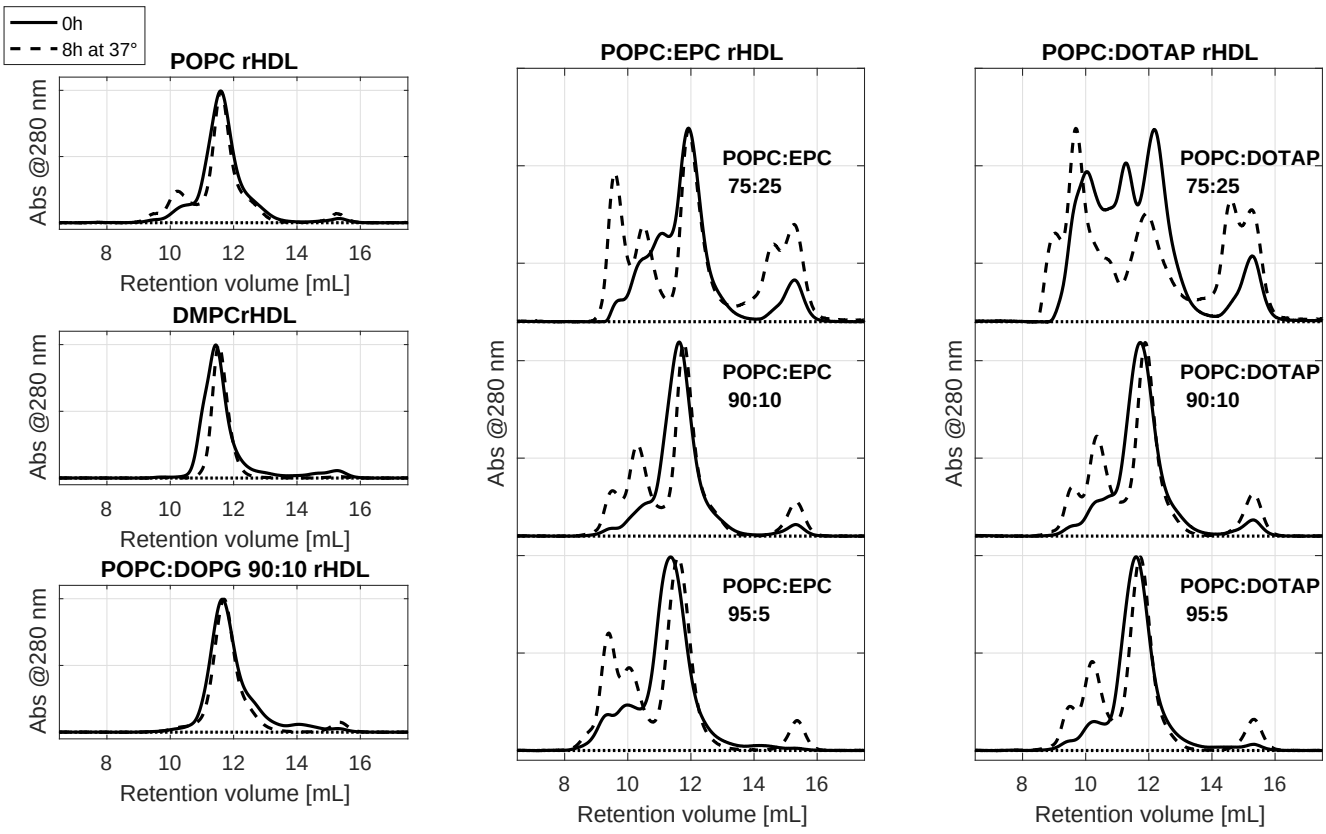


**Figure 4.20:** Investigation of the stability of the rHDL at 37 °C. The solid and dashed lines are SEC chromatograms obtained immediately after preparation and after 8 hours at 37 °C, respectively. A lipid/protein ratio of 100 was used for DMPC rHDL, while all the other formulations used a lipid/protein ratio of 80. The chromatograms are normalized, and only the retention volumes of interest are shown.

that formulation of POPC:DOPG 90:10 rHDL yielded a relatively monodisperse distribution without the shoulder to the left of the major peak. The negative charge might interact with the positive part of apoA-I, and these electrostatic interactions might favour the formation of stable rHDL. The charged lipids used in natural lipid bilayers are all negatively charged [67], hence, the endogenous HDL might also be stabilised by some negatively charged lipids. The incorporation of cationic lipids apparently impairs the structure of the rHDL by shifting the size distribution to larger sizes, however, when only 10% cationic lipids or lower are incorporated the effect seems to be minimal, though it induces some instability which becomes apparent after storage at 37 °C. Although there are some limitations when incorporating cationic lipids, it is illustrated that several types of lipids, fluorophore and drugs can be incorporated in the rHDL.

The rHDLs were in this project formulated by the detergent depletion method. Bio-Beads were primarily used to remove the used detergent cholate, however, other methods are also available which might be more favourable for some applications. The Bio-Beads can potentially interact with other substances in the sample than the cholate with it has to remove. It was for example observed by measuring the absorbance before and after applying the Bio-Beads during formulation of rHDL that the absorbance at 280 nm decreased approximately 20%. This is most likely because apoA-I binds to the Bio-Beads. It was also found that when using an increased amount of Bio-Beads during formulation of rHDL, an even larger decrease in absorbance at 280 nm was measured. The lipids might also bind, however, this could not be assessed by measuring absorbance. If it is mainly apoA-I which binds to the beads, it will clearly affect the lipid/protein ratio, and the ratio might differ between the samples, if the amount of used Bio-Beads vary. Furthermore, when incorporating drugs into the rHDL, these might also bind to the Bio-Beads. The drugs could potentially have an even higher affinity towards the Bio-Beads, thus resulting in a decreased amount of incorporated drugs. It was in this project observed that the TMX-201 concentration did not decrease significantly after incorporation with the drugs (Martin Kisha Kræmer measured the concentration of TMX-201 in the samples by reverse phase HPLC before and after treatment with Bio-Beads), however, it obviously has to be kept in mind that the Bio-Beads can interact with the substances in the sample. In some cases it might be more favourable to use dialysis to remove the cholate instead of Bio-Beads. The effect of using dialysis instead of Bio-Beads was also investigated, and as seen from figure 4.21, rHDL could seemingly be formulating successfully using dialysis as well. The chromatograms seem slightly different, and it is evident that the temperature used during dialysis also affect the size distribution of rHDL. It seems most favourable to conduct the dialysis at 4 °C, if a monodisperse distribution is desired. The substances of the samples might also bind to the dialysis membrane, however, it was found to be less than when using the Bio-Beads. The dialysis might also remove the cholate more effectively, and if the rHDLs have to be used for biomedical application the complete removal of cholate is important, since the detergent can cause cell lysis, resulting toxicity to healthy cells.

It must also be noted that other methods than the detergent depletion method can be used for formulation of rHDL, e.g. they can be formulated by mixing the apoA-I with liposomes or by mixing a lipid film with the apoA-I solution [1]. It was found in this project that cholesterol did not dissolve in the cholate solution, hence, if cholesterol was to be incorporated in the rHDL, other methods than the detergent depletion method might have to used.

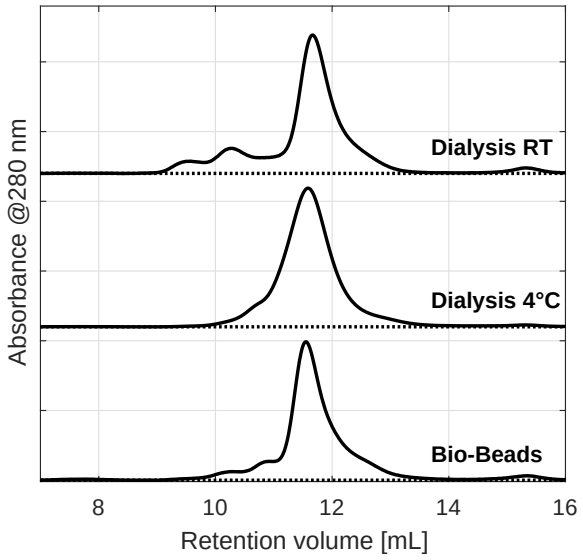


**Figure 4.21:** Investigation of using dialysis or Bio-Beads for removal of the detergent cholate during the formulation of rHDL. The dialysis was conducted at both 4 °C and room temperature. The chromatograms are normalized, and only the retention volumes of interest are shown.

## 4.3 Monocyte targeting and adjuvant delivery

The association of rHDL with leukocytes were investigated in order to be able to design rHDL which could target monocytes with the incorporated adjuvant TMX-201, thus being able to activate the TLR7 in monocytes which potentially can initiate an immune response that can fight the cancer cells.

The association of rHDL with leukocytes in WHB were studied by flow cytometry, while the cytokine secretion obtained when delivering TMX-201 with the rHDL was studied by ELISA. It is indeed relevant to use both methods since the flow cytometry only detects if the rHDLs associate with the cells, e.g. rHDLs which only adhere to the surface of the cells would be detected by the flow cytometry. If the rHDLs are not able to deliver TMX-201 to the endosomes, where the TLR7 is located, there would be no activation of the immune response, and consequently on cytokine secretion. Note that several leukocytes can secrete cytokines, as previously discussed, and it can be difficult to assess if the cytokines are caused by activation of TLR7 in monocytes, however, if both a high specific association of rHDL with monocytes and a significant cytokine secretion are observed, it would be an indication of an effective delivery of TMX-201 to the monocytes.

### 4.3.1 rHDL association with leukocytes

The association of rHDL with monocytes, lymphocytes and granulocytes, which are the main leukocytes in WHB, were studied by flow cytometry. They can be distinguished based on their morphology using FSC and SSC as discussed in section 2.4. In order to distinguish monocytes more accurately, they were stained with a CD14 antibody, since one of the characteristics of monocytes is their expression of CD14[50]. Hence, if cells were positive both for CD14 and atto488, they were considered to be monocytes with associated rHDL. Lymphocytes and granulocytes were only identified by their morphology gate. rHDLs formulated with both a lipid/protein ratio of 80 and 200 were used for the experiments. These results will be presented separately. Note that DMPC was formulated with a lipid/protein ratio of 100, but will be compared and discussed when considering the POPC based rHDL which use a lipid/protein ratio of 80.

**Using rHDLs with a lipid/protein ratio of 200**

A size distribution of the rHDLs appears when using a lipid/protein ratio of 200, hence, they can be used to assess if there was any association with monocytes for any of the different sized rHDL particles. Two donors were used for the experiments. rHDLs with lipid composition consisting of POPC, POPC:TMX-201 95:5, POPC:DOTAP 90:10 and POPC:DOTAP:TMX-201 85:10:5 were used for the experiments, all with 0.1 mol% DOPE-atto488 incorporated. The results from the experiments are seen in figure 4.22. The used gating strategy can be seen in appendix B.

It clearly seems that the rHDLs have a tendency to associate with the monocytes rather than to lymphocytes and granulocytes. It is interesting that the POPC rHDLs also associate with monocytes, since Pia T. Johansen et al.[50] did not observe any significant monocyte association when they used liposomes of similar lipid composition. When comparing the results with the results from the liposomes, it has to be noted that the rHDL is overall negatively charged, even though it has neutral lipid composition, due to the negative charge of apoA-I. However, since neither neutral nor anionic liposomes were found by Pia T. Johansen et al.[50] to associate significantly with monocytes, it indicates that the rHDL might be recognised by cellular receptors which do not recognise liposomes.

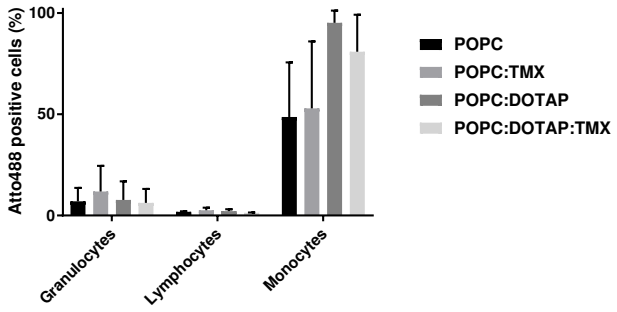


**Figure 4.22:** The association of rHDL with leukocytes using rHDLs formulated with a lipid/protein ratio of 200. The lipid composition of the rHDLs were: POPC, POPC:TMX-201 95:5, POPC:DOTAP 90:10, POPC:DOTAP:TMX-201 85:10:5. Furthermore, all rHDLs were formulated with 0.1 mol% DOPE-atto488.

The association of rHDL with monocytes is apparently higher when using rHDL consisting of POPC:DOTAP 90:10 compared to rHDL without DOTAP. The average amount of atto488 positive cells are approximately 95% for the POPC:DOTAP 90:10 rHDL without TMX. This result is comparable, and actually slightly higher, than the result observed by Pia T. Johansen et al.[50] when they used liposomes of similar composition. Hence, although the rHDL might still have a net negative charge, there seem to be an additional association with the monocytes which might be mediated by the same pathway that are responsible for the uptake of cationic liposomes. Incorporation of TMX-201 seems to decrease the association rHDL with monocytes, which might be because TMX-201 is negatively charged thus reducing the net charge of the rHDL. If this is the case, it does again indicate that the additional association with monocytes depend on the charge of the rHDLs, as it was observed for liposomes. Hence, there might be a charge dependent as well as a receptor mediated association of the rHDL with the monocytes. The results of this analysis are indeed promising since a seemingly preferred association to the monocytes is observed, especially when using DOTAP in the rHDL. However, cationic lipids such as DOTAP are often considered toxic, and though the use of relatively low concentration of DOTAP in liposomes have shown not to cause any toxicity[50], avoiding cationic lipids in the particles must be favourable, since risk of potential accumulation of toxic components in patients thereby is removed.

The rHDLs with a lipid/protein ratio of 200 are apparently a mixture of different sized rHDL particles and potentially some liposomes, as discussed in section 4.2.2. The POPC rHDL with a lipid/protein ratio of 200 seemingly yielded more liposomes than POPC:DOTAP 90:10 rHDL did, and since the POPC based liposomes apparently do not associate with monocytes, the lower association with monocytes observed for the POPC rHDL might be attributed to the presence of liposomes. Hence, further investigation were made on rHDL using lipid/protein ratio of 80 (and 100 for DMPC rHDL), since a more monodisperse distribution of these rHDLs were obtained, thus allowing for more accurate consideration of the effect from rHDL. Note that if no preferred association of rHDL with monocytes was observed for these rHDL, the effect observed in figure 4.22 must be ascribed to the larger sized rHDL particles.

**Using rHDLs with a lipid/protein ratio of 80**

The results from the experiments which used rHDLs with a lipid/protein ratio of 80 (and 100 for the DMPC rHDL) are seen in figure 4.23, where WHB from one donor was used. An important difference between these results and the results presented in figure 4.22, is that the concentration of DOPE-atto488 in the rHDL was increased from 0.1 to 1 mol% of the lipids. Due to the small size of rHDLs there might not be DOPE-atto488 in all the rHDLs when using 0.1 mol% DOPE-atto488, thus several rHDL particles might have to be associated with each leukocytes in order to yield a positive signal. Therefore, the concentration was increased to 1 mol% DOPE-atto488 such that each rHDL statically should contain at least one fluorophore, i.e. the association of a single rHDL would make the leukocyte positive for atto488.

It is evident from figure 4.23 A that all the used formulation of rHDL, i.e. POPC, POPC:DOTAP 90:10, POPC:EPC 90:10, POPC:DOPG 90:10 and DMPC rHDLs (all with 1 mol% DOPE-atto488 and corresponding decrease in amount of POPC/DMPC), show high association with monocytes. For each rHDL formulation, almost all of the monocytes are associated with rHDL. The use of higher concentration of DOPE-atto488 could potentially have increased signal compared to the results from figure 4.22, where all monocytes might have had associated rHDL but some of the rHDLs might not have contained DOPE-atto488. The use of different lipid/protein ratios might also have affected the results, e.g. if the smaller rHDLs are preferably taken up in monocytes. It might mainly be the ∼10 nm sized rHDL which associated with monocytes when using a lipid/protein ratio of 200, and since a rather larger fraction of the rHDLs in the batch presumably was larger sized rHDL particles or potentially liposomes, this might have reduced the effect compared to the relative monodisperse rHDL formulated with a lipid/protein ratio of 80, which all yielded high association with monocytes. It must be noted that the detection of rHDL is based on the fluorescence from atto488, hence, if DOPE-atto488 leaks out of the rHDL when incubated with WHB, and the free DOPE-atto488 associates with the cells, it would yield a positive signal which could be misinterpreted as if rHDL was associated with the cell. However, since the DOPE-atto488 seems to be successfully incorporated into the rHDL, refer section 4.2.4,

it is likely that the leakage would be minimal during the one hour of incubation with WHB, though this cannot be assessed explicitly based on the current results.

It is also evident from figure 4.23 A that there do seem to be some of the rHDL associating with granulocytes and lymphocytes, i.e. though there is a high association with monocytes, the association with other leukocytes decreases the specificity towards monocytes. The DMPC rHDL seemingly also associate with granulocytes to a relatively high extent. However, it is important to note that results presented in figure 4.23 A and 4.22 represent how many of the cells that are positive for atto488, hence, it does not give information about how many rHDLs that are associated with each cell. An indication of the relative amount of rHDLs associated with each cell can be obtained by considering the mean fluorescence intensity (MFI). The measured MFIs (normalized with the MFI of an untreated sample) are presented in figure 4.23 B. It is seen that there are differences between the different rHDL formulation when considering the MFI. Furthermore, the MFI for the lymphocytes and the granulocytes are relatively low, indicating that only a minimal amount of rHDLs are associated with each of these cells. Incorporation of cationic lipids, seem to increase the MFI from the monocytes compared with the MFI obtained when using POPC rHDL, and incorporation of DOTAP seems to cause a higher increase in MFI than EPC. Using POPC and POPC:DOPG 90:10 rHDL yield comparable MFI from the monocytes. The MFI for the DMPC clearly stays out. It is evident that though the percentage of granulocytes associated with DMPC rHDL is relatively high, a much higher amount of DMPC rHDL associate with each of the monocytes than with each of the granulocytes.

As previously discussed, there could potentially be several mechanisms involved in the association, and potential uptake, of rHDLs with the monocytes. There might be a receptor mediated uptake as well as a charge dependent uptake, i.e. additional rHDLs with slightly cationic lipid composition might be taken up due to the charge. There could also be other explanations for additional association with the rHDL with cationic lipid composition. For example, it was observed that the incorporation of cationic lipids induces instability at 37 °C, refer section 4.2.6, hence, the instability might have caused structural changes in the rHDL after only one hour, thus resulting in leakage of the DOPE-atto488, and the free DOPE-atto488 could have been taken up by the monocytes thereby resulting in a higher signal.

The fact that high amount of DMPC rHDLs associate with the monocytes is indeed interesting. The DMPC seems to pack better into the rHDL than POPC, and the resulting DMPC rHDL seems to be more stable than POPC rHDL. Hence, they could potentially be more susceptible to be recognised by cellular receptors. Nature primarily uses unsaturated lipids[67], and it might also be an uptake from the monocytes initiated by the recognition of a foreign HDL. However, neither

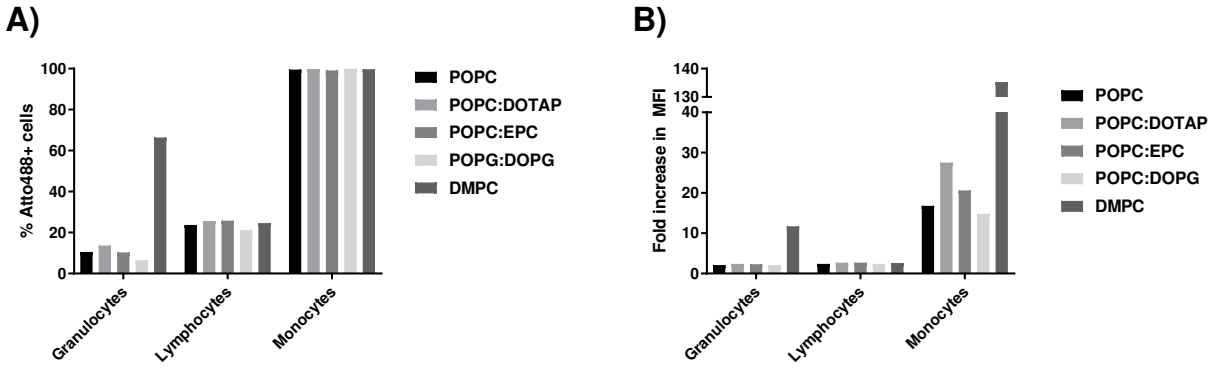


**Figure 4.23:** The association of rHDL with leukocytes. The used rHDLs had following lipid compositions: POPC:atto488 99:1, POPC:DOTAP:atto488 89:10:1, POPC:EPC:atto488 89:10:1, POPC:DOPG:atto488 89:10:1 and DMPC:atto488 99:1. **(A):** The amount of either granuocytes, lymphocytes and monocytes associated with rHDL. Almost 100 % of the monocytes (gated CD14 positive) have apparently associated rHDL **(B):** The measured MFIs (normalized with the MFI of an untreated sample) which show some difference between the different rHDL formulations, and indicate that more rHDLs accumulate in each of the monocytes compared to each of the granulocytes and lymphocytes.

the isolated DMPC nor apoA-I should cause a significant immune response, and it seems more likely that it is a receptor mediated process which take up DMPC, probably because it is less dynamic than the POPC based formulations. Note that none of the formulations can be compared directly with endogenous HDL, since the lipid composition of endogenous HDL probably will consist of several types of phospholipids as well as cholesterol.

Another important consideration is the fact that only one donor was used for these experiments. There can be a relatively large variation between the donors, and obviously more experiments with additional donors are required to confirm the observed effects explicitly.

### The presence of SR-B1 on leukocytes

There are various receptors on the monocytes which could be responsible for the seemingly preferable association of rHDL with the monocytes. As efflux of cholesterol from endogenous HDL is mediated by the SR-B1, it could be interesting to study if this receptor is present on monocytes and not on granulocytes or lymphocytes. Experiments were conducted using a SR-B1 Antibody from Novus Biologicals (England) when analysis WHB by flow cytometry (the measurements were conducted by Ditte Villum Madsen). The results can be seen in figure 4.24. The SR-B1 receptor does indeed seem to be present on most of the monocytes while only relatively low amount of lymphocytes and granulocytes seem to express the SR-B1. Furthermore, the measured MFIs indicate that each monocytes express more SR-B1 than lymphocytes and granulocytes. Since it is known that the SR-B1 recognises HDL, this could explain the observed preferred association with monocytes. Note that the SR-B1 receptor might not necessarily mediate an uptake into the endosomes[19], thus a SR-B1 mediated uptake might not be favourable if the delivered cargo is the TLR7 agonist, since it requires endocytic uptake to be effective.

The presence of SR-B1 on monocytes does not necessarily guarantee that the observed preferred monocyte association is SR-B1 mediated. Thus, in order to more effectively study if the preferred association depended on the SR-B1 receptor, the antibody specific for the SR-B1 was used to block the receptor during experiments with the rHDL. However, this yielded inconclusive results, since some of the formulation had higher association with the cells when blocking the SR-B1 while other formulation did not, and an isotype control yielded similar effects as when using the SR-B1 antibody. The data are consequently not shown. These inconclusive results might be because the SR-B1 antibody was not purified, and other substances in the samples might have interfered with the leukocytes. Hence, further studies are needed in order to assess if the association actually is SR-B1 mediated.

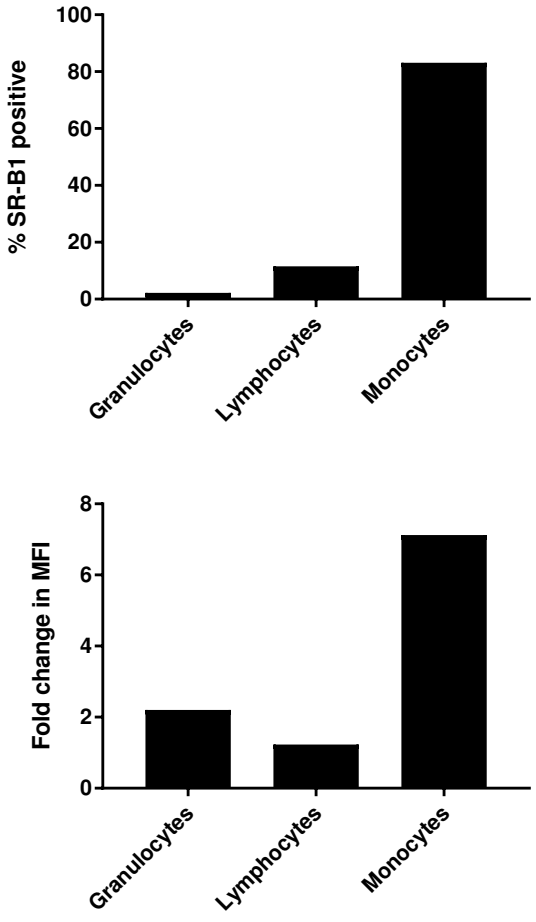


**Figure 4.24:** Estimation of the presence of SR-B1 on granulocytes, lymphocytes and monocytes using an antibody specific for the SR-B1 during flow cytometry analysis of WHB. The top figure shows percentage of cells associated with the SR-B1 antibody, and the bottom figure shows the MFI which indicates the relative amount of SR-B1 on each cell. The measurements were conducted by Ditte Villum Madsen, and the figures are printed with her permission.

### Estimation of the amount of associated rHDL

The MFI gives an indication of the relative amount of rHDLs in each cell, however, other methods have to

be used to estimate the total amount of rHDL associated with the cells. One way that this could be achieved is by SEC analysis of the supernatant obtained after incubating the rHDLs with WHB for one hour, since the non-associated rHDLs would be present herein. The absorbance could be followed during SEC analysis at 500 nm, and since the serum should not absorb significantly at 500 nm, it should be possible to detect the atto488, which is incorporated in the rHDL. The chromatograms from SEC analysis of the supernatant from both an untreated sample and a sample treated with DMPC rHDL are seen in figure 4.25. The pure DMPC rHDL was also characterized by SEC prior to the incubation with WHB. For a valid comparison between the chromatograms of pure rHDL and the supernatant from the experiments, the absorbance values were adjusted taking the dilution of the supernatant and different volume loaded onto the Superdex-200 column into account. The amount of rHDL was estimated by the integral of chromatograms between retention volumes of 10 mL and 13.3 mL. The integral from the untreated sample was subtracted from the integral from the sample treated with rHDL, and compared with the integral from the chromatogram of the pure rHDL. Using this approach it was estimated that approximately 70% of the applied DMPC rHDLs were associated with the cells. Similar results were obtained for the other rHDL formulations where 60-72% of the rHDLs seemingly were associated with the cells. The amount of associated rHDLs might be increased further by using a lower incubation time with WHB. Also, it is noted that the majority of the DOPE-atto488 still seems to be incorporated in the rHDL, as it probably would be detectable at other retention volumes if DOPE-atto488 had leaked out. Thus, it is indicated that a relatively large fraction of the rHDLs is associated with the cells, which are indeed promising for the immunotherapeutic applications.

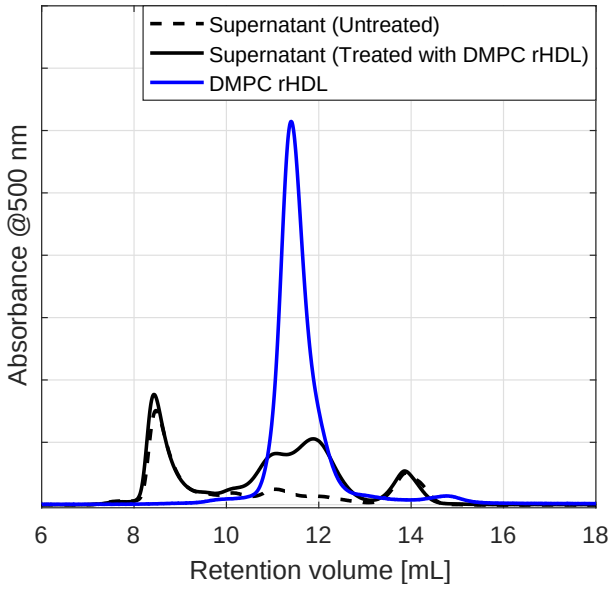


**Figure 4.25:** Estimation of amount of DMPC rHDL associated with the cells using SEC analysis of the supernatant removed after incubating the rHDLs with WHB. The chromatograms are adjusted based on dilution and different amount loaded to the SEC column. It was estimated that ~70% of the DMPC rHDLs were associated with the cells.

### 4.3.2 Study of cytokine secretion

In order to investigate if rHDLs loaded with the TLR7 agonist, TMX-201, could initiate an immune repsonse, they were incubated in WHB for one hour, and the resulting cytokine secretion was studied by ELISA. The cytokines IL-6, IL-10, IL-12p70 and IFN-$\alpha$ were investigated. As previously discussed, these cytokines can be secreted from various leukocytes, hence, even though a preferred association with monocytes were observed, the cytokines might also be secreted by the other leukocytes to which the rHDLs also associated to a minor extent. The measurement of secreted cytokines can, however, still be used to assess if an immune response actually is initiated. The result can be seen in figure 4.26. The lipid composition of the used rHDLs are noted in the figure caption. The rHDL formulations are similar to the formulations used when the HDL association with leukocytes was considered, refer figure 4.23, with the exception that 5 mol% TMX-201 and no DOPE-atto488 are incorporated. Experiments were also conducted with rHDLs without TMX-201 (using POPC and POPC:DOTAP 90:10 rHDL with lipid/protein ratio of 200), which confirmed that no cytokines were secreted when formulated without TMX-201 (data not shown).

It is evident that only low amount of IL-12p70 is secreted. The measured values are lower than the minimal value of the used standard curve, and cannot be considered valid as it might merely be uncertainties associated with the measurements. It is also evident from the results that the free TMX-201 cause much cytokine secretion for especially IL-6 and IL-10. In contrast, when Pia T. Johansen et al.[50], who studied monocyte targeting liposomes, conducted similar measurements

of cytokine secretion, they observed only minimal amount of IL-6 secretion when using free TMX-202, refer figure 1.10. It is unlikely that this difference is caused by the difference between TMX-201 and TMX-202 as it is only the length of the hydrophobic tail that differs, however, they might have used other experimental parameters which have limited the amount of cytokine secreted when using free TMX-202. As previously mentioned free TLR agonists can cause an undesirable cytokine storm, hence, though the observed effect differs from what was observed by Pia T. Johansen et al.[50], it does seem likely that free TMX-201 cause some cytokine secretion, and the results are believed to be reliable.

Except for IFN-$\alpha$, all rHDL formulations cause secretion of less cytokines than the free TMX-201. Hence, it cannot be excluded that a minor fraction of the TMX-201 which has not been incorporated into the rHDLs or has leaked out, have yielded some of the observed effects. However, the fact that equivalent, or slightly higher, amount of IFN-$\alpha$ is secreted when using most of the rHDL formulations indicate that the rHDLs do deliver the TMX-201 to the cells. The cytokine secretion might be preserved over longer time period when using the rHDL, or the effect might be more pronounced if a longer incubation were used, hence, the seemingly minor amount of cytokine secreted does not necessarily mean that the delivery of TMX-201 is ineffective. It has to be taken into account that too much cytokines can be secreted, especially of the IL-6 and IL-10 which are unfavourable for an anticancer immune response. The R848 is a water soluble TLR7 agonist, and it seems to cause a more favourable cytokine secretion because a relatively high amount of IFN-$\alpha$ is secreted, and the amount of IL-6 and IL-10 are lower than for free TMX-201. Although, lower amount IFN-$\alpha$ is secreted when using the rHDLs compared to R848, the secreted amount of IL-6 is only slightly lower when using rHDL formulations of POPC:DOTAP, POPC:EPC and POPC:DOPG compared to R848. All rHDL formulations secrete only a minor amount of IL-10.

It is interesting that almost no cytokines are secreted when delivering TMX-201 with DMPC rHDL, especially as relatively high amount of these DMPC rHDLs

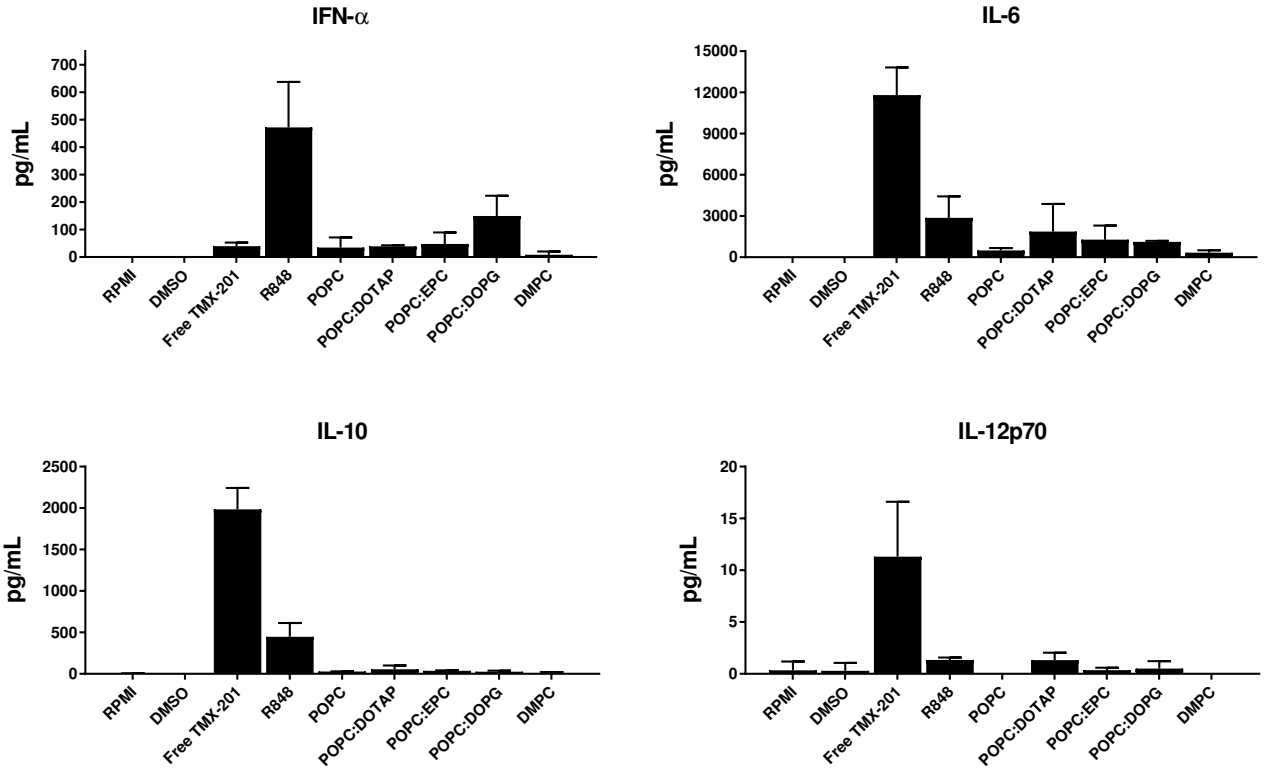


**Figure 4.26:** Study of cytokine secretion by ELISA caused by delivering TMX-201 with rHDLs. The lipid compositions of the used rHDLs were as follows: POPC:TMX-201 95:5, POPC:DOTAP:TMX-201 85:10:5, POPC:EPC:TMX-201 85:10:5, POPC:DOPG:TMX-201 85:10:5, DMPC:TMX-201 95:5. The concentration of TMX-201 was approximately 10 $\mu$M after mixing the rHDL with WHB. The data are based on results from two donors.

were found to associate with monocytes, and some of them also associated with granulocytes, refer figure 4.23. There could be several explanations for this. The observed high association of DMPC rHDL with monocytes might for example not be the same when using another donor. Also, the DMPC rHDL was shown to be more stable than POPC based rHDL formulations, and it might be that the TMX-201 in the DMPC rHDL cannot interact with the TLR7 after being taken up in the endosomes due to a too tight packing into the DMPC bilayer. Another explanation could be that DMPC rHDL interact with receptors, e.g. SR-B1, which can facilitate a non-endocytic uptake, thereby circumventing the endosomes where the TLR7 is located. However, Rui Kuai et al. [55] did use DMPC based rHDL with a TLR9 agonist and observed an immunotherapic effect when using the TLR9 agonist, illustrating delivery of their formulated rHDLs to the endosomes where the TLR9 is located. Despite this result, the DMPC rHDL of this project could still be taken up differently, since Rui Kuai et al. [55] formulated the DMPC rHDL differently, e.g. they used apoA-I mimicking peptides instead of apoA-I purified from human plasma.

It has previously been discussed that IFN-$\alpha$ and IL-12p70 are favourable for an anticancer immune response while secretion of IL-6 and IL-10 is unfavourable. Hence, considering the ratio between IFN-$\alpha$ and the sum of IL-6 and IL-10, the applicability of the formulation for cancer immunotherapy is better illustrated, see figure 4.27. Note that IL-12p70 is not including in the calculations, as these results are considered unreliable. The results from the POPC and DMPC rHDL are rather arbitrary seeing as only minimal amount of cytokines are secreted when using these formulations, and minor fluctuations would affect the ratio significantly. The other rHDL formulations do yield a ratio which is higher than the ratio obtained from using free TMX-201 which again indicates that the rHDLs have interacted with the cells to deliver TMX-201, since leakage of TMX-201 most likely would have resulted in an effect comparable with the effect observed for free TMX-201. The POPC:DOPG 90:10 rHDL yields the highest ratio of the rHDLs formulations due to the highest secretion of IFN-$\alpha$.

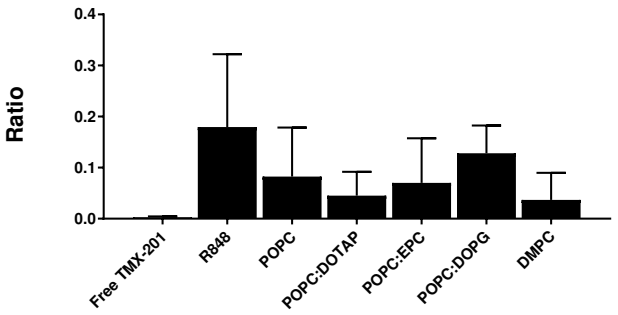


**Figure 4.27:** The ratio between IFN-$\alpha$ and the sum of IL-6 and IL-10 for each sample. The IFN-$\alpha$ is favourable for an anti-cancer immune response, while the IL-6 and IL-10 are unfavourable, hence, higher ratios indicate a better anti-cancer immune response. The data are based on results from two donors.

The observed results indicate that the rHDLs interact with the leukocytes and deliver TMX-201 which cause cytokine secretion, however, it cannot be assessed how much of the applied TMX-201 is delivered effectively. Furthermore, based on these results, it cannot be evaluated if the cytokines are secreted by monocytes or other cells, e.g. since pDCs secrete much IFN-$\alpha$ it is likely that the secreted IFN-$\alpha$ is from pDCs. Comparing the results with the results from Pia T. Johansen et al. [50] presented in figure 1.10, it is seen that the amount of secreted IL-6 caused by using rHDL is in the same range as the amount that they measured when using liposomes with 10 $\mu$M TMX-202. They also measured a relatively high amount of IL-12p40. Although IL-12p40 is a subunit of IL-12p70, they might not be directly correlated since more IL-12p40 could be secreted prior to the assembly into the IL-12p70, thus these data cannot be compared. It would have been interesting to study the secretion of IL-12p40 as well as other cytokines caused by delivering the TMX-201 with the rHDLs to more explicitly confirm that an immune response actually was initiated. In order to investigate if the cytokine secretion was initiated by monocyte activation, cytokines such as IL-1 and IL-15 which are secreted from monocytes [44] could be investigated. Note that these cytokines also can be secreted from other types of cell, but if high amounts are measured, it would give a clear indication of monocyte activation.

## 4.4 Antigen delivery to dendritic cells

For an effective immune response against the cancer cells, the delivery of adjuvant, as described in the previous section, might not be sufficient, since it only boosts the immune response, and more specifically directing the immune response to eliminate the cancer cells might be required. This can be achieved by delivering tumour antigen to DCs, which in turn can present the antigens to cytotoxic T-cells. There are several types of DCs, and the focus will in the following be cDC1s, cDC2s and mDCs. It was investigated if antigen could be taken up by the DCs and presented through the MHC-I. The peptide SIINFEKL was used as the model antigen, and in order to detect when SIINFEKL was presented as desired, an antibody specific for the SIINFEKL:MHC-I complex was used. The SIINFKEL peptide was cholesterol-anchored in order to make incorporation into the rHDL feasible. The cholesterol-anchor needs to be removed for SIINFEKL to be presented through the MHC-I. The cholesterol is linked to SIINFEKL by a disulfide bridge which can be reduced in the reductive environment of the cytosol. Hence, if taken up in the endosomes, it needs to be cross-presented to make presentation by MHC-I possible. Furthermore, free cholesterol-anchored SIINFEKL which are neither taken up by the DCs nor cross-presented and processed (if taken up by endocytosis), cannot yield an observable signal, since it is only the SIINFEKL:MHC-I complex which is detectable.

The rHDLs loaded with cholesterol-anchored SIINFEKL were mixed with isolated DCs, and the cells were subsequently analysed by flow cytometry for atto488 and the SIINFEKL:MHC-I complex. POPC:DOTAP:SIINFEKL:atto488 84.5:9.5:5:1 rHDL formulated with a lipid/protein ratio of 75 were used for the experiments. The results can be seen in figure 4.28. It is evident from figure 4.28 A that all the DCs seem to have some associated rHDLs, however, the mDC apparently take up more rHDLs relative to the other types of DCs. Note that since DOPE-atto488 is incorporated in the rHDL, the measurement of atto488 indicates the presence of rHDL. Furthermore, rHDLs which only adhere to the cell surface would also yield a positive signal, hence, these measurements do not directly correlate with uptake of rHDL. All the DCs seem to express the SIINFEKL:MHC-I complex with approximately equal intensity, as seen from figure 4.28 B. Hence, when considering the ratio between MFI of the SIINFEKL:MHC-I complex and atto488, see figure 4.28 C, the cDC1s yield a much higher ratio than for the other types of DCs. This indicates that though cDC1s do not take up much of the rHDLs, they are very effective at presenting the SIINFEKL that they do take up. The different types of DCs have different properties, and it is illustrated from these results that cDC1s seem better at presenting antigens through the MHC-I though it is not as effective at engulfing foreign material. If the rHDLs are taken up in endosomes, it could be because the cDC1s are better at cross-presenting the cholesterol-anchored SIINFEKL. It could also be that the cDC1s do not take up the rHDLs in the endosomes but another mechanism

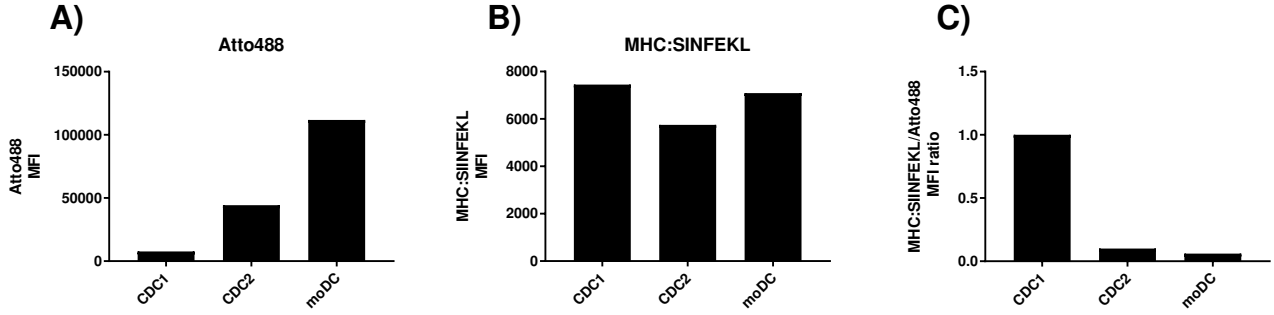


**Figure 4.28:** Delivery of SIINFEKL to DCs by rHDLs. The rHDLs were formulated with lipid composition of POPC:DOTAP:SIINFEKL:atto488 84.5:9.5:5:1, and a lipid/protein ratio of 75. The cholesterol-anchored SIINFEKL needs to be processed by the cells before it can be presented on the MHC-I. **(A):** The MFI from atto488 in each type of DC. The measured atto488 indicate uptake of rHDL. **(B):** The SIINFEKL:MHC-I complex was detected using a specific antibody. **(C):** The ratio between MFI from the antibody detecting the SIINFEKL:MHC-I complex and atto488, which indicate the cDC1s are better at presenting the SIINFEKL which they have taken up, compared to the other types of DCs.

is involved such that the cargo of the rHDL is delivered to the cytosol, which could lead to a more effective presentation of SIINFEKL through the MHC-I.

One of the purposes of delivering the TLR7 agonist to monocytes was, besides causing cytokine secretion, to initiate differentiation of the monocytes into mDCs, which then should be capable of presenting antigen to T-cells. These results indicate the mDCs are less effective at presenting the antigen compared to other types of DCs, however, the mDCs seem to take up relatively many rHDLs, thus when targeting TLR receptors located in the endosomes, the high uptake is clearly favourable, if it is endocytic. It is likely that the monocytes and mDCs have various similar properties which might explain the high potential uptake of rHDLs in both monocytes and mDCs. In order to optimize the antigen presenting, it might be more effective to design systems which targeted the cDC1 specifically. However, the presentation of SIINFEKL might be limited to the amount of MHC-I present on the cells, and all MHC-I might be saturated with SIINFEKL. In this case it would not increase the presentation of antigen, if more rHDLs were taken up by the cDC1s. Note that certain cytokines can increase the amount of MHC-I on the cells[44], hence, delivering adjuvants might induce the secretion of these cytokines and increase the antigen presentation.

More experiments are obviously needed to evaluate the observed effect more thoroughly. It is, however, evident that the rHDLs seem capable in delivering antigen to DCs such that the antigen can be processed and presented by the MHC-I.

## 4.5 The application of rHDL for cancer immunotherapy

The application of rHDL to immunotherapy is motivated by their biocompatibility, biodegradability as well as their high tolerance and long circulation time in humans. The small size of the rHDL is also an attractive property, especially seeing as other nanoparticles commonly used for DDSs, e.g. liposomes, are limited to larger sizes. This project has shown that rHDL can be designed to effectively associate with monocytes, which can be utilized for adjuvant delivery. Furthermore, the rHDLs have also proven capable in delivering antigen to DCs. This obviously illustrates the applicability of rHDL for cancer vaccine. The rHDLs might also be utilized merely as adjuvant therapy to boost the immune response during for example radio- or chemotherapy.

It is interesting that the endogenous HDLs have anti-inflammatory properties such as down-regulation of the proinflammatory properties of certain leukocytes by modification of the cell membrane structure. However, it might in fact be these properties which are responsible for the association of rHDL with the monocytes and DCs and allows for the delivery of immunotherapeutic drugs, which can initiate a proinflammatory immune response. The rHDLs might still cause some anti-inflammatory effects during the association with leukocytes, however, this effect would probably be minimal compared to the proinflammatory response from the delivered cargo. It must also be noted that the properties of the endogenous HDL and rHDL might differ due to structural differences, e.g. the rHDL might be so tightly packed that the cholesterol influx to the rHDL is minimized, and consequently only minor modification of the cell membrane structure can occur.

Another important consideration when using rHDL for biomedical applications is the possible transformation into spherical HDL. Endogenous HDL transforms from discoidal to spherical when cholesterol is esterified by LCAT and internalized into the core of the HDL.This could happen for the rHDL as well, however, when the rHDL is not formulated with cholesterol, an influx of cholesterol to the rHDL is required before a possible transformation can occur. The tight packing of the lipids in the rHDL might minimize the influx of cholesterol, however, it cannot be ruled out that some cholesterol will accumulate in the rHDL over time, and can be internalized into the rHDL after being converted into cholesteryl ester by the LCAT. The possible transformation into spherical can lead to leakage of drugs, as it has been shown in other studies[36], thereby, illustrating the importance of understanding the biological fate of the rHDL when applying them for biomedical applications.

Although the rHDLs were found to associate preferably with monocytes in WHB, some of the rHDLs also as-

sociated with granulocytes and lymphocytes. Furthermore, DCs could take up the rHDLs, and especially the mDCs seemed to take up much of the rHDL. As the mDCs are derived from monocytes it might be the similar mechanisms that is responsible for the uptake in both cell types. Even though the POPC:DOTAP 90:10 rHDL was the only formulation investigated for the DC uptake, it is likely that similar effects would be seen for other rHDL formulations. Hence, when applying the rHDLs for immunotherapeutic applications, one must consider the fact that the rHDLs are taken up in several leukocytes, and will probably accumulate in both monocytes and DCs depending on the administration route. This means that the used immunotherapeutic drugs have to be designed not to cause undesirable effect when taken up by other leukocytes than the target cells.

It could be interesting to study the mechanism responsible for the preferred association with monocytes. As previously discussed, it could be a SR-B1 mechanism as monocytes seemingly express more SR-B1 than granulocytes and lymphocytes, however, more studies are needed to confirm that this receptor is involved. If it is found that the mechanism indeed is SR-B1 mediated, the rHDL would not necessarily be taken up in the endosomes as this receptor can also mediate a delivery of cargo to the cytosol. Uptake of the cargo to the cytosol would hinder an effect when using the TLR7 agonist, since TLR7 is located in the endosomes. However, a direct delivery to the cytosol could be of great potential for antigen delivery to DCs. The antigens need to be presented by the MHC-I for presentation to cytotoxic T-cells, and since the MHC-I is only accessible through the cytosol, it is likely that it would be more effective to deliver antigens directly to the cytosol than to the endosomes, where subsequent cross-presentation of the antigen is required. Thus, the rHDL could prove to be very useful for antigen delivery to DCs. However, the fact that cytokine secretion is observed during the experiments of this project indicate that some of the rHDLs are taken up in the endosomes of certain cells. Rui Kuai et al.[55] co-delivered antigen and a TLR9 agonist with rHDLs to DCs, and since TLR9 is located in the endosomes, these rHDLs had to be taken up in the endomses for an effect of the adjuvant. Hence, it seems that the rHDLs can be taken up by DCs by endocytosis though this do not exclude the possibility for a direct delivery to the cytosol. If the DCs express the SR-B1 as the monocytes, which is likely that mDCs do, the rHDL might be designed to utilize the SR-B1 for direct delivery to the cytosol. It might also be effective to deliver the antigen to the cytosol of the monocytes, and subsequently deliver adjuvants which can cause them to differentiate into DCs, which then can express the pre-delivered antigen. Further studies are needed to evaluate the mechanism involved in the interaction between rHDL and the leukocytes, and as evident from the above discussion, a deeper insight into the mechanism would aid the development an optimized design of the rHDL for immunotherapeutic applications.

It was found in this project that it was possible to design rHDLs which associated with monocytes to similar extent, as it had been observed for liposomes by Pia T. Johansen et al.[50]. Furthermore, the fact that a preferred association with monocytes was observed even when using rHDLs with a neutral lipid composition is of great interest, since the use of potentially toxic cationic lipids are avoided. A slightly cationic charge was observed by Pia T. Johansen et al.[50] to be required for the liposomes to obtain a similar monocyte association, illustrating the advantage of using rHDL.

Although the rHDL has several advantages for immunotherapeutic applications compared to other commonly used nanoparticles, they lack the possibility to deliver the immunotherapeutic drugs in a continuously manner[19]. A controlled release is one of the advantages of polymeric nanoparticles, and one could imagine that an effective cancer immunotherapeutic treatment would require continuous supply of either adjuvants or antigens to ensure a sustained anticancer immune response until tumour elimination. It has been reported in literature that rHDL can be designed with a polymeric core from which a sustained release can be obtained[19], illustrating even more possibilities for modification of the rHDLs. Thus, the design of the rHDL is not limited to simple variations in the lipid composition, and the promising results of this project could potentially be optimized further by other modification of the rHDLs.

As it is the case for several of the immunotherapeutic cancer therapies, the rHDL based cancer immunotherapy investigated in this project, might work even better in combination with other cancer treatments such as radio- or chemotherapy. rHDLs also have the potenti-

al to deliver chemotherapeutic drugs to the tumours, hence, a cocktail of rHDLs with either chemotherapeutic and immune stimulating drugs designed to reach the tumour or monocytes/DCs, respectively, has the potential to be an effective cancer treatment.

In order to confirm the observed effects of this project explicitly, the studies needs to be supported by more experiments. These additional experiments should also include other types of nanoparticles, e.g. liposomes, for a valid comparison between the commonly used nanoparticles and the rHDLs. However, the results of the project do indeed indicate that the rHDLs are promising candidates for carrier in a potent cancer immunotherapeutic DDS.

# 5. Conclusion

ApoA-I was purified from human plasma to ensure the necessary supply required for the formulation of rHDL. The purification method was optimized over several purification experiments, and the optimized method yielded a relatively high yield and high purity, i.e. 12 mg apoA-I (>99%) was obtained from 50 mL plasma.

The purified apoA-I was used to formulate discoidal rHDLs by the detergent depletion method using Bio-Beads to remove the detergent cholate. The lipid/protein ratio prove to be an important parameter, since it could affect the size distribution of the rHDLs, i.e. there seems to be an optimal ratio for a monodisperse distribution, which depends on the used lipid. Larger sized rHDL particles could seemingly be obtained by increasing the lipid/protein ratio above the optimal ratio, however, formation of smaller rHDLs seemed more favourable. The size of the smaller rHDLs was estimated by SEC and TEM to be between 10 - 12 nm, however, this estimate was associated with some uncertainty, and as the size of the endogenous discoidal HDL is 9.6 nm, it is likely that the rHDLs actually had similar size.

Incorporation of cationic lipids (DOTAP and EPC) in POPC based rHDLs was found to affect the size distribution of the rHDLs by shifting it to larger sizes, and induced instability at 37 °C, though they seemed stable at 4 °C for one week. POPC based rHDL with a slightly anionic lipid composition (POPC:DOPG 90:10) and DMPC rHDL did, in contrast, yield a monodisperse distribution of rHDLs which were stable at 37 °C for at least 8 hours.

Flow cytometry was used to assess the association of rHDLs to leukocytes in WHB, distinguishing between granulocytes, lymphocytes and monocytes. All the used rHDL formulations associated preferably with monocytes. Even rHDL with neutral lipid composition associated with monocytes, which is remarkable since liposomes require potential toxic cationic lipids for association with monocytes. The lipid composition of the rHDL also affected the extent of monocyte association, since incorporation of 10% cationic lipids (DOTAP and EPC) in POPC based rHDLs seemingly increased the amount of rHDLs associating with the monocytes compared to rHDL which only consisted of POPC, while incorporation of 10% anionic lipids (DOPG) did not affect the observed association. Hence, there might be a receptor mediated uptake as well as a charge depended uptake of the rHDL. Interestingly, DMPC rHDLs were found to associate with monocytes to a higher extent than observed for the POPC based rHDLs, however, some of the DMPC rHDLs also accumulated in the granulocytes. The SR-B1 receptor, which is known to interact with endogenous HDL, might be involved in the preferred association with monocytes, as it was found that monocytes express more SR-B1 than granulocytes or lymphocytes. However, further studies are needed to investigate if SR-B1 actually is involved in the observed association of rHDL with monocytes.

The rHDLs were used to deliver TMX-201 (a TLR7 agonist). After incubation of these rHDLs in WHB, secretion of certain cytokines were measured, indicating they that were able to initiate an immune response. Although, it could not be assessed if these cytokines were secreted from the monocytes, and less cytokines were secreted than when using free TMX-201, the results did indicate that a better anti-cancer immune response was obtained when delivering TMX-201 with rHDL compared to the free TMX-201. Interestingly, almost none cytokines were secreted when using DMPC rHDL as the carrier, hence, it might be that the TMX-201 are packed too tightly in the DMPC rHDL such that it cannot interact with the TLR7, or the TMX-201 from DMPC rHDL might be delivered directly to the cytosol, thus circumventing the endosomes where TLR7 is located. Again, further studies are needed, e.g. with more cytokines, to make explicit conclusions concerning these effects.

The adjuvants can be used to boost the immune response, however, tumour antigen is also required for a specific immune response. It was found that rHDL was capable of delivering antigen (SIINFEKL) to DCs, such that it could be presented through the MHC-I to

cytotoxic T-cells. Furthermore, a difference between the different types of DCs were observed, since the rHDLs were found to associate primarily with mDCs, but the mDCs seemed less effective in presenting the antigen on the MHC-I compared to cDC1s which were highly effective in presenting the minimal amount of antigen that they had taken up.

Although more studies are needed to confirm several of the effects observed in this project, the results are indeed promising, and show that the rHDLs have great potential as carrier in an immunotherapeutic DDS.

# 6. Outlook

Several of the experiments of this project obviously require replications to confirm the observed effects, especially for the experiments where only one donor is used. However, other approaches for the experiments could also be used which will be discussed further in the following.

**Effect of incubation time**

In several of the experiments of this project, the rHDLs were only incubated with WHB at a fixed time period, e.g. one hour of the experiments consider adjuvant delivery. The effect might be time-dependent, and it could be interesting to study both the association of rHDL with leukocytes and the resulting cytokine secretion over a longer period of time and with more time point measurements. Furthermore, the antigen presentation might also depend on the time point where the analysis is taken. The use of rHDL might result in a prolonged effect compared with the free drug, even without a sustained release from the rHDL, and it could be interesting to study this in more detail.

***in vivo* experiments**

It could be relevant to continue the experiments of the project with *in vivo* experiments. The association of rHDL with leukocytes could be evaluated after incubating the rHDLs in mice models. Obviously, there are differences between applying rHDLs to a sample of WHB and incubate them *in vivo*, however, the experiments could illustrate the effect of applying the rHDLs into the bloodstream.

Mice models could also be used to evaluate the biodistribution of the rHDLs. The endogenous HDL naturally interact with the liver, hence, it could be interesting to study if most of the rHDLs just accumulated in the liver, or if the rHDLs could be designed to be taken up by leukocytes, before accumulation in the liver. The rHDLs could potentially also accumulate elsewhere, and the biodistribution are clearly important when designing a potent DDS with minimal side-effects.

After optimizing of the rHDL for cancer immunotherapy, it could also be relevant to study if the rHDLs were able to eliminate tumours in mice models.

**Further investigation of larger rHDL particles**

It was found in the project that increasing the lipid/protein ratio of the rHDL led to a polydispersed distribution of presumably different sized rHDLs. It did not seem possible to obtain a monodisperse distribution of larger rHDL particles immediately after preparation, however, it might be possible to isolate the different subpopulations of the rHDLs by collecting fractions after the Superdex-200 column. The presumably larger sized rHDL particles could then be investigated to confirm that it in fact was well-defined structures and not just aggregates. TEM could be used to assess the shape and size of the rHDLs, while SEC could be used to study the stability of the isolated rHDLs with varying size. The larger rHDL particles might consist of more than two apoA-I proteins per particle, and it could also be interesting to investigate this. This might be achieved by cross-linking the proteins while in the rHDL configuration, and subsequently analysing them by SDS-page. This approach has successfully been used elsewhere[37].

The incorporation cationic lipids also seemed to shift the distribution to larger sized rHDLs, and it could be interesting to investigate if the cationic lipids preferably accumulated in the larger rHDL particles. Incorporation of cationic lipids in rHDLs has also shown some difficulties in other studies[58], however, these difficulties might be resolved by using larger sized rHDLs. Note that instability at 37 °C was observed for the rHDLs with cationic lipids incorporated, however, the isolated larger rHDL particles might be more stable, or higher stability might be achieved by using DMPC based rHDLs instead of POPC based rHDLs.

**rHDL with other apolipoproteins**

The apoA-I has been used for formulation of rHDLs in this project, however, there are also other apolipoproteins which could be used for the formulation of rHDLs[1].

An example is apoA-II, which is smaller than apoA-I, i.e. it has a molecular weight of approximately 17.4 kDa compared to 28 kDa of apoA-I. It was found using SDS-page that during the purification of apoA-I, a protein of approximately 17 kDa was discarded when using the SP-column. It might be that this was the apoA-II, hence, it might be possible to collect and further purify this protein, thus allowing for supply of apoA-II for formulation of rHDLs. It could be interesting to study if rHDL formulated with apoA-II had different properties than rHDL formulated with apoA-I.

Another apolipoprotein which could to used to formulate rHDL is apoE. It is known that apoE can bind the LDL receptor thus facilitating endocytosis of the rHDL[1]. Hence, using apoE in the rHDL might be more favourable when aiming to activate TLRs located in the endosomes of the cells.

### Spherical rHDL

This project has primarily focused on discoidal rHDL but spherical rHDL can also be formulated. The discoidal rHDL might transform into spherical rHDL when applied to blood, which could lead to unfavourable leakage of incorporated drugs, hence, it might be more favourable to use spherical rHDL. The spherical rHDL could potentially also be modified with a polymeric core from which the drug can be release substantially, as observed in other studies[19]. For immunotherapeutic purposes this could be utilized to deliver adjuvant or antigen substantially, such that immune response is preserved until the tumour is eliminated.

### Using other TLR agonists

Adjuvants have to be delivered along with antigens for an effective cancer vaccine. The used adjuvant in this project was a TLR7 agonist, however, it should also be possible to use other adjuvants to activate other TLRs. There are several types of TLRs, and while some of them are located in the endosomes, there are also several of them expressed on the cell surface[18]. The cascade of reactions which happen when the TLRs are activated needs to be evaluated, since the targeted TLR obviously need to initiate a immune response which is effective against cancer cells, e.g. by initiating the secretion of the cytokines IFN-$\alpha$, IFN-$\gamma$ or IL-12.

### rHDL for cytokine therapy

Cytokine therapy is another approach for cancer immunotherapy where cytokines are administrated to the patient. As previously discussed, rHDLs have been used to increase the circulation half-life of the cytokine IL-15[54]. It might also be possible to incorporate other cytokines in the rHDL in order to achieve a more effective cytokine therapy. The rHDLs could potentially also alter the biodistribution of the cytokines such that the cytokine accumulate at favourable sites, e.g. lymph nodes or the tumour tissue.

### PEGylated rHDL for tumour targeting

The rHDL can also be used to deliver chemotherapeutics directly to the tumour. PEGylation of nanoparticles are often used to increase their circulation time in order to achieve a more effective accumulation in the tumour by the EPR effect[10]. The circulation time of rHDL in mice models has been shown to increase many fold by PEGylation[70], however, this effect has seemingly not been utilized to optimize tumour targeting. The PEGylation of rHDL could potentially shield rHDL from interactions with receptors, e.g. the SR-B1, due to steric hindrance effects, and thereby change the biodistribution such that the uptake in the liver is limited and accumulation in the tumour is achieved. A variety of cancer cells overexpress SR-B1[1], and after the PEGylated rHDLs have accumulated in the tumour, orientation of the rHDL might at some point make interactions with the SR-B1 receptor on the cancer cells feasible thus enabling delivery of drugs from the rHDL to the cancer cells. This approach is illustrated in figure 1. The PEGylated rHDLs might also be used to deliver immunotherapeutic drugs, e.g. cytokines, to the tumour tissue.

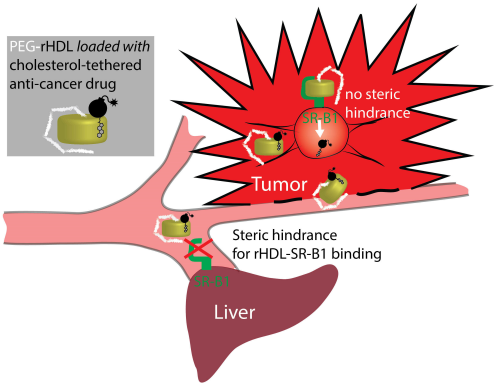


**Figure 6.1:** Illustration of the purposed effect when using PEGylated rHDL for tumour targeting.

# Bibliography


[1] Jens B. Simonsen. Evaluation of Reconstituted High-Density Lipoprotein (rHDL) as a Drug Delivery Platform – a Detailed Survey of rHDL Particles ranging from Biophysical Properties to Clinical Implications. *Nanomedicine: Nanotechnology, Biology, and Medicine*, **12**:2161–2179, 2016.

[2] S.K. Sahoo, S. Parveen, and J.J. Panda. The Present and Future of Nanotechnology in Human Health Care. *Nanomedicine: Nanotechnology, Biology, and Medicine*, **3**:20–31, 2007.

[3] Ernest S. Kawasaki and T Audrey Player. Nanotechnology, Nanomedicine, and the Development of New, Effective Therapies for Cancer. *Nanomedicine: Nanotechnology, Biology, and Medicine*, **1**:101–109, 2005.

[4] Michael Holzinger, Alan Le Goff, and Serge Cosnier. Nanomaterials for Biosensing Applications: a Review. *Frontiers in Chemistry*, **2**(63):1–10, 2014.

[5] Yiyao Liu, Hirokazu Miyoshi, and Michihiro Nakamura. Nanomedicine for Drug Delivery and Imaging: A Promising Avenue for Cancer Therapy and Diagnosis using Targeted Functional Nanoparticles. *Int. J. Cancer*, **120**:2527–2537, 2007.

[6] Larissa Y Rizzo, Benjamin Theek, Gert Storm, Fabian Kiessling, and Twan Lammers. Recent Progress in Nanomedicine: Therapeutic, Diagnostic and Theranostic Applications. *Current Opinion in Biotechnology*, **24**:1159–1166, 2013.

[7] Theresa M. Allen and Pieter R. Cullis. Drug Delivery Systems: Entering the Mainstream. *Science*, **303**:1818–1822, 2004.

[8] Biana Godin, Jason H. Sakamoto, Rita E. Serda, Alessandro Grattoni, Ali Bouamrani, and Mauro Ferrari. Emerging Applications of Nanomedicine for the Diagnosis and Treatment of Cardiovascular Diseases. *Trends in Pharmacological Sciences*, **31**(5):199–205, 2010.

[9] Kewal K.Jain. Role of Nanotechnology in Targeted Drug Delivery and Imaging: A Concise Review. *Nanomedicine: Nanotechnology, Biology, and Medicine*, **1**:193–212, 2005.

[10] Omid C. Farokhzad and Robert Langer. Impact of Nanotechnology on Drug Delivery. *American Chemical Society Nano*, **1**(1):16–20, 2009.

[11] Dennis Pedersbæk, Magnus Tudsborg Frantzen, and Peter Fojan. Electrospinning of Core-Shell Fibers for Drug Release Systems. *Journal of Self-Assembly and Molecular Electronics*, **1**:17–30, 2017.

[12] Dan Peer, Jeffrey M. Karp, Seungpyo Hong, Omid C. Farokhzad, Rimona Margalit, , and Robert Langer. Nanocarriers as an Emerging Platform for Cancer Therapy. *nature nanotechnology*, **2**:751–760, 2007.

[13] Rebecca A. Bader and David A. Putnam. *Engineering Polymer Systems for Improved Drug Delivery*, pages 46–49,60–63. Number ISBN: 978-1-118-09847-9. Wiley, 2014.

[14] Anna Meiliana, Nurrani Mustika Dewi, and Andi Wijaya. Cancer Immunotherapy: A Review. *The Indonesian Biomedical Journal*, **8**(1):1–20, 2016.

[15] Robert D. Schreiber, Lloyd J. Old, and Mark J. Smyth. Cancer Immunoediting: Integrating Immunity's Roles in Cancer Suppression and Promotion. *Science*, **331**:1565–1570, 2011.

[16] Michael Holzinger, Alan Le Goff, and Serge Cosnier. Application of Nanostructured Drug Delivery Systems in Immunotherapy of Cancer: A Review. *Artificial Cells, Nanomedicine, and Biotechnology*, **45**(1):18–23, 2017.

[17] Joana M. Silva, Mafalda Videira, Rogério Gaspar, Véronique Préat, and Helena F. Florindo. Immune System Targeting by Biodegradable Nanoparticles for Cancer Vaccines. *Journal of Controlled Release*, **168**:179–199, 2013.

[18] Holger Kanzler, Franck J Barrat, Edith M Hessel, and Robert L Coffman. Therapeutic Targeting of Innate Immunity with Toll-Like Receptor Agonists and Antagonists. *Nature Medicine*, **13**(5):552–559, 2007.

[19] Rui Kuai, Dan Li, Y. Eugene Chen, James J. Moon, and Anna Schwendeman. High-Density Lipoproteins: Nature's Multifunctional Nanoparticles. *American Chemical Society*, **10**:3015–3041, 2016.

[20] F Re, R Moresco, and M Masserini. Nanoparticles for Neuroimaging. *Journal of Physics D: Applied Physics*, **45**(073001):53–65, 2012.

[21] Shawn C. Owen, Dianna P.Y. Chan, and Molly S. Shoichet. Polymeric Micelle Stability. *Nano Today*, **7**:53–65, 2012.

[22] Ole G. Mouritsen. Lipids, Curvature, and Nano-medicine. *Eur. J. Lipid Sci. Technol.*, **113**:1174–1187, 2011.

[23] Leonie E Paulis, Subhra Mandal, Martin Kreutz, and Carl G Figdor. Dendritic Cell-based Nanovaccines for Cancer Immunotherapy. *Current Opinion in Immunology*, **25**:389–395, 2013.

[24] Nazila Kamaly, Zeyu Xiao, Pedro M. Valencia, Aleksandar F. Radovic-Moreno, and Omid C. Farokhzad. Targeted Polymeric Therapeutic Nanoparticles: Design, Development and Clinical Translation. *Chem. Soc. Rev.*, **41**:2971–3010, 2012.

[25] Singh Davinder, Harikumar S L, and Nirmala. Nanoparticles: An Overview. *Journal of Drug Delivery & Therapeutics*, **3**(2):169–175, 2013.

[26] Masayuki Yokoyama. Polymeric Micelles as Drug Carriers: Their Lights and Shadows. *Journal of Drug Targeting*, **22**(7):576–583, 2014.

[27] Meredith L. Hans and Anthony M. Lowman. *Nanomaterials Handbook, Chapter 23: Nanoparticles for Drug Delivery.* Number ISBN: 978-1-4200-0401-4. Taylor and Francis Group, 2006.

[28] Sungwon Kim and Kinam Park. *Targeted Delivery of Small and Macromolecular Drugs, Chapter 19: Polymer Micelles for Drug Delivery.* Number ISBN: 978-1-4200-8773-4. CRC Press, 2010.

[29] Kazunori Kataoka, Atsushi Harada, and Yukio Nagasaki. Block Copolymer Micelles for Drug Delivery: Design, Characterization and Biological Significance. *Advanced Drug Delivery Reviews*, **64**:37–48, 2012.

[30] Giuseppina Bozzuto and Agnese Molinari. Liposomes as Nanomedical Devices. *International Journal of Nanomedicine*, **10**:975–999, 2015.

[31] Theresa M. Allen and Pieter R. Cullis. Liposomal Drug Delivery Systems: From Concept to Clinical Applications. *Advanced Drug Delivery Reviews*, **65**:36–48, 2013.

[32] C. Shad Thaxton, Jonathan S. Rink, Pratap C. Naha, and David P. Cormode. Lipoproteins and Lipoprotein Mimetics for Imaging and Drug Delivery. *Advanced Drug Delivery Reviews*, **106**:116–131, 2016.

[33] Nirupama Sabnis and Andras G Lacko. Drug Delivery via Lipoprotein-based Carriers: Answering the Challenges in Systemic Therapeutics. *Therapeutic Delivery*, **3**(5):599–608, 2012.

[34] Patrick C.N. Rensen, Remco L.A. de Vrueh, Johan Kuiper, Martin K. Bijsterbosch, Erik A.L. Biessen, and Theo J.C. van Berkel. Recombinant Lipoproteins: Lipoprotein-like Lipid Particles for Drug Targeting. *Advanced Drug Delivery Reviews*, **47**:251–276, 2001.

[35] Jeremy M. Berg, John L. Tymoczko, and Lubert Stryer. *Biochemistry*, pages 70–75, 90–91, 1031–1040. Number ISBN: 978-1-4292-7635-1 in 7th ed. W.H. Freeman and Company, 2012.

[36] Ji Wang, Junting Jia, Jianping Liu, Hongliang He, Wenli Zhang, and Zhenghua Li. Tumor Targeting Effects of a Novel Modified Paclitaxel-loaded Discoidal Mimic High Density Lipoproteins. *Drug Delivery*, **20**(8):356–363, 2013.

[37] John B. Massey and Henry J. Pownall. Cholesterol is a Determinant of the Structures of Discoidal High Density Lipoproteins formed by the Solubilization of Phospholipid Membranes by Apolipoprotein A-I. *Biochimica et Biophysica Acta*, **1781**:245–253, 2008.

[38] Andras G. Lacko, Nirupama A. Sabnis, Bhavani Nagarajan, and Walter J. McConathy. HDL as a Drug and Nucleic Acid Delivery Vehicle. *Frontiers in Pharmacology*, **6**:247, 1–6, 2015.

[39] Jeffrey K. Actor. *Introductory Immunology: Basic Concepts for Interdisciplinary Applications*, pages 1–27. Number ISBN: 978-0-12-420030-2. Elsevier Inc., 2014.

[40] Kathleen Park Talaro and Barry Chess. *Foundations in Microbiology*, pages 424–481. Number ISBN: 978-0-07-337529-8 in 8th ed. The McGraw-Hill Companies, 2012.

[41] Jeffrey D. Price and Kristin V. Tarbell. The Role of Dendritic Cell Subsets and Innate Immunity in the Pathogenesis of Type 1 Diabetes and other Autoimmune Diseases. *Frontiers in Immunology*, **6**(288):1–12, 2015.

[42] Olivier P. Joffre, Elodie Segura, Ariel Savina, and Sebastian Amigorena. Cross-Presentation by Dendritic Cells. *Nature Reviews*, **12**:557–569, 2012.

[43] Jan Mauer, Jesse L. Denson, and Jens C. Brüning. Versatile Functions for IL-6 in Metabolism and Cancer. *Trends in Immunology*, **36**(2):92–101, 2015.

[44] Sylvia Lee and Kim Margolin. Cytokines in Cancer Immunotherapy. *Cancers*, **3**:3856–3893, 2011.

[45] Hélène Gary-Gouy, Pierre Lebon, and Ali H. Dalloul. Type I Interferon Production by Plasmacytoid Dendritic Cells and Monocytes is Triggered by Viruses, but the Level of Production is Controlled by Distinct Cytokines. *Journal of Interferon and Cytokine Research*, **22**:653–659, 2002.

[46] Nahideh Asadi, Soodabeh Davaran, Yunes Panahi, Arash Hasanzadeh, Javad Malakootikhah, Hadi Fallah Moafi, and Abolfazl Akbarzadeh. Application of Nanostructured Drug Delivery Systems in Immunotherapy of Cancer: a Review. *Artificial Cells, Nanomedicine, and Biotechnology*, **45**(1):18–23, 2017.

[47] Samar Hamdy, Azita Haddadi, Anooshirvan Shayeganpour, John Samuel, and Afsaneh Lavasanifar. Activation of Antigen-Specific T Cell-Responses by Mannan-Decorated PLGA Nanoparticles. *Pharm Res*, **28**:2288–2301, 2011.

[48] Rodney A. Rosalia et al. CD40-Targeted Dendritic Cell Delivery of PLGA-Nanoparticle Vaccines Induce Potent Anti-Tumor Responses. *Biomaterials*, **40**:88–97, 2015.

[49] Thomas C.B. Klauber, Janne M. Laursen, Daniel Zucker, Susanne Brix, Simon S. Jensen, and Thomas L. Andresen. Delivery of TLR7 Agonist to Monocytes and Dendritic Cells by DCIR Targeted Liposomes Induces Robust Production of Anti-Cancer Cytokines. *Acta Biomaterialia*, **53**:367–377, 2017.

[50] Pia T. Johansen, Daniel Zucker, Ladan Parhamifar, Houman Pourhassan, Ditte Villum Madsen, Jonas R. Henriksen, Monika Gad, Alcide Barberis, Roberto Maj, Thomas L. Andresen, and Simon S. Jensen. Monocyte Targeting and Activation by Cationic Liposomes Formulated with a TLR7 Agonist. *Expert Opinion on Drug Delivery*, **12**(7):1045–1058, 2015.

[51] Hidesuke Kaji. High-Density Lipoproteins and the Immune System. *Journal of Lipids*, **2013**(684903):8 pages, 2013.

[52] Alberico Luigi Catapano, Angela Pirillo, Fabrizia Bonacina, and Giuseppe Danilo Norata. HDL in Innate and Adaptive Immunity. *Cardiovascular Research*, **103**:372–383, 2014.

[53] Emiel P.C. van der Vorst et al. High-Density Lipoproteins Exert Pro-inflammatory Effects on Macrophages via Passive Cholesterol Depletion and PKC-NF-$\kappa$B/STAT1-IRF1 Signaling. *Cell Metabolism*, **25**:197–207, 2017.

[54] Maria C. Ochoa et. al. Antitumor Immunotherapeutic and Toxic Properties of an HDL-Conjugated Chimeric IL-15 Fusion Protein. *Cancer Research*, **73**(1):139–149, 2017.

[55] Rui Kuai, Lukasz J. Ochyl, Keith S. Bahjat, Anna Schwendeman, and James J. Moon. Designer Vaccine Nanodiscs for Personalized Cancer Immunotherapy. *Nature Materials*, **16**:489–496, 2017.

[56] Ernst J. Schaefer et al. Human Apolipoprotein A-I and A-II Metabolism. *Journal of Lipid Research*, **23**:850–862, 1982.

[57] Matthew R. Whorton, Beata Jastrzebska, Paul S.-H. Park, Dimitrios Fotiadis, Andreas Engel, Krzysztof Palczewski, , and Roger K. Sunahara. Efficient Coupling of Transducin to Monomeric Rhodopsin in a Phospholipid Bilayer. *Journal of Biological Chemistry*, **283**(7):4387–4394, 2008.

[58] Maria Wadsäter, Selma Maric, Jens B. Simonsen, Kell Mortensen, and Marité Cardenas. The Effect of using Binary Mixtures of Zwitterionic and Charged Lipids on Nanodisc Formation and Stability. *The Royal Society of Chemistry*, **9**:2329–2337, 2013.

[59] Daniel L. Sparks, Sissel Lund-Katz, and Michael C. Phillips. The Charge and Structural Stability of Apolipoprotein A-I in Discoidal and Spherical Recombinant High Density Lipoprotein Particles. *Journal of Biological Chemistry*, **267**(36):25839–25847, 1992.

[60] Rajan Katoch. *Analytical Techniques in Biochemistry and Molecular Biology*, pages 47–62. Number ISBN: 978-1-4419-9784-5. Springer, 2011.

[61] Aysun Adan, Günel Alizada, Yağmur Kiraz, Yusuf Baran, and Ayten Nalbant. Flow Cytometry: Basic Principles and Applications. *Critical Reviews in Biotechnology*, **37**(2):163–176, 2017.

[62] Mark Winey, Janet B. Meehl, Eileen T. O'Toole, and Jr. Thomas H. Giddings. Conventional Transmission Electron Microscopy. *Molecular Biology of the Cell*, **25**:319–323, 2014.

[63] Lei Zhang, Huimin Tong, Mark Garewal, and Gang Ren. Optimized Negative-Staining Electron Microscopy for Lipoprotein Studies. *Biochimica et Biophysica Acta*, **1830**:2150–2159, 2013.

[64] Denys Bashtovyy, Martin K. Jones, G. M. Anantharamaiah, and Jere P. Segrest. Sequence Conservation of Apolipoprotein A-I Affords Novel Insights into HDL Structure-Function. *Journal of Lipid Research*, **52**:435–450, 2011.

[65] Yujie Wanga, Pengxiao Lou, Guangyue Bai, Caoying Fan, and Margarida Bastos. Cationic Gemini and Sodium Cholate – Following the Interaction of Oppositely Charged Surfactants by Calorimetry, Turbidity and Conductivity. *The Journal of Chemical Thermodynamics*, **73**:225–261, 2014.

[66] Yelena V.Grinkova, Ilia G.Denisov, and Stephen G.Sligar. Engineering Extended Membrane Scaffold Proteins for Self-Assembly of Soluble Nanoscale Lipid Bilayers. *Protein Engineering, Design & Selection*, **23**(11):843–848, 2010.

[67] Ole G. Mouritsen. *Life - As a Matter of Fat: The Emerging Science of Lipidomics*, pages 23–31. Number ISBN: 978-3-540-23248-3. Springer, 2005.

[68] Jan-Christer Janson. *Protein Purification: Principles, High Resolution Methods, and Applications*, pages 61–63. Number ISBN: 978-0-471-77661-4. Wiley and Sons, Inc., 2011.

[69] Markus Johnsson and Katarina Edwards. Liposomes, Disks, and Spherical Micelles: Aggregate Structure in Mixtures of Gel Phase Phosphatidylcholines and Poly(Ethylene Glycol)-Phospholipids. *Biophysical Journal*, **85**(6):3839–3847, 2003.

[70] Andrew J. Murphy, Samuel Funt, Darren Gorman, Alan R. Tall, and Nan Wang. Pegylation of High-Density Lipoprotein Decreases Plasma Clearance and Enhances Antiatherogenic Activity. *Circulation Research*, **113**:e1–e9, 2013.

# Appendix A

# Supporting Information

### Calibration of the SDS-page

The SDS-page can give information about the mass of a protein as well as the purify of a protein in solution. Furthermore, it can seemingly also be used to estimate the concentration of a protein in a sample. This can be achieved by considering the intensity of the protein bands in a gel. Higher concentration of protein will lead to more pronounced/darker protein bands. The intensity over each lane was plotted by the software imageJ. In order to relate the measured intensity to the concentration of apoA-I, a calibration was conducted using four samples with known concentration of apoA-I, see figure A.1. It was found that there was a linear correlation between the integral measured over the peaks (related to the protein band) and the concentration of apoA-I, see figure A.2. Thus, using minimum two samples of apoA-I when running the SDS-pages, it seems possible to estimate the amount of apoA-I quantitatively. However, it might not be a very accurate estimate, and should only be use to get an idea of the quantitative amount. The method of using the integral seems more reliable when used for relative estimates of proteins in the same gel, e.g. to assess the purity.

### Determine volume shift of the fraction collection on the HPLC

The fraction collector on the HPLC is obviously of major importance during the purification of apoA-I. The volume between detection by the UV-detector and fraction collector was initially unknown. Hence, experiments were conducted in order to estimate this volume. This was done by injection of a BSA solution on the Superdex-200 column, and collecting fractions of 0.5 mL which could be further analysed by absorption spectroscopy. The shift in retention volume between the result from the SEC analysis and the fractions analysed by the spectrophotometer can be estimated to be the volume difference between UV-detector and fraction collector. The results from these data are seen in figure A.3. It is evident that a suggested shift of 0.5 mL seems reasonable.

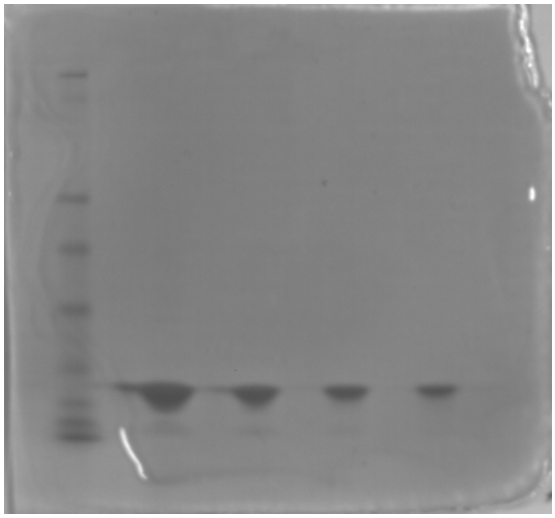

**Figure A.1:** The SDS-page with three different concentrations of the supplied apoA-I. From the left the wells contain: The ladder, 0.0842 mM apoA-I, 0.0421 mM apoA-I, 0.0210 mM apoA-I, 0.0105 mM apoA-I.

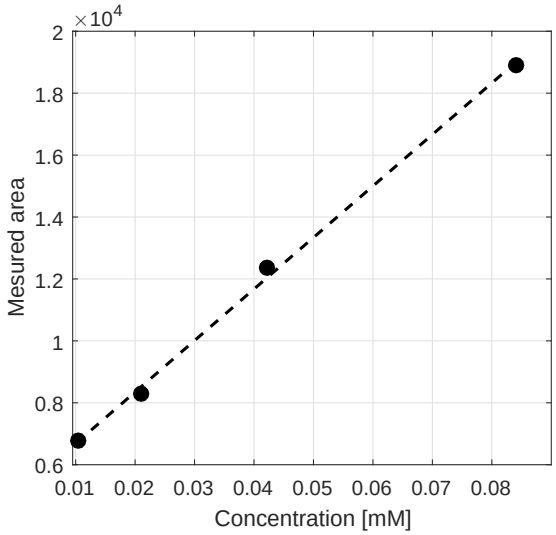


**Figure A.2:** Plotting the intensity of the lanes, and measuring the integral over the peaks by the software imageJ, indicate that this integral seem to by proportional to the concentration of apoA-I.

### Liposomes prepared by the detergent depletion method

The detergent depletion method was used to formulate rHDLs, however, it could apparently also be used to formulate liposomes. This was found by using the same approach as used to formulate rHDLs but without adding of apoA-I. The resulting solution was analysed by dynamic light scattering, and it was found that the average size of particles in the solution was 190 ± 14 nm, which could be attributed to liposomes since this is a reasonable size of self-assembled liposomes. Hence, assuming that it indeed is liposomes, this illustrates that liposomes can be prepared by the same method as used to formulate rHDL if no apoA-I is present.

The solution, which presumably contained liposomes, were also analysed by SEC, see figure A.4. The liposomes should be eluted at the void of the Superdex-200 column due to their relatively large size. Hence, it is seen from figure A.4 that the void of the column seems to be between retention volumes of approximately 7-8 mL.

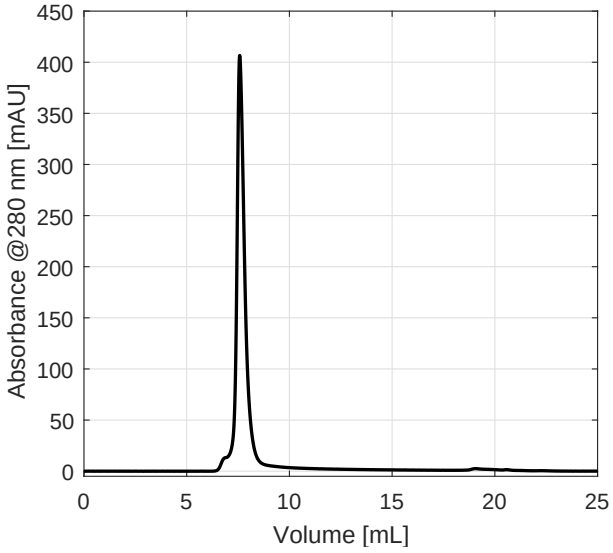


**Figure A.4:** SEC analysis of the liposomes prepared by the detergent depletion method. The liposomes should be eluted at the void of the column illustrating that the void is at retention volumes at approximately between 7-8 mL.

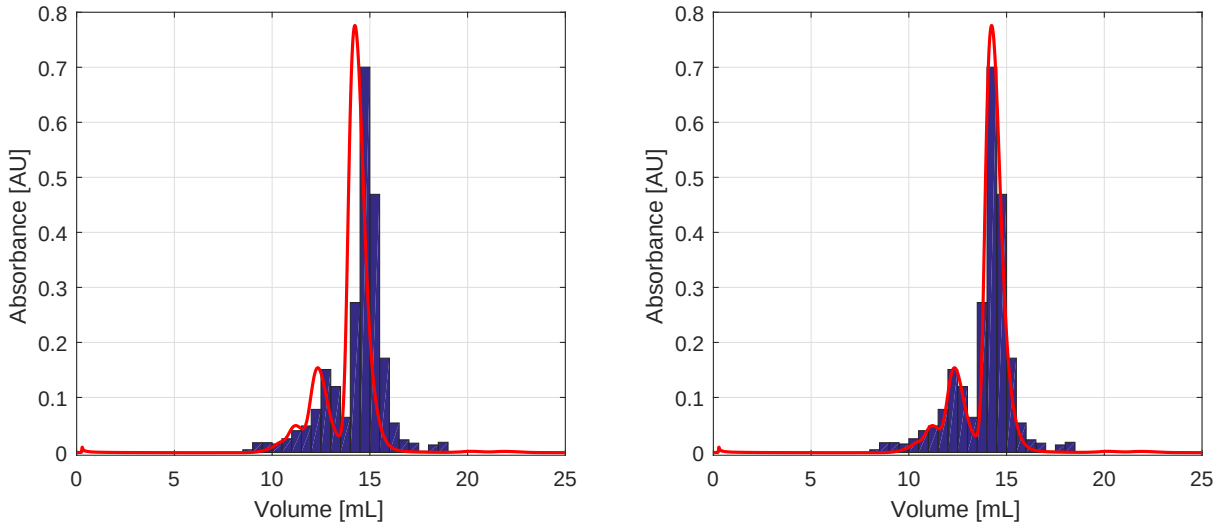


**(A)** **(B)**

**Figure A.3:** Comparison between the absorbance at 280 nm measured by the HPLC UV-detector and absorbance of the collected fraction at 280 nm measured by the spectrophotometer. The red line is the data from the HPLC while the blue bars represent the absorbance of the collected fractions. **(A):** Clearly, a shift in volume is observed. **(B):** A volume shift of 0.5 mL is suggested and applied to the collected fractions. The suggested shift seem reasonable.

# Appendix B

## B.1 Gating strategy for flow cytometry analysis in figure 4.22

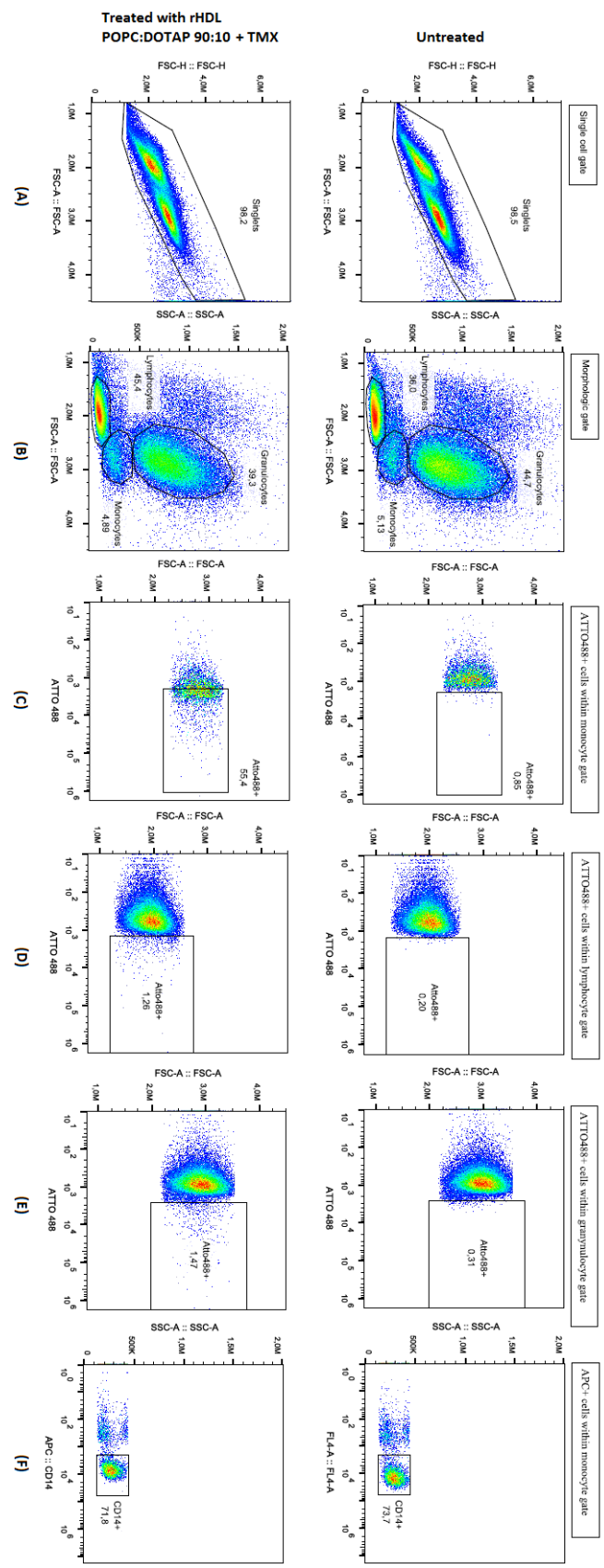


**Figure B.1:** A untreated sample was used as reference to set the gates. Data are only shown for gating of the untreated sample and the sample containing rHDH with POPC:DOTAP:TMX-201 85:10:5 and 0.1% DOPE-atto488, however, similar gating strategy was used for all of the formulation presented in figure 4.22. **(A):** Gating for single cells. **(B):** The morphology gates (using FSC and SSC) which identifies the granulocytes, lymphocytes and monocytes. (**C-E**:) The cells within the morphology gates are analysed further for the fluorescence from DOPE-atto488. **(F):** Analysis of the CD14 antibody within the monocytes gate, which can identify the monocytes more accurately.

## B.2 Gating strategy for flow cytometry analysis in figure 4.23

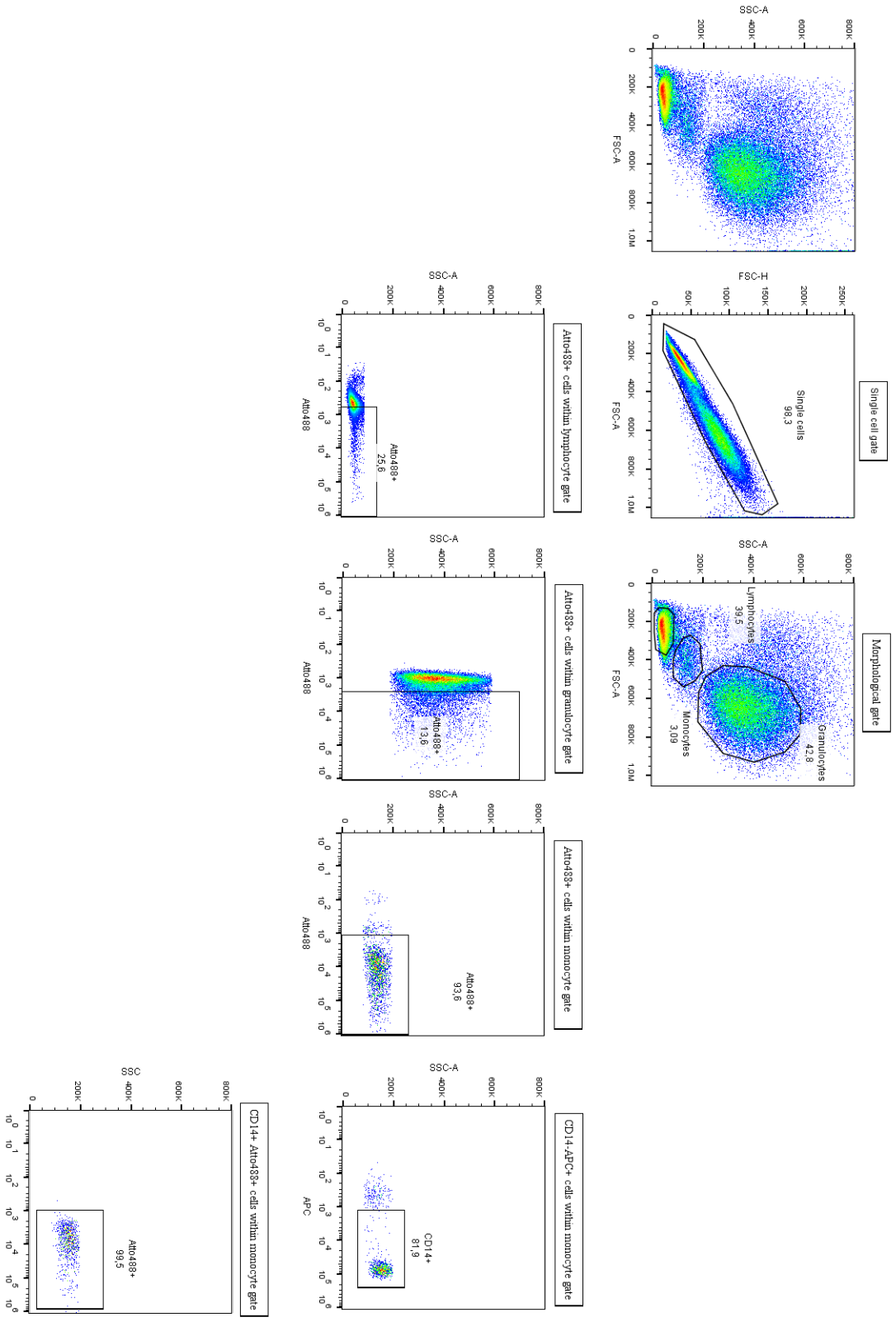


**Figure B.2:** The gating strategy for the flow cytometry experiments presented in figure 4.23. A untreated sample was used as reference to set the gates (data not shown). The data is shown for the POPC:DOTAP rHDL sample. Similar principles apply as described in the caption of figure B.1

## B.3 Gating strategy for flow cytometry analysis in figure 4.28

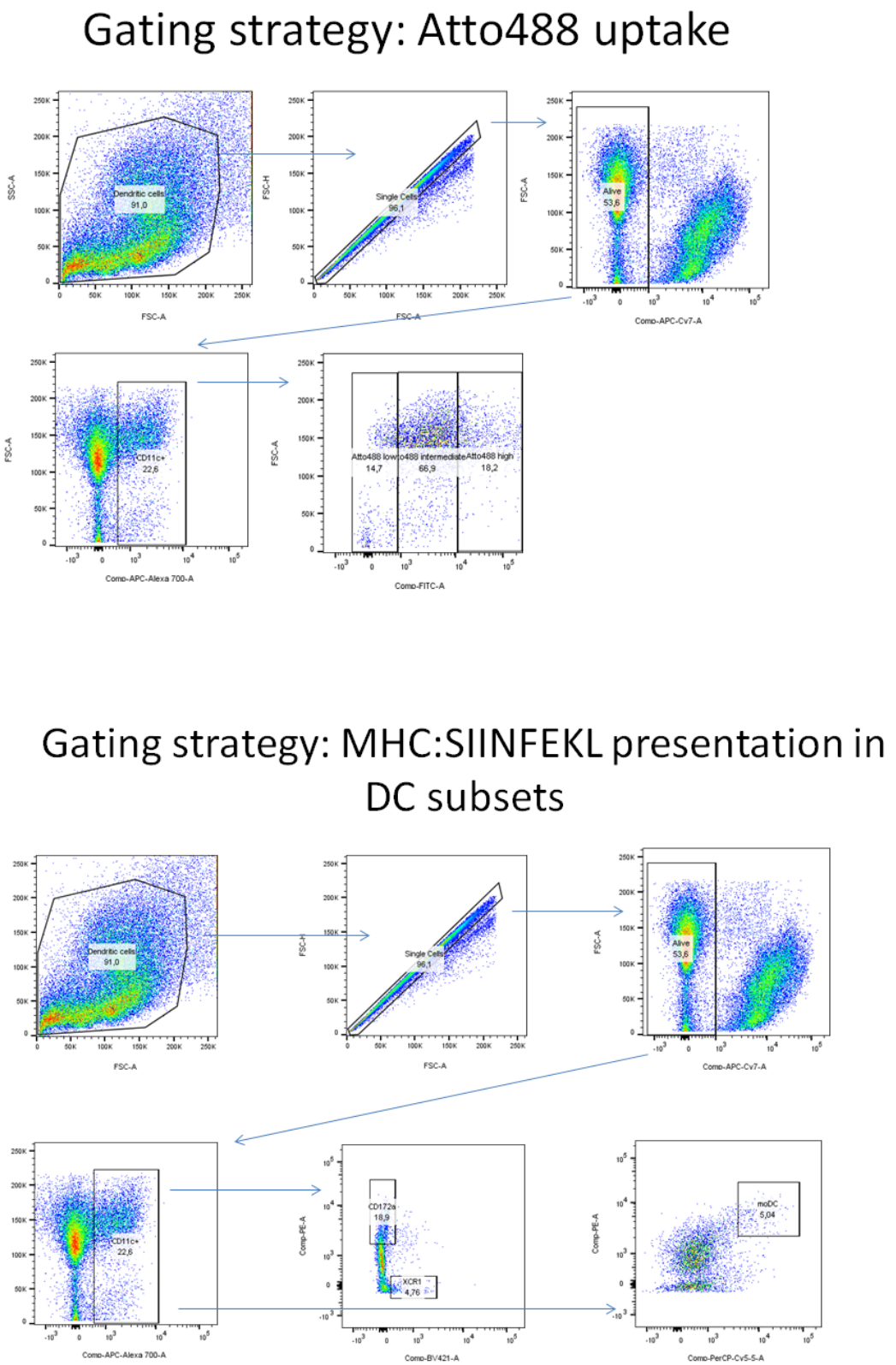


**Figure B.3:** The gating strategy for the flow cytometry experiments presented in figure 4.28. The gating strategies used to assess both the association of atto488 (which indicate uptake of the rHDLs) and the MHC-I:SIINFEKL presentation are shown.